



Virginia Commonwealth University  
VCU Scholars Compass

---

Theses and Dissertations

Graduate School

---

2011

## Synthesis and Biological Screening of a Series of Novel Chemokine Receptor CCR5 Antagonists

Soundarya Vaithianathan  
*Virginia Commonwealth University*

Follow this and additional works at: <https://scholarscompass.vcu.edu/etd>

 Part of the [Pharmacy and Pharmaceutical Sciences Commons](#)

© The Author

---

Downloaded from

<https://scholarscompass.vcu.edu/etd/243>

This Dissertation is brought to you for free and open access by the Graduate School at VCU Scholars Compass. It has been accepted for inclusion in Theses and Dissertations by an authorized administrator of VCU Scholars Compass. For more information, please contact [libcompass@vcu.edu](mailto:libcompass@vcu.edu).

SYNTHESIS AND BIOLOGICAL SCREENING OF A SERIES OF NOVEL  
CHEMOKINE RECEPTOR CCR5 ANTAGONISTS

A Dissertation submitted in partial fulfillment of the requirements for the degree of Master of  
Science at Virginia Commonwealth University.

by

SOUNDARYA VAITHIANATHAN  
Bachelor of Pharmacy, Mumbai University, India, 2009

Director: DR. YAN ZHANG  
ASSOCIATE PROFESSOR OF MEDICINAL CHEMISTRY

Virginia Commonwealth University  
Richmond, Virginia  
July, 2011

### Acknowledgement

This research project would not have been possible without the support of many people. I would start by thanking my advisor, Dr. Yan Zhang, for his supervision, advice, and guidance at every stage of the research. He has been extremely patient and always willing to help me. I will always be thankful to him for giving me the opportunity to work in his lab, and improve my knowledge and understanding of chemical synthesis and medicinal chemistry.

I would like to thank Ms. Kendra Haney for her invaluable support and help. I am much indebted to her for her valuable advice and help in biological screening. I would sincerely like to thank Dr. Yunyun Yuan for teaching me the basics in chemical synthesis, answering my numerous questions and also performing HPLC for my final compounds. My sincere thanks to Dr. Feng Zhang for always being ready to offer his help! Tackling some challenging reactions would have been extremely difficult without his help. I would also convey my thanks to Dr. Guo Li, whose chemical synthesis notebook helped me invariably.

Many thanks go to Dr. Martin Safo and Dr. David Gewirtz, that in the midst of all their activities, they agreed to be the members of my defense committee. I was benefited by the advice and guidance from Dr. Gewirtz, who kindly granted me his time for explaining the intricate aspects of cancer biology.

It was nice to work with our research group members, Shilpa, Orgil, Chris, Ashley, Yamini and Saheem who made working in the lab fun. I would also like to thank my other friends in the department, Hardik, Rio, Shrenik, Rakesh, PreetPal and Akul who have helped me

at various instances. I would also like to express my sincere gratitude to my undergraduate chemistry professors; Mrs. Raheja and Mrs. Poonam who instilled in me the love for chemistry.

My parents require a special mention for always supporting my decision; my sister for being my source of inspiration. I would like to mention my friends outside the department; Sayali, Soumya, Vidya, Della, Vikram and Sriram who have always been extremely supportive.

And last but not the least I would like to thank Department of Medicinal Chemistry and School of Pharmacy at VCU for giving me this opportunity to study here.

## Table of Contents

	Page
Acknowledgements .....	ii
List of Tables.....	vi
List of Figures .....	vii
<b>Chapter</b>	
1 General Introduction .....	1
1.1 Inflammation and cancer .....	1
1.2 Tumor microenvironment.....	2
1.2.1 Cellular components.....	2
1.2.2 Humoral components .....	4
1.3 Chemokines .....	6
1.4 Chemokine receptors .....	8
1.5 CCR5 .....	13
2 Disease Involvement of CCR5.....	17
2.1 Prostate Cancer .....	17
2.2 Breast Cancer.....	24
2.3 HIV/AIDS.....	26
3 CCR5 Antagonists.....	32
4 Project Objectives and Design .....	42
4.1 Background work.....	43

4.2	Molecular Modeling based Drug Design.....	49
4.3	Project Design.....	55
4.4	Project Objectives.....	57
5	Results and Discussion.....	59
5.1	Chemical synthesis of CCR5 Antagonists.....	59
5.2	Biological Screening.....	75
5.2.1	Calcium Mobilization Assay.....	75
5.2.2	Anti-proliferation Assay.....	78
6	Experimental Section.....	85
6.1	Chemical Synthesis.....	85
6.1.1	Synthesis of Intermediates.....	85
6.1.2	Synthesis of Final Compounds.....	100
6.2	Biological Screening.....	119
6.2.1	Calcium Mobilization Assay.....	119
6.2.2	Anti-proliferation Assay.....	120
7	Conclusions.....	122
	References.....	124

## List of Tables

	Page
Table 1: Total cell surface and intracellular expression of CCR1, CCR3 and CCR5 in PC-3, LNCaP and DU145 cell lines.....	21
Table 2: Possible substitutions at R <sub>1</sub> , R <sub>2</sub> , and R <sub>3</sub> . .....	48
Table 3: Possible substituents at R <sub>1</sub> and R <sub>3</sub> .....	56
Table 4: IC <sub>50</sub> values from the calcium mobilization assay.....	76
Table 5: The IC <sub>50</sub> values for PC-3 and M12 cell lines.....	80

## List of Figures

	Page
Figure 1: Signaling of chemokine receptors upon chemokine binding.....	12
Figure 2: Schematic diagram of CCR5 G-protein-coupled receptor.....	15
Figure 3: Expression of CCL5 mRNA in prostate cancer cell lines .....	20
Figure 4: Inhibition of CCL5 (RANTES) mediated cell proliferation in DU 145 prostate cancer cell line by CCR5 antagonist TAK-779.....	22
Figure 5: Steps involved in the entry of HIV into the host cell via the CD4 and CCR5/CXCR4 receptors. ....	29
Figure 6: Initial lead (1) and TAK-779 (2) .....	33
Figure 7: TAK-652.....	34
Figure 8: Aplaviroc/ONO-4128 .....	34
Figure 9: Initial leads developed by Schering-Plough .....	35
Figure 10: SCH-C / SCH351125.....	36
Figure 11: Initial leads in piperazino-piperidine series of Schering-Plough CCR5 antagonists.....	37
Figure 12: SCH-D/ Vicriviroc/ SCH-417690.....	38
Figure 13: Initial leads for Merck CCR5 antagonists .....	38
Figure 14: Cyclic CCR5 antagonists developed by Merck.....	39
Figure 15: Initial leads for CCR5 antagonists developed by Pfizer .....	40
Figure 16: Pfizer CCR5 antagonists.....	41
Figure 17: CCR5 antagonists .....	43



Figure 18: Molecular scaffold .....	44
Figure 19: SCH-D docked into CCR5 receptor .....	45
Figure 20: Novel skeleton .....	46
Figure 21: Model Compound .....	47
Figure 22: Model compound docked into binding pocket of CCR5 .....	47
Figure 23: Lead compound .....	49
Figure 24: Binding mode of Maraviroc (purple) in the homology model of CCR5 .....	50
Figure 25: Binding mode of Aplaviroc (yellow) in the homology model of CCR5 .....	52
Figure 26: The three compounds that were aligned together .....	53
Figure 27: Maraviroc (purple), Aplaviroc (orange) and compound from our lab (cyan) aligned together .....	54
Figure 28: Molecular skeleton with new substituents at R1 .....	55
Figure 29: The different commercially available hydrophobic substituents .....	57
Figure 30: Substitution and Grignard reactions .....	59
Figure 31: Experimental set-up for Grignard reaction .....	61
Figure 32: Hydrogenation and protection reactions .....	61
Figure 33: Nitration and reduction reactions .....	63
Figure 34: Amide formation and base catalyzed de-protection reactions .....	65
Figure 35: Amide formation and base catalyzed de-protection reactions .....	65
Figure 36: Diaryl ethers with six different substituents at R1 .....	66
Figure 37: Bromobenzenes to be coupled with p-cresol .....	67
Figure 38: Ullman coupling reaction for electron donating groups .....	67

Figure 39: Ullmann Coupling reaction for electron withdrawing groups .....	68
Figure 40: Different substituents that were attached to 10 and 11 .....	69
Figure 41: Final compounds.....	70, 71
Figure 42: Reaction for para substituents at R .....	72
Figure 43: Reaction for ortho and meta substituted R .....	73
Figure 44: Ullmann coupling and bromination reactions.....	74
Figure 45: Our initial lead and compound 19 .....	77
Figure 46: Role of WST-1 in the Anti-proliferation Assay .....	79
Figure 47: Compounds 19, 14, and 24 .....	82

## Abstract

### SYNTHESIS AND BIOLOGICAL SCREENING OF A SERIES OF NOVEL CHEMOKINE RECEPTOR CCR5 ANTAGONISTS

By Soundarya Vaithianathan, MS

A Dissertation submitted in partial fulfillment of the requirements for the degree of Master of  
Science at Virginia Commonwealth University.

Virginia Commonwealth University, 2011

Major Director: Dr. Yan Zhang

Associate Professor, Department of Medicinal Chemistry

The chemokine receptor CCR5 has been implicated in the pathogenesis of cancers and AIDS. A series of novel piperidine derivatives were designed, synthesized, and evaluated as CCR5 antagonists. The ability of the new ligands to inhibit the increment of intracellular calcium level stimulated by endogenous ligand CCL5 was measured in the calcium mobilization assay as an indication of its CCR5 receptor antagonism. The anti-proliferation assay was performed to measure the ability of these new compounds to inhibit the proliferation of prostate cancer cell lines, PC-3 and M12. A new lead compound has been identified which showed micromolar level of inhibition to PC-3 cell line proliferation as well as calcium mobilization. These studies are the

beginning of a thorough analysis of the CCR5 receptor antagonist binding pocket in the CCR5 receptor. Further examination may help identify next generation lead to develop highly selective CCR5 receptor antagonists and anti prostate cancer agents.

## 1. General Introduction

### 1.1 Inflammation and cancer:

Inflammation is a fundamental physiologic process that is necessary for wound repair and recovery from infection.<sup>1</sup> This process acts as a defense mechanism helping the host fight against infections. However, inflammation is a self-limiting process.<sup>2</sup> Uncontrolled or abnormal regulation of this process can lead to carcinogenesis.<sup>1</sup> As early as the 19<sup>th</sup> century, Rudolf Virchow noticed leucocytes in neoplastic tissue and made a connection between inflammation and cancer.<sup>3</sup> Currently it has been reported that 25% of the cancers worldwide are caused due to infectious agents or an inflammatory condition.<sup>2</sup> For example; papillomavirus serves as the inflammatory stimuli in cervical cancer. A similar analogy can be drawn between hepatocellular carcinoma and hepatitis virus (B and C), gastric cancer and *H. pylori*, and colorectal cancer and inflammatory bowel disease.<sup>3</sup>

The main purpose of an inflammatory response is to create a tissue microenvironment. The microenvironment recognizes foreign particles and repairs cellular damage thus, leading to eradication of the foreign particles and infected cells.<sup>6</sup> The environment is rich in inflammatory cells which is an integral part of the neoplastic process, leading to proliferation, migration, and survival of cells.<sup>5</sup>

Under homeostatic conditions, when tissues are either exposed to some chemical irritant or wounded, inflammatory cells remove these wounded and damaged cells. This is done by induction of cell death or phagocytosis. The inflammatory cells also promote cell growth and proliferation to facilitate tissue regeneration and wound healing. The process

of proliferation and inflammation subsides once the chemical irritant or inflammatory stimulus is removed, and the wound is repaired. Chronic inflammation brings about alterations in the normally growing cells by affecting oncogenes leading to continued and sustained proliferation of the cells. This causes the uncontrolled growth of cells which eventually leads to neoplasm.<sup>5</sup>

### **1.2 Tumor Microenvironment:**

In 1889, Stephen Paget emphasized the importance of the tumor microenvironment in tumor growth and progression. The “seed and soil” hypothesis was postulated by him. This hypothesis stated that factors in the tumor microenvironment constitute the fertile soil which promotes the growth and metastasis of cancer. This hypothesis has been validated and continues to hold true in associating the ability of the tumor cell (seed) to metastasize successfully to the microenvironment (soil).<sup>7</sup>

The tumor microenvironment comprises of two major components. These include the cellular and the humoral components. The cellular components include macrophages, dendritic cells, lymphocytes and leucocytes. The humoral components include cytokines and chemokines.<sup>6</sup> Tumors, their stromal areas, and precancerous tissues have a large and diverse population of the cellular and humoral components thus, contributing in cancer initiation, promotion and metastasis.<sup>5</sup>

#### **1.2.1 Cellular components:**

Macrophages are the major component of the tumor microenvironment.<sup>3</sup> They are also known as tumor-associated macrophages (TAM).<sup>4</sup> They are differentiated monocytes

that mainly originate from the bone marrow. Macrophages in the body are in continuous search of foreign antigens which are phagocytosed and processed.<sup>8</sup> Due to this function, TAMs are recruited to sites of tissue injury and inflammation.<sup>4</sup> Under homeostatic conditions, macrophages are appropriately activated. Upon activation, TAMs have the ability to kill tumor cells and cause tissue destruction. However, TAMs can also produce angiogenic and growth factors which stimulates tumor-cell proliferation and angiogenesis. They also produce protease enzymes which can degrade the extracellular matrix and hence, favor invasion and metastasis.<sup>3</sup> The major pro-tumoral function of TAM is the suppression of anti-tumor immune response.<sup>9</sup>

There are two types of macrophages: M1 and M2 macrophages. M1 macrophages are anti-tumor in function. They perform tumor surveillance functions. TAMs are M2 type of macrophages which contributes to the immuno suppressive tumor microenvironment. These macrophages show several pro-tumoral functions such as angiogenesis, matrix remodeling and suppression of adaptive immunity. When the macrophages are recruited into the tumor microenvironment, they are exposed to very high levels of inflammatory cytokines. This selectively leads to activation of the M2 subtype of macrophages which are pro-tumor in function.<sup>8</sup>

Dendritic cells, also known as tumor-associated dendritic cells (TADC) are another important component of the tumor microenvironment. They maintain both innate and adaptive immunity by activating antigen specific immunity and maintaining tolerance.<sup>9</sup> Dendritic cells are the first cells to migrate to the tumor site for recognizing the tumor

cells and inducing anti-tumor immunity. There are two forms of dendritic cells present in humans which are dendritic cells 1 and dendritic cells 2. They are myeloid and lymphoid lineage pathways respectively, which differentiate from hematopoietic progenitor cells under the control of complex network of cytokines and chemokines. Dendritic cells 1 originates in the bone marrow as immature dendritic cells.<sup>8</sup> TADC with an immature phenotype are defective in stimulating T cells. The immature TADC are usually present in the tumor mass.<sup>9</sup> They mature once they process foreign antigens which are brought about by inflammatory signals.<sup>8</sup> Mature TADC are present in the peri tumoral area.<sup>9</sup> Cancer cells are active in attracting immature dendritic cells which are accumulated with in the tumor. As a result of this, tumor cells contain an abundant amount of immature dendritic cells, which are unable to exert their function of antigen presenting although they can take up antigens.<sup>8</sup>

### **1.2.2 Humoral components:**

The humoral components of the tumor microenvironment include cytokines and chemokines predominantly. Cytokines are a large group of polypeptides which are secreted by living cells. They regulate cellular functions such as immune cell activity, and proliferation and differentiation of a wide variety of cell types. Interleukins (IL), tumor necrosis factor (TNF) and chemokines are the cytokines which are an integral part of the inflammatory process.<sup>10</sup>

Cytokines produced by leucocytes which affect other leucocytes are termed as interleukins. Interleukins stimulate the proliferation and differentiation of T and B



lymphocytes as well as other cells involved in the immune response.<sup>10</sup> Malignant cells secrete cytokines like interleukin-1 (IL-1) and interleukin-6 (IL-6) which promotes tumor cell growth and resistance to therapy.<sup>3</sup>

One of the major mediators of inflammation is tumor necrosis factor. They perform actions which mediate both tissue destruction as well as recovery. It stimulates fibroblast growth at the site of inflammation and thus, induces cell death of mutated and diseased cells. Anti-tumor activities like destruction of tumor associated blood vessels are performed by TNF at malignant sites. However, when they are chronically produced, they perform pro-tumor functions. This contributes in tissue remodeling and stromal development which is necessary for tumor growth and metastasis. TNF is often detected in breast, ovarian, prostate, colorectal, and bladder cancer.<sup>3</sup>

Besides the cellular and humoral components, a number of other factors are present in the tumor microenvironment with potentiates cancer progression. Reactive oxygen species (ROS) and reactive nitrogen species (RNS) are produced in inflamed tissues. They attack the invading infectious agents and other foreign bodies by oxidation, nitration, and other reactions. Excessive production of these reactive species can cause DNA damage and mutations, and injure the host cells leading to neoplasm.<sup>5</sup> The tumor microenvironment is also made up of extracellular matrix and stromal cells. The stromal cells include fibroblasts and vascular cells. There is a specific stromal fibroblast fraction known as carcinoma-associated fibroblasts (CAFs). CAF has striking tumor-promoting properties. CAFs were found to exhibit increased levels of chemokines which recruits

endothelial progenitor cells (EPCs) into the tumor mass, thus favoring and supporting tumor angiogenesis. *In vivo*, the CAF's can promote tumor progression.<sup>8</sup>

The various components in the tumor microenvironment are recruited to the sites of inflammation by a process known as chemotaxis. Chemotaxis is a phenomenon in which the migrating cell's direction is determined by the concentration gradient of extracellular chemicals. Chemotaxis plays an important role in many diverse physiological processes like recruitment of leucocytes to the sites of infection and trafficking of lymphocytes. A number of molecular components are involved in chemotaxis. For example, leucocyte migration is guided by a set of short peptides known as chemokines.<sup>11</sup>

### **1.3 Chemokines:**

Chemokines are chemo attractant cytokines. They were initially characterized because of their association with inflammatory responses by stimulation of leucocyte chemotaxis during inflammation. These small proteins activate G-protein-coupled receptors (GPCRs) and thereby induce cells to migrate in a concentration gradient. They are a family of small proteins typically defined by four cysteine residues. The first cysteine forms a disulfide bond with the third cysteine residue and the second cysteine residue in the sequence forms a disulfide bond with the fourth cysteine residue. The family of chemokines comprises over 40 members.<sup>12, 13</sup> Typical chemokines can be found easily in genome sequences owing to their relatively small size. Each of them is made up of 70-90 amino acids.<sup>11</sup>

Chemokines are sub-classified into four classes based on the location of the first two cysteine residues in the molecule. Those chemokine which have an intervening amino acid between the first two cysteine residues are termed as CXC or  $\alpha$ -chemokines.<sup>13</sup> There are 17 members in this family of chemokines.<sup>14</sup> The CC chemokines or the  $\beta$ -chemokines are those which have no intervening amino acid. In other words, the first two cysteine residues are adjacent to each other. A few chemokines from this family have six cysteine residues instead of four. All of them are disulfide bonded to each other.<sup>13</sup> 28 members so far have been identified in this family.<sup>14</sup> The third sub-family is the CX3C or the  $\gamma$ -chemokine family. There are three intervening amino acids between the first two cysteine residues. Presently, only one protein has been identified in this family. The CX3C chemokine is unusual because it is a part of a cell surface receptor. The last sub class is the C or  $\gamma$ -chemokine. This class is an exception to the four-cysteine paradigm and has only two cysteine residues.<sup>13</sup> XCL1 and XCL2 are examples of chemokines belonging to this class which lack two out of the four cysteine residues.<sup>14</sup>

Chemokines can also be classified according to their functional properties. Inducible (inflammatory) and constitutive (homeostatic) chemokines are the two classes. Inducible chemokines are induced by inflammatory stimuli. Thus, they control the recruitment of leucocytes into inflamed and injured tissue. Constitutively expressed chemokines perform various housekeeping functions.<sup>8</sup>

The CXC family of chemokines can be further classified based on the existence of glutamate-leucine-arginine (E-L-R) motif which is located upstream from the CXC

sequence. They are classified into ELR+ and ELR- chemokines which stand for ELR positive and ELR negative respectively. This motif is important as the NH<sub>2</sub> terminal of the chemokines is responsible for attracting inflammatory cells. This motif is also necessary for eliciting the angiogenic properties of the chemokines. CXCL1, CXCL2, CXCL3, CXCL5, CXCL6, CXCL7 and CXCL8 are examples for ELR+ chemokines. ELR- chemokines usually have angiostatic and anti-invasive properties. Examples of such chemokines are CXCL4, CXCL4L1, CXCL9, CXCL10, CXCL11 and CXCL14. There is an exception to the class of ELR- chemokines. CXCL12 is an ELR- chemokine which possesses angiogenic properties.<sup>14</sup>

Chemokines can form dimers or other high order structures at chemokine rich sites like the sites of inflammation. Such chemokines have synergism, thus, strongly enhancing leucocyte migration and activation.<sup>8</sup> Due to the similarity between the processes of cancer invasion and metastasis, and entry of leucocytes into inflamed tissue, cancer biologists postulated that tumor cells may use chemokine mediated mechanisms during the process of metastasis.<sup>8</sup> Chemokines exert their functions by interacting with cell surface receptors known as chemokine receptors.

#### **1.4 Chemokine Receptors:**

Chemokine receptors are members of a large super family of cell membrane receptors called G protein coupled receptors. They have seven trans-membrane spanning helices. Chemokines function by activating the chemokine receptors.<sup>15</sup> Twenty chemokine receptors have been identified to date.<sup>12</sup> These receptors are embedded in the cell surface

lipid bilayer. The chemokine receptors have been designated as CXCR1 through 6, CCR1 through 11, XCR1 and CX3CR1. This nomenclature is given to them based on the type of chemokines they bind. CXCR1 through 6, CCR1 through 11, XCR1 and CX3CR1 bind to CXC, CC, C and CX3C chemokines sub family respectively.<sup>13</sup>

All these receptors contain around 350 amino acids each and have a molecular weight of about 40 kDa. Most of the chemokine receptors initiate ligand induced signaling cascades by receptor dimerization.<sup>8</sup> They form homo dimers and occasionally hetero dimers.<sup>12</sup> Unlike other GPCRs, chemokines and their receptors have overlapping specificities for each other.<sup>11</sup> There are multiple ligands for a single receptor and vice-versa. For example, the CXCR2 has 8 different CXC chemokines which can bind to it. In a case where CXCR2 is defective, CXCL8 and CXCL5 still exert their actions via another CXCR receptor, CXCR1.<sup>8</sup> However; receptors interacting with multiple chemokines are capable of doing so with chemokines belonging to the same sub family. Binding of chemokines across sub families is rare.<sup>13</sup>

Infiltrating leucocytes are not the only cells that respond to chemokine gradients. Cancer cells themselves express chemokine receptors and respond to chemokine gradient.<sup>16</sup> Around 23 different types of human cancers express the chemokine receptor CXCR4. However not all cancer cells in the primary tumor express CXCR4. For instance, in ovarian and lung cancer only a small population of cells expresses the CXCR4 receptor. The expression of CXCR4 is low or absent in normal breast and lung cancer cells. Therefore, its expression is characteristic of malignancy.<sup>16</sup>

Organ specific metastasis is governed by interaction between chemokine receptors and chemokine gradients in target organs.<sup>16</sup> This can be explained with an example of a comprehensive survey of chemokines and their receptors in breast cancer patients performed by Muller and co-workers. It was found that the chemokine receptor CXCR4 was expressed more in breast cancer tissue than normal breast tissue. The endogenous ligand CXCL12 was expressed in many organs such as lymph nodes, bone marrow and lungs. These were the organs where breast cancer metastasized.<sup>8</sup>

Over expression of CXCR4 on neoplastic cells assists the cancer cells in adhering to the vascular endothelium in distant tissues. This is one of the first steps in establishing a metastatic niche. Various growth factors such as vascular endothelial growth factor (VEGF), epidermal growth factor (EGF) and inflammatory cytokines such as tumor necrosis factor- $\alpha$  (TNF- $\alpha$ ), interferon- $\gamma$  have also been found to correlate to chemokine receptor expression in cancer.<sup>8</sup>

Chemokine receptors function as allosteric molecular relays. When chemokine binds to the receptor, the tertiary structure of the receptor is modified.<sup>14</sup> This activates the hetero trimeric G proteins. This activation causes activation of a signaling network leading to chemotaxis.<sup>11</sup> It was initially assumed that chemokine receptor function is governed entirely by G<sub>i</sub> –mediated processes. This was further confirmed as it was found that the chemokine functions are blocked in cells pre-treated with pertussis toxin.<sup>17</sup> However, recent evidence suggests that chemokines function through other G protein subtypes as well as non-G-protein mediated pathways.<sup>18</sup>

When the chemokine binds to the extracellular part of the receptor; the receptor is stabilized in a conformation such that the hetero trimeric G-protein is activated (**Figure 1**). G-protein is present in the intracellular part. The G protein has three subunits:  $\alpha$ ,  $\beta$ ,  $\gamma$ . The  $G\alpha$  subunit is tightly associated with the  $\beta$  subunit, which in turn is in tight association with the  $\gamma$  subunit. The  $G\alpha$  subunit interacts with the intracellular loops two and three, as well as the C terminal domain. Intracellular loop two has the important DRY motif which is essential for interaction with the  $G\alpha$  subunit. GDP is bound to  $G\alpha$  in the inactive state of the receptor. When an agonist binds, GDP is replaced by GTP. The  $G\alpha$ -GTP subunit and the  $G\beta\gamma$  subunit dissociate from each other as well as the receptor, and subsequently activate a number of signaling pathways downstream.<sup>18</sup> Adenylyl cyclase is the only effector known to be regulated directly by  $G\alpha$  subunit.<sup>19</sup> The  $\beta\gamma$  subunit causes transient accumulation of phosphatidylinositol-3,4,5-triphosphate (PIP3). This is coupled to the activation of proteins containing PIP3 binding motifs.<sup>12</sup>

If there is continued stimulation of the receptor by the chemokine, receptor desensitization and internalization occurs. This process occurs by phosphorylation of certain residues in the C-terminal domain of the receptor by G-protein receptor kinases (GRK). Receptor phosphorylation stimulates the binding of arrestins which acts as a steric block thus, preventing the further interaction of the receptor. This eventually leads to receptor desensitization and internalization (**Figure 1**).<sup>18,20</sup>

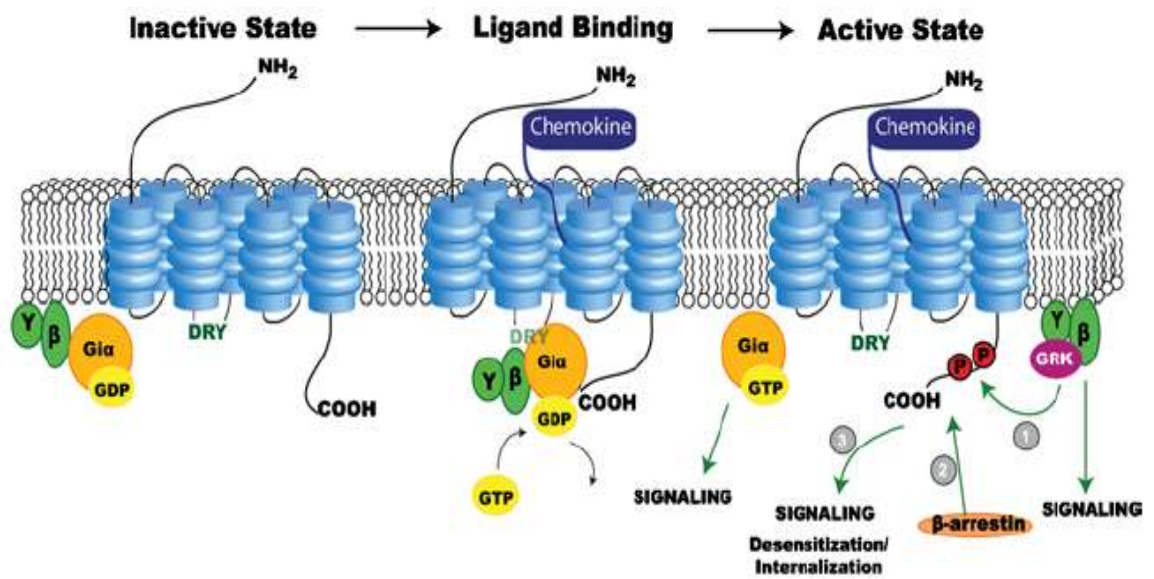


**Figure 1:** Signaling of chemokine receptors upon chemokine binding.<sup>16</sup>



Decoy receptors are types of chemokine receptors that negatively regulate the immune and inflammatory response.<sup>12</sup> DARC, D6 and CCX-CKR are three decoy receptors that have been identified. DARC is expressed by erythrocytes and vascular endothelial cells. This receptor is up regulated during inflammation. It binds pro inflammatory chemokines belonging to the CC and CXC sub class. This receptor lacks the intracellular signaling motifs, and hence, it does not support ligand induced signaling and migration. It neutralizes chemokines at extracellular barriers. Humans who lack the erythroid DARC may contribute to the increased progression and mortality of prostate cancer. Almost all inflammatory CC chemokines binds to the D6 receptor. This receptor undergoes rapid internalization. This leads to degradation of the ligand, however the receptor recycles back. Similar to DARC and D6 receptors, the CCX-CKR receptor lacks signaling motifs.<sup>14</sup>

A chemokine receptor of considerable interest to researchers is the CC chemokine receptor CCR5. CCR5 has been widely studied owing to its implication in various disease states. It has been found that prostate and breast cancer tissues express the CCR5 receptor. CCR5 is also expressed on human CD4<sup>+</sup> T cells and hence, is a critical mediator in the human immune deficiency virus (HIV) entry into the host cell. Thus, due to its diversity, the CCR5 receptor serves as an important therapeutic target.

### **1.5 CCR5:**

The CC chemokine receptor 5 (CCR5) was first identified in 1996.<sup>21</sup> It is a seven trans-membrane, G-protein-coupled receptor. CCR5 has 352 amino acids with a mass of

about 40.6 kDa. It shares 71% sequence identity with CCR2. Most of the differences are located in the extracellular and cytoplasmic domains. It has four cysteine residues in the extracellular domains as well as a conserved DRYLAVHA sequence which is important for interaction with the G protein (**Figure 2**).<sup>22-24</sup> Macrophage inflammatory protein 1 $\alpha$  (MIP-1 $\alpha$ , CCL3), MIP-1 $\beta$  (CCL4) and regulated on activation, normal T cell expressed and secreted (RANTES, CCL5) are the endogenous chemokine agonists that bind to CCR5.<sup>21</sup> Also, monocyte chemo attractant protein 2 (MCP-2, CCL8) and MCP-4 (CCL13) show reasonable activity at CCR5.<sup>25</sup>

CCR5 receptor activation involves two steps. This includes an initial interaction between the chemokine and amino terminal domain of the receptor as well as the adjoining extra cellular loops. This is followed by interaction of the amino terminal with the trans-membrane domain which leads to receptor activation.<sup>22</sup> Like other chemokine receptors, CCR5 binds to inhibitory G<sub>i/o</sub> guanine nucleotide binding protein thus inhibiting 3'-5'-cyclic adenosine monophosphate production (cAMP) by inhibiting adenylyl cyclase. They also stimulate the release of intracellular Ca<sup>2+</sup>. Effects on adenylyl cyclase are mediated via G protein  $\alpha$  subunits whereas effects on Ca<sup>2+</sup> mobilization occur due to signaling mediated by the  $\beta\gamma$  subunit. Treatment with pertussis toxin inhibits [<sup>35</sup>S]GTP $\gamma$ S binding which is stimulated by CCL3, CCL4, CCL5 and CCL8. It can also partially inhibit internalization of the receptor which is induced by the chemokines. These two features indicate that CCR5 function through G<sub>i/o</sub> proteins.<sup>26</sup>

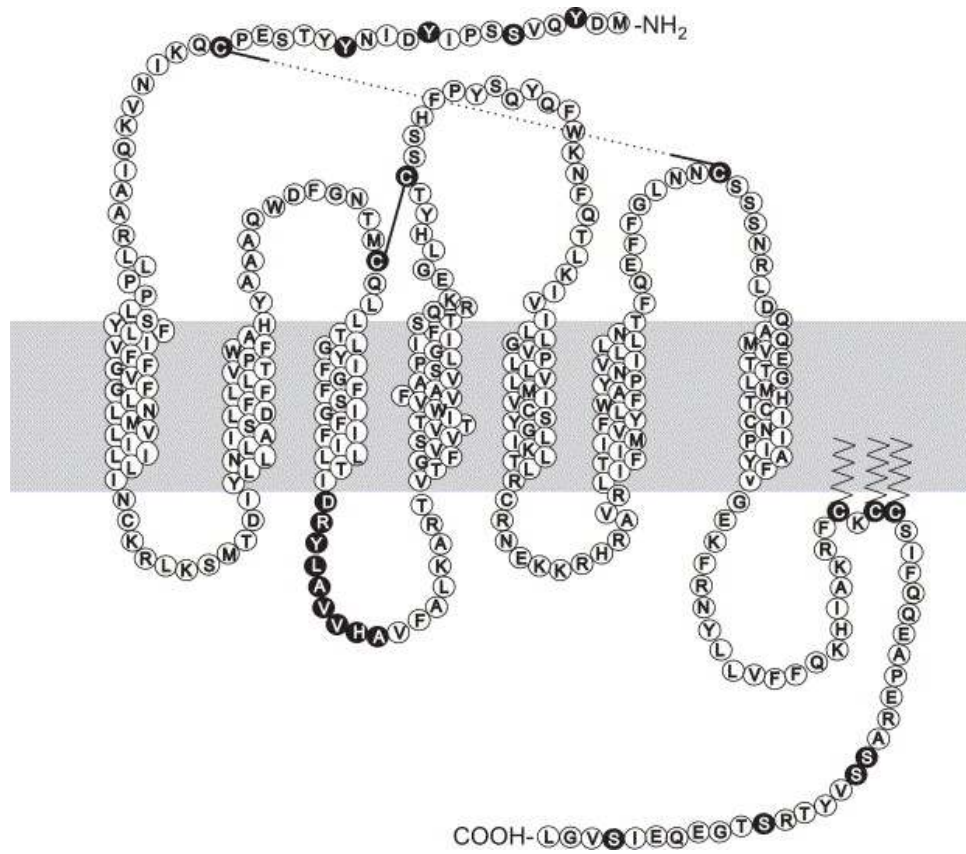


**Figure 2:** Schematic diagram of CCR5 G-protein-coupled receptor.<sup>27</sup>

Phospholipase C (PLC) is activated via CCR5 which results in the production of diacyl glycerol (DAG). This subsequently leads to the activation of protein kinase C (PKC). It mediates receptor regulation by receptor phosphorylation which is carried out by a class of serine threonine protein kinases known as G protein receptor kinases (GRK). This leads to receptor desensitization. The CCR5 ligands mainly activate three main members of the MAP (mitogen activated protein) kinase family. These include ERK1/2 (extracellular signal-regulated kinase), p38 and SAPK/JNK which are critical for T cell proliferation and transcriptional activation of cytokine genes.<sup>27</sup>

The chemokine receptor CCR5 serves as a portal of cellular entry for the human immunodeficiency viruses (HIV-1 and HIV-2). CCR5 and CXCR4 act as co receptors along with CD4 *in vivo* for the attachment and entry of HIV into the host cell.<sup>26, 27</sup> Also, studies have shown that the chemokine CCL5 which is a potent chemotactic factor for inflammatory cells is important in the progression of breast cancer. The chemokine CCL5 and its receptor CCR5 are over expressed in human prostate cancer cell lines.<sup>28</sup> This makes the chemokine receptor CCR5 attractive as a therapeutic target.

## **2. Disease Involvement of CCR5**

The chemokine receptor CCR5 is implicated in various disease conditions. Some of these include Alzheimer's disease, atherosclerosis, and cardiovascular diseases. However, its implication in cancer and acquired immune deficiency syndrome (AIDS) has been extensively studied by researchers. CCR5 receptor and its endogenous ligand CCL5 (RANTES) are over expressed in cancer, specifically prostate and breast cancer. This receptor also serves as the co-receptor for the entry of Human immune deficiency virus (HIV) along with CD4 receptor and hence is involved in the pathogenesis of AIDS. The role and involvement of CCR5 in prostate cancer, breast cancer and AIDS are discussed below.

### **2.1 Prostate Cancer:**

Prostate cancer is an extremely common malignancy of the male genitourinary tract.<sup>15</sup> It is the most frequently diagnosed cancer and the second leading cause of cancer death among the men in the United States and Western Europe. The American Cancer Society estimates 240,890 new cases of prostate cancer and 33,720 deaths due to prostate cancer in 2011.<sup>29</sup> North American men are at a higher risk of acquiring prostate cancer as compared to Asian men. This is due to a typical Western diet rich in saturated fats and little or devoid of fruits and vegetables which is most likely the culprit in the promotion of prostate cancer. Thus, diet and lifestyle are the important risk factors associated with prostate cancer.<sup>30, 31</sup>

It has been widely known and accepted that there is a functional relationship between inflammation and cancer.<sup>3</sup> Prostate cancer precursor lesions often show inflammatory infiltrates in close proximity. This has led scientists to consider inflammation in the etiology of prostate cancer.<sup>32</sup> Several case studies have shown an association between prostate cancer and prostatitis, which is inflammation of the prostate gland.<sup>6</sup> The anatomic position of the prostate gland is such that easy exposure to various infectious agents present in urine and sexual activity can lead to inflammation.<sup>33, 34</sup>

Prostate specific antigen (PSA) is a membrane protein that is found predominantly in the epithelial cells of the prostate gland.<sup>35</sup> This antigen is expressed in low levels in epithelial cells of the normal prostate gland in contrast to its high expression in metastatic, and androgen-insensitive prostate cancer. Thus, PSA is one of the most commonly used biomarker in the diagnosis and treatment of prostate cancer.<sup>36</sup> However, biopsy of the prostate tissue is the only confirmatory diagnostic test for prostate cancer.<sup>15</sup>

Many types of cancer cells including prostate cancer cells express chemokines and their receptors. It has been stated that chemokines and their receptors are involved in the growth and metastasis of prostate cancer.<sup>34</sup> Vaday and co-workers performed a series of experiments to characterize the expression of CCL5 (RANTES) and its receptor CCR5 in prostate cancer cell lines. Four cell lines were used which were PC-3, LNCaP, DU145, and human prostatic adenocarcinoma cells (E-CA-65). MCF-7, which is human breast carcinoma cell line, was used as the positive control. It was seen that CCL5 was expressed

in all these cell lines with DU145 and LNCaP expressing the highest levels (**Figure 3**). PC-3 and E-CA-65 secreted low levels of CCL5.<sup>28</sup>

CCL5 was capable of binding to three receptors; CCR1, CCR3 and CCR5 to exert its action. Anti-bodies were used against each of these three receptors to measure their cell surface expression in prostate cancer cell lines. The receptor CCR5 was expressed on the cell surface of all three prostate cancer cell lines PC-3, DU145 and LNCaP. Also, large amounts of intracellular CCR5 were seen in PC-3 cell lines. On examining the expression of receptors CCR1 and CCR3 in the three prostate cancer cell lines, it was found that large amounts were expressed in the intracellular pools. However, their cell surface expression was lower than the levels of CCR5 (**Table 1**). Thus, it could be concluded that the cell surface expression of CCR5 was greater than that of CCR1 and CCR3 in prostate cancer cell lines.<sup>28</sup>

The effect of CCL5 on the invasion and proliferation of cancer cells was studied. It was seen that CCL5 causes the migration of PC-3 and LNCaP cell lines. TAK-779 which is an antagonist of the receptor CCR5 was used to assess CCL5 induced cell invasion and proliferation. It was noted that TAK-779 was capable of inhibiting CCL5 induced invasion as well as proliferation of PC-3 and LNCaP cells (**Figure 4**).<sup>28</sup> Thus, CCR5 antagonists can be used to prevent the cell proliferation, invasion and metastasis that occurs in prostate cancer.

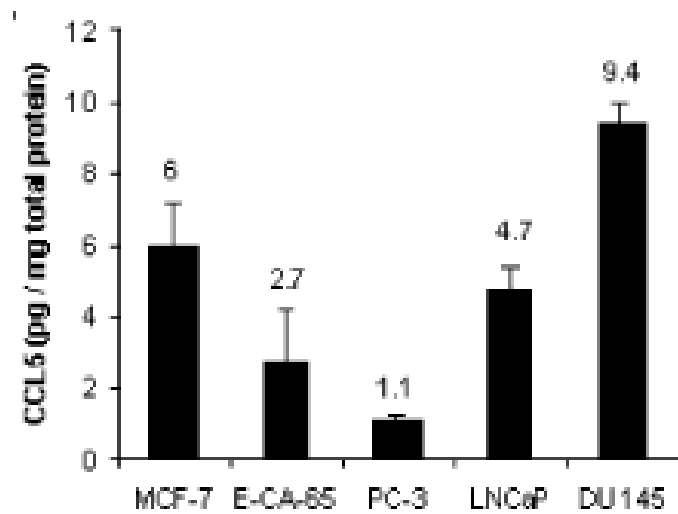


**Figure 3:** Expression of CCL5 mRNA in prostate cancer cell lines

CCL5 (RANTES) expression was analyzed in prostate cancer cell lines PC-3, DU145, LNCaP and primary cultures of prostate adenocarcinoma. The positive control used was MCF-7 breast carcinoma cell line. Serum free conditioned media was collected after 24 hour incubation for CCL5 ELISA experiment.<sup>28</sup>



**Table 1:** Total cell surface and intracellular expression of CCR1, CCR3 and CCR5 in PC-3, LNCaP and DU145 cell lines.

	<b>PC-3</b>	<b>LNCaP</b>	<b>DU 145</b>
<b>CCR1 surface</b>	0	22.6	16.6
<b>CCR1 total cellular</b>	35.2	52.4	50.2
<b>CCR3 surface</b>	6.1	29.5	8.0
<b>CCR3 surface</b>	95.0	88.6	77.8
<b>CCR5 surface</b>	28.8	48.3	38.8
<b>CCR5 total cellular</b>	88.3	89.5	98.6

The data represents the percentage of positive cells in the total cell population. Cells were stained with anti-CCR1, anti-CCR3, and anti-CCR5 antibodies. Their fluorescence was compared with the fluorescence of mouse isotype control cells stained with antibody.<sup>28</sup>

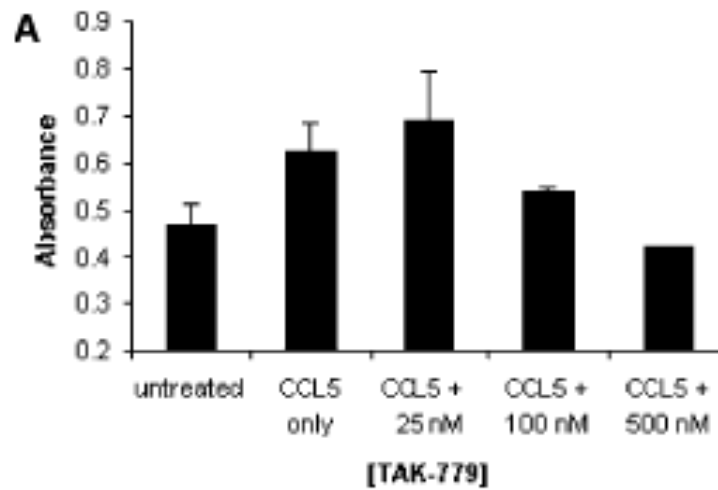


**Figure 4:** Inhibition of CCL5 (RANTES) mediated cell proliferation in DU 145 prostate cancer cell line by CCR5 antagonist TAK-779.

DU 145 cells were exposed to either CCL5 alone in a concentration of 10 ng/ml or both CCL5 (ng/ml) and TAK-779 (10-500 nM). This was incubated for 24 hours followed by the addition of colorimetric reagent WST-1. Absorbance was measured at 450 nM.<sup>28</sup>

### **2.1.1 CCR5 $\Delta$ 32:**

CCR5 $\Delta$ 32 is a non-functional allele resulting from 32-bp deletion in CCR5 gene. This results in non-functional receptor. CCR5 $\Delta$ 32 encodes a truncated protein that is not detected or present on the surface of the cell. This is due to 32 base pair deletion which causes a shift in the reading frame. There is creation of an early stop codon thus leading to the production of a truncated protein. This truncated protein is retained in the endoplasmic reticulum.<sup>37</sup> CCR5 $\Delta$ 32 is common among Centenarians.

Ballitri.C *et al* performed a study to evaluate whether CCR5 $\Delta$ 32 deletion of the CCR5 gene may be associated with susceptibility to prostate cancer. This study consisted of 50 human prostate cancer tissues which were obtained from patients affected by prostate cancer. The DNA samples were genotyped for CCR5 $\Delta$ 32 deletion. The control group consisted of Centenarians. Centenarians have no history of cancer or any other age related disease. This control group had previously been genotyped for CCR5 $\Delta$ 32 deletion. On analyzing the data, it was found that the anti-inflammatory CCR5 $\Delta$ 32 allele was under expressed in prostate cancer patients while CCR5 $\Delta$ 32 deletion was over-expressed in Centenarians. This suggested that CCR5 $\Delta$ 32 deletion is a resistance factor in the development of prostate cancer.<sup>38</sup>

### **2.2 Breast Cancer:**

Carcinoma of the breast is the second leading cause of cancer related death among women in the United States.<sup>39</sup> The American Cancer Society estimates about 232,620 new cases and 39,970 deaths due to breast cancer in 2011.<sup>29</sup> Only modest improvements in

survival rates have been achieved despite advances in the diagnosis and treatment of breast cancer. Thus, there is a continuous search for new insights into the role of various cellular effectors in the progression of this disease.<sup>40</sup>

The tumor microenvironment in breast cancer consists of various inflammatory mediators such as inflammatory cells, cytokines and chemokines.<sup>41</sup> The chemokines are capable of promoting tumor growth. They also play a prominent role in tumor cell migration which could lead to increased invasive and metastatic propensity.<sup>39</sup> However; several chemokines are expressed by normal breast tissue even though they are expressed at low levels. For example, the chemokines CXCL1, 2, 3, 4, 5, 6, 7 and 8 have been detected in human milk. The normal breast tissue also secretes other cytokines like IL-6 and TNF- $\alpha$ .<sup>14</sup>

In breast cancer tissue, the chemokines CXCL12, CCL2, and CCL5 have been detected at high levels. These chemokines are expressed minimally by normal breast epithelial cells. This indicates that these chemokines are acquired in the course of transformation to malignancy. They are critical mediators and play an important role in the progression of the tumor.<sup>42</sup> Along with chemokines; their receptors are also over expressed. The receptor CXCR4 is up regulated in breast cancer compared to normal breast tissue. Also, its ligand CXCL12 shows peak mRNA level expression in the metastatic sites of breast cancer.<sup>14</sup>

Youngs *et al.* performed a study to monitor the chemotactic response of MCF-7 breast cancer cell lines to  $\alpha$  and  $\beta$  chemokines. The MCF-7 cell line was obtained from a

pleural effusion of a 69 year old female with metastatic mammary carcinoma. It was noted that MCF-7 cells migrated in the presence of both  $\alpha$  and  $\beta$  chemokines. However, the  $\beta$  chemokines elicited a greater chemotactic response. MIP-1 $\alpha$  induced significant migration of MCF-7 cells in 5 out of 6 experiments. Similarly MIP-1 $\beta$  and RANTES (CCL5) induced migration in 5 out of 6 and 6 out of 6 experiments respectively.<sup>39</sup>

RANTES (CCL5) expression is rarely observed in those patients with benign breast disorders. Advanced breast carcinoma patients over-express RANTES. In such patients, only the malignant epithelial cells expressed RANTES. Non-malignant benign lumps and mammary ducts that were in close proximity to the malignant epithelial cells rarely expressed RANTES. On evaluation of the RANTES expression in different pathological stages of breast cancer, it was found that higher expression was seen in patients with disease in stages II and III. About 83% patients in stage II and 83.3% patients in stage III expressed RANTES. On the other hand, only 55% patients who were in stage I of the disease were positive for RANTES expression.<sup>43</sup> This indicated that RANTES was expressed more in the advanced and later stages of breast cancer than the initial stages.

Robinson *et al.* performed a study to obtain evidence if the action of an antagonist for the CCR5 receptor would inhibit the tumor promoting role of the chemokine CCL5 (RANTES). Met-CCL5 was used as the antagonist.<sup>44</sup> *Escherichia Coli* expressed RANTES in which the protein retains the initiating methionine residue. This was known as Met-CCL5. The retention of the initiating methionine residue renders it inactive as an

agonist despite being correctly folded. However, it shows antagonistic activity. It is capable of antagonizing the effects induced both by RANTES and MIP-1 $\alpha$ .<sup>45</sup>

The activity of Met-CCL5 was tested against 410.4 tumor cells. The mice were injected with an intra-peritoneal injection of Met-CCL5 daily. The volume of the tumor was measured at regular intervals. The tumors were excised and weighed after five weeks of growth. The tumor weights were significantly lower which showed that Met-CCL5 did slow down tumor growth. There was also a substantial decrease in the proportion of macrophages in those tumors which were treated with Met-CCL5.<sup>44</sup> Thus, CCR5 antagonists can be used to decrease the progression of breast cancer as well as significantly lower the leukocyte population within the tumor.

### **2.3 HIV/AIDS:**

The retro virus, human immune deficiency virus-1 (HIV-1), causes the disease acquired immuno deficiency syndrome (AIDS). Almost 30 years ago, in 1981, AIDS was first identified in the United States of America. About 2.7 million people are infected with HIV each year and around 33 million people are living with AIDS. Women comprise about 50% of the population living with AIDS. This is mainly because women have limited or no freedom to insist condom use, or choose sexual situations in developing countries.<sup>34</sup>

A number of anti-retroviral agents are available. Highly active anti-retroviral therapy (HAART) is an extremely powerful treatment for AIDS which was introduced in the early 90s. This is defined as three or more drugs concomitantly administered to

achieve suppression of the virus.<sup>46, 47</sup> Recent studies have shown that 90% of the patients respond well to HAART and survive for at least five years if the treatment is initiated early. The different classes of anti-retroviral agents which are used in HAART include the reverse transcriptase inhibitors, the protease inhibitors and the integrase inhibitors which target the viral proteins.<sup>48</sup>

The chemokine receptor CCR5 was identified about a decade ago as one of the major co-receptor that was used by HIV to gain entry into cells.<sup>49</sup> The viral envelope contains two glycoproteins, gp120 and gp41. The main receptor protein is CD4 and a co-receptor which is a chemokine receptor. This co-receptor is typically either CCR5 or CXCR4. The HIV-1 strains are classified into three major groups based on the co-receptor which they use for entering into the host cell. They could either be R5 (CCR5-tropic), X4 (CXCR4-tropic) and R5/X4 (they are able to use either CCR5 or CXCR4).<sup>50</sup>

A number of steps are involved in the entry of HIV into the host cell which is shown in **Figure 5**. Complex interaction between the glycoproteins present in the viral envelope and the host cell surface receptors (CD4 and CCR5 or CXCR4) is the initial step. This involves binding of the glycoprotein gp120 to the host cell surface receptor CD4. This brings about a conformational change in the viral gp120 thus creating or exposing a binding site for the chemokine receptor. Once gp120 binds to the chemokine receptor, another conformational change is induced which allows the viral glycoprotein gp41 to initiate fusion. The gp41 glycoprotein contains two alpha-helices that form a hairpin configuration. A hydrophobic fusion peptide is inserted into the cell membrane of the host.

This leads to spanning of gp41 between the virus and host cell membrane. The helices of gp120 then folds into a six helix bundle. This brings the N terminal and the C terminal close eventually bringing the viral and cell membranes close. This proximity leads to contact between them thus allowing mixing.<sup>50, 51</sup>



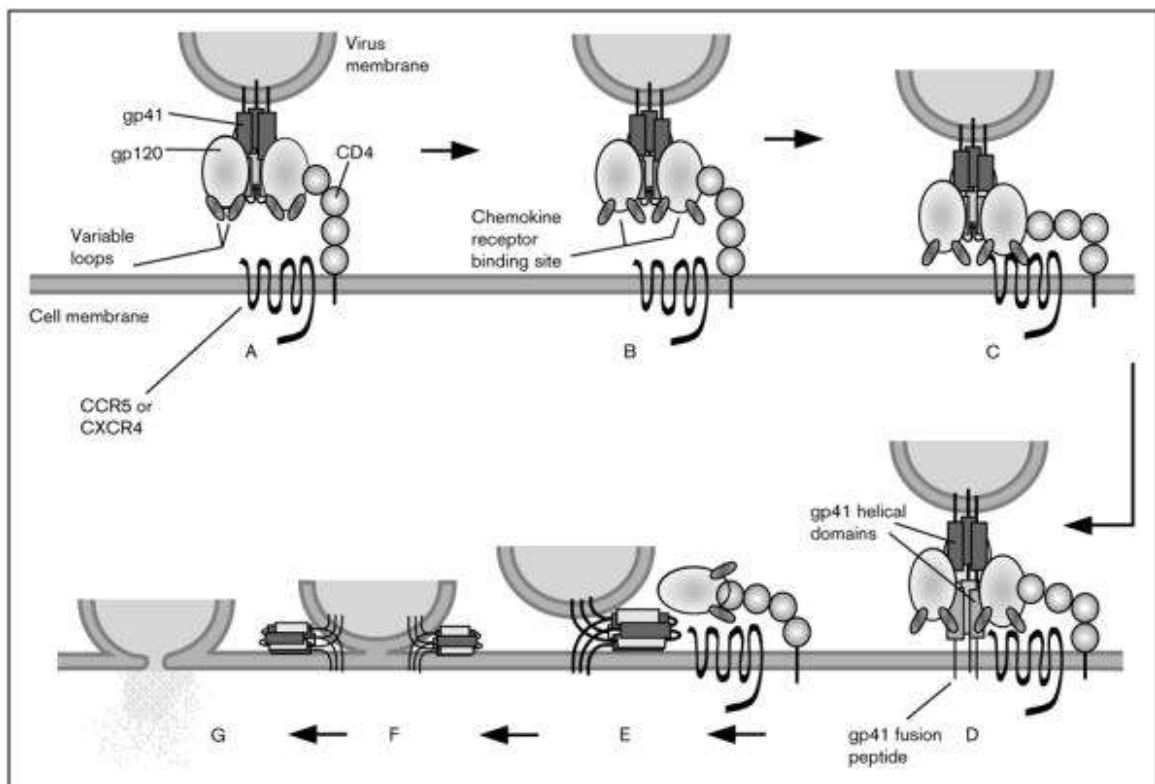


**Figure 5:** Steps involved in the entry of HIV into the host cell via the CD4 and CCR5/CXCR4 receptors.

The CC chemokines RANTES, MIP-1 $\alpha$ , and MIP-1 $\beta$  suppress infection caused by R5 tropic HIV. It was demonstrated that these chemokines sterically block the site where the viral envelope interacts with the receptor. This is the proposed mechanism of inhibition which leads to receptor down modulation. SDF-1, which is the endogenous ligand for the receptor CXCR4, leads to down regulation of CXCR4 thereby blocking infection caused by X4 tropic HIV. This ability of chemokines to inhibit HIV-1 infection made these molecules attractive targets for the development of anti-HIV therapeutic agents.<sup>46, 52</sup>

CCR5 antagonists can thus be successfully used as anti-retroviral drugs in therapeutics. Maraviroc was the first and only CCR5 antagonist approved for use in both treatment-experienced and treatment naïve patients.<sup>37</sup> CCR5 antagonists are allosteric and non-competitive inhibitors of the receptor. They bind to the receptor thus inhibiting the interaction between gp120 and the co-receptor.<sup>53</sup> However, there is a limitation in treating AIDS patients with CCR5 antagonists. It would be ineffective in patients where HIV uses CXCR4 as the co-receptor.<sup>37</sup> On the other hand, only advanced stages of the disease use CXCR4 as the co-receptor. HIV-1 strains use CCR5 as the co-receptor in the early stages of the disease. Thus, CCR5 antagonists can prevent the progression of AIDS.<sup>37</sup>

A naturally occurring 32-bp deletion in the human CCR5 gene is known as CCR5 $\Delta$ 32. Individuals who carry two alleles of this CCR5 $\Delta$ 32 mutation (CCR5 $^{-/-}$ ) are those who are highly protected against infection by HIV-1. Those who are heterozygous for this mutant allele (CCR5 $^{+/-}$ ) are not protected against infection. However, such

individuals have a delayed progression of the disease. This indicates that a partial resistance can occur if there is a single copy of CCR5 $\Delta$ 32. In very rare cases, people homozygous for CCR5 $\Delta$ 32 allele showed HIV infection. The mechanism of infection in such cases has not been identified. Exclusive use of CXCR4 by the virus could probably be the reason.<sup>50, 54</sup>

Thus, the CC chemokine receptor CCR5 has been implicated in the progression of various human cancers like the prostate and breast cancer. It is also an important co-receptor which mediates the entry of the HIV virus into the host cell. Therefore, CCR5 antagonists could prevent the entry of the HIV into the host cell by blocking the receptor. These antagonists can also be used as anti-proliferative agents in prostate and breast cancer. Detailed study of the CCR5 antagonists previously synthesized will help in better understanding of the CCR5 as a therapeutic target.

### 3. CCR5 Antagonists

Highly active anti-retroviral therapy (HAART) has significantly affected the treatment and epidemiology of HIV-1 infection. Since 1989, HAART has successfully contributed in saving around 3 million years of life in the United States. However, the rate of resistance in patients infected with HIV-1 has drastically increased.<sup>69</sup> A new and attractive strategy for treating HIV-1 infection is inhibition of viral entry into the host cell. Since the chemokine receptor CCR5 serves as a co-receptor for the entry of the virus into the host cell, targeting this receptor could serve as a new therapeutic approach in treating AIDS. Thus, identifying CCR5 receptor antagonists, which inhibits the binding and entry of HIV-1 into the host cell, would serve as a novel approach in the treatment of AIDS.<sup>70</sup>

The CCR5 receptor is also implicated in cancer, specifically prostate and breast cancer with an inflammation etiology. The endogenous ligand CCL5 (RANTES) and CCR5 are over expressed in prostate and breast cancer. This may lead to proliferation, invasion and metastasis of tumor cells.<sup>43, 71</sup> CCR5 receptor antagonists which can inhibit the binding of the endogenous ligand to the receptor may inhibit the proliferation and growth of tumor cells. Thus, the chemokine receptor CCR5 has been of interest to researchers due to its implication in various disease states. CCR5 antagonists would thus serve as a novel therapeutic approach in the treatment of several disease conditions.<sup>43</sup>

A number of pharmaceutical companies conducted high throughput screenings of their in-house compounds in search of small molecule CCR5 antagonists. Compound **1** was obtained as the initial lead from high throughput screening. This quaternary ammonium salt was optimized chemically which led to the discovery of TAK-779 (**2**).<sup>56</sup>

TAK-779 (**2**) was the first small molecule CCR5 antagonist that was reported in 1999 by Takeda chemicals, Japan (**Figure 6**).<sup>55</sup>

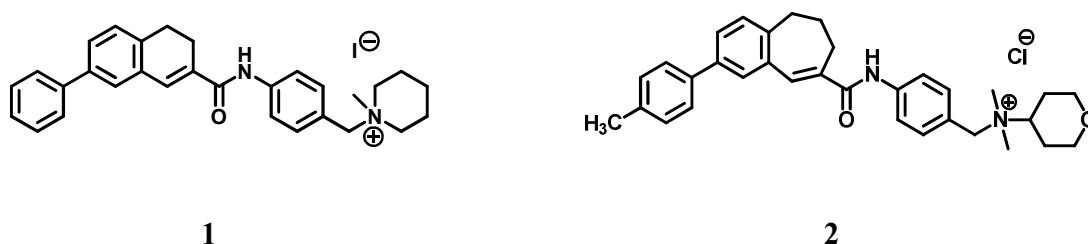


**Figure 6:** Initial lead (**1**) and TAK-779 (**2**)

Radiolabelled ligand, [<sup>125</sup>I]-RANTES, binds to CHO-CCR5 cell (Chinese hamster ovary cell expressing CCR5) with a high affinity ( $K_d = 0.45$  nM). TAK-779 was able to inhibit the binding of [<sup>125</sup>I]-RANTES to CCR5 expressing CHO cells with an  $IC_{50}$  of 1.4 nM. TAK-779 was a selective antagonist for the CCR5 receptor as it did not inhibit the binding of ligand to other chemokines receptors expressed by CHO cells namely, CCR1, CCR3, and CCR4. However, this potent and selective CCR5 antagonist was not developed further due to poor oral bioavailability and toxicity at the site of injection.<sup>56, 58</sup>

Due to its drawbacks, the structure of TAK-779 was further modified. This included replacement of the quaternary ammonium moiety with a sulfoxide group, ring expansion to (6,8) fused nuclei, and replacement of the methyl group with 4-(2-butoxyethoxy) group. This resulted in TAK-652 (**3**) which had increased potency and bioavailability (**Figure 7**).<sup>59</sup> It inhibited the binding of [<sup>125</sup>I]-RANTES to CCR5 expressing CHO cells with an  $IC_{50}$  of 3.1 nM. TAK-652 was also active against R5 HIV-1 strains with an  $EC_{50}$  of 0.061 nM and  $EC_{90}$  of 0.25 nM. A single dose Phase I study for

TAK-652 has been completed.<sup>57</sup> Administration of this drug up to 100 mg once a day was safe and well tolerated in humans. However, the clinical efficacy of TAK-652 in HIV-1 infected individuals and further clinical data are awaited. It is currently being studied in Phase II clinical trials.<sup>72</sup>

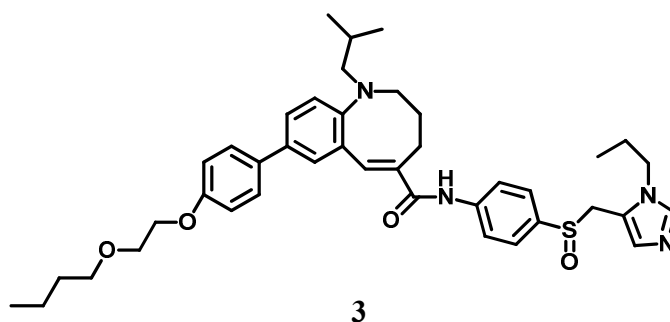


**Figure 7:** TAK-652

Ono pharmaceuticals in collaboration with GlaxoSmithKline developed spirodiketopiperazine derivatives as CCR5 antagonists. ONO-4128/Aplaviroc (**4**), a highly potent CCR5 antagonist was developed by Ono pharmaceuticals (**Figure 8**). This antagonist inhibited the replication of R5 viruses with an  $IC_{50}$  of 30-60 nM. Aplaviroc was selective for R5 tropic strains of HIV-1; it did not inhibit the X4 tropic strains of HIV-1.<sup>73</sup>

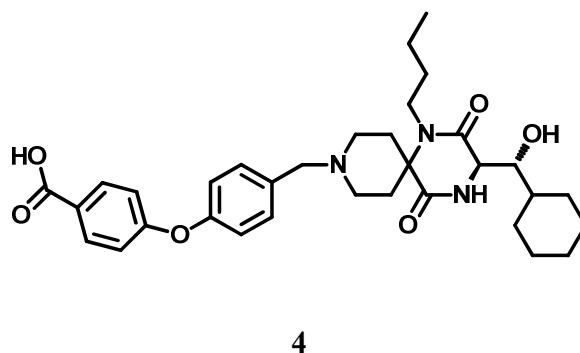


**Figure 8:** Aplaviroc/ONO-4128

In early clinical studies, a dose of 600 mg of Aplaviroc twice a day for ten days was well tolerated and demonstrated reduction in viral load. However, three subjects developed hepatotoxicity in Phase II-b clinical trial. Also, in phase III clinical trial, one patient in a group of 44 patients developed idiosyncratic hepatotoxicity. Thus, the clinical studies of Aplaviroc were discontinued.<sup>72</sup>

Schering-Plough developed two series of CCR5 antagonists: piperidino–piperidine and piperazino-piperidine. The initial lead (**4**) for the piperidino-piperidine series had moderate affinity for both the CCR5 ( $K_i = 64$  nM) and M2 muscarinic receptor ( $K_i = 230$  nM). Medicinal chemistry optimization of compound **4** afforded compound **5**; which had a  $K_i$  of 66 nM for the CCR5 receptor and  $K_i$  of 1323 nM for the M2 muscarinic receptor (**Figure 9**).<sup>58, 61, 62</sup>

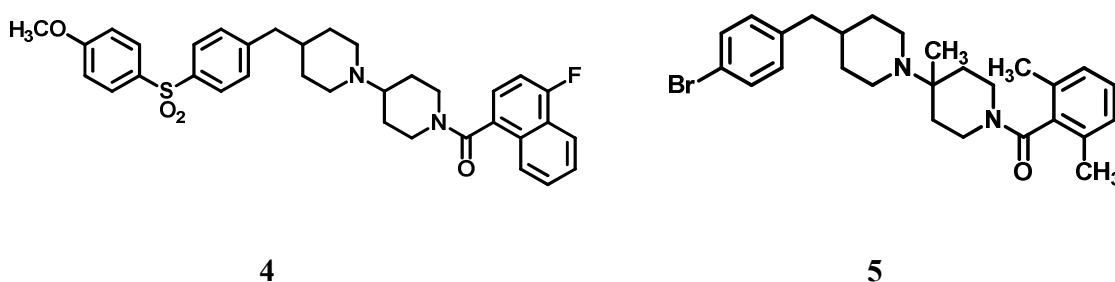


**Figure 9:** Initial leads developed by Schering-Plough.

SCH-C/SCH351125 (**6**) was Schering-Plough's first clinical candidate (**Figure 10**). This antagonist was developed by making certain structural changes to compound **5**.

These included addition of an oxime at the benzylic position and replacement of 2,6-dimethylbenzamide with 2,6-dimethylnicotinamide *N*-oxide. SCH-C demonstrated excellent anti-viral properties with an  $IC_{50}$  of 3 to 78 nM against R5 tropic HIV-1 isolates.<sup>61, 62</sup> In clinical efficacy studies, a dose of 25 mg twice daily demonstrated a significant drop in viral load in ten out of twelve subjects. However, at the highest dose tested (400 mg), cardiac side effects were noted. Thus, further clinical efficacy studies of SCH-C were not conducted.<sup>60, 74</sup>

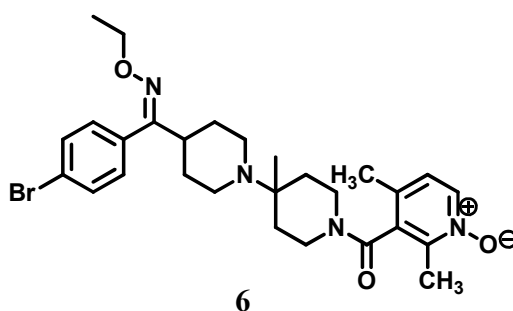


**Figure 10:** SCH-C / SCH351125

Compound **7** (**Figure 11**), a potent antagonist for the M2 muscarinic receptor ( $K_i = 0.8$  nM), was the initial lead obtained in the piperazino-piperidine series of Schering-Plough CCR5 antagonists. This compound had only moderate affinity for the CCR5 receptor with a  $K_i$  of 440 nM. In an effort to improve affinity for the CCR5 receptor and reduce the affinity for the M2 muscarinic receptor, structural modifications were made to compound **7**. Truncation of the left side and leaving a small para substituent on the phenyl ring afforded compound **8**, which had high affinity for the CCR5 receptor ( $K_i = 20$  nM)



and reduced affinity for M2 muscarinic receptor. However, the major drawback of **8** was poor oral bioavailability in rat and hence, could not be developed further (**Figure 11**).<sup>58,74</sup>

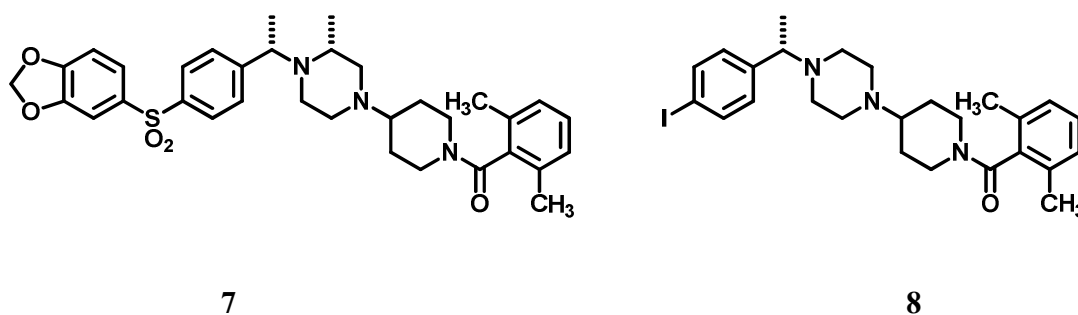


**Figure 11:** Initial leads in piperazino-piperidine series of Schering-Plough CCR5 antagonists.

SCH-D/Vicriviroc/SCH-417690 (**9**) developed later by Schering-Plough, was a potent CCR5 antagonist ( $K_i = 1.6$  nM) (**Figure 12**). This compound was 2 to 40 times more potent than SCH-C against R5 HIV-1 isolates. Vicriviroc also demonstrated good oral bioavailability in preclinical studies. In clinical studies, vicriviroc was well tolerated at a dose of 50 mg twice daily.<sup>59,60</sup> However, the Phase II clinical studies of vicriviroc were discontinued because there was a viral breakthrough in the group receiving this drug compared to the control group. This indicated that vicriviroc was not effective for use in treatment naïve patients. Phase II studies were then carried out in treatment-experienced patients. The results of this showed that vicriviroc exhibited strong antiviral activity, however five participants had an incidence of malignancy. Despite this, the study was continued as there was no causal association of the malignancy and vicriviroc. Phase III clinical trials were initiated in treatment experienced patients in late 2009.<sup>61,62,72</sup> In 2010

Merck halted the phase III clinical studies of Vicriviroc in treatment-experienced patients due to no significant superior efficacy.<sup>84</sup>

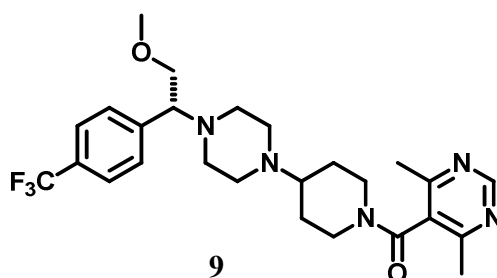


**Figure 12:** SCH-D/ Vicriviroc/ SCH-417690

Acyclic and cyclic scaffold based CCR5 antagonists were developed by researchers at Merck. The initial lead (**10**) had an *N*-methylbutane amine core with a spirocyclic piperidine moiety at the 4<sup>th</sup> position and a (*S*)-phenyl moiety at the second position. This compound had moderate affinity for the CCR5 receptor ( $IC_{50} = 40$  nM). However, it demonstrated very weak anti-viral activity and hence, compound **10** was further modified to afford compound **11** (**Figure 13**).<sup>58, 75, 76</sup>

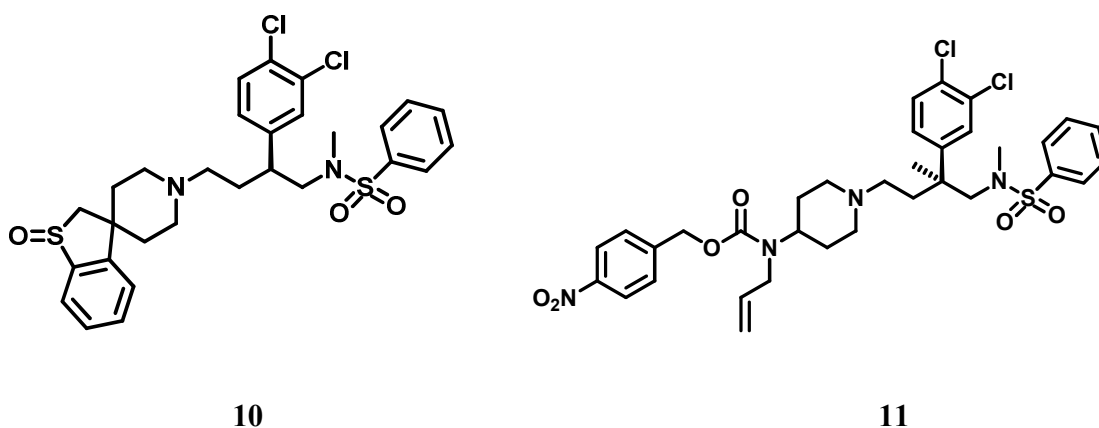


**Figure 13:** Initial leads for Merck CCR5 antagonists.

Compound **11** was an extremely potent CCR5 antagonist with an  $IC_{50}$  of 0.1 nM with good oral bioavailability in rats. The active conformation of this compound was locked in place with a 1,3,4-trisubstituted pyrrolidine to create a cyclic scaffold leading to compound **12** which was an even more potent CCR5 antagonist with an  $IC_{50}$  of 0.8 nM. The pyrrolidine scaffold in compound **12** gave rise to the cyclopentane template in compound **13**, which was a potent CCR5 antagonist ( $IC_{50} = 1.1$  nM). It demonstrated good anti-viral activity with an  $IC_{95}$  less than 8 nM (**Figure 14**). However, these CCR5 antagonists were not pursued further and did not enter clinical efficacy studies.<sup>58, 75, 76, 77</sup>

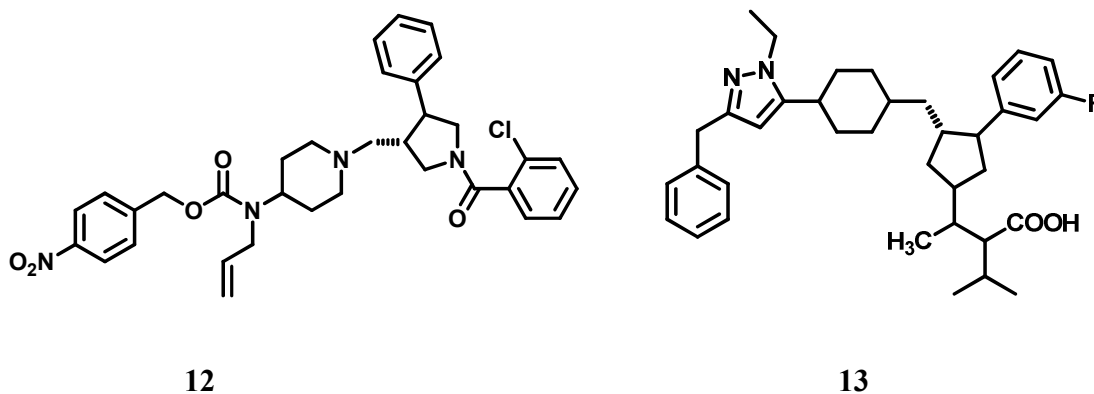


**Figure 14:** Cyclic CCR5 antagonists developed by Merck.

Researchers at Pfizer developed piperidine-based CCR5 antagonists. The initial hit (**14**) identified from high throughput screening had good affinity for the CCR5 receptor ( $IC_{50} = 4$  nM) despite the lack of anti-viral activity. Thus, the structure of **14** was modified

in an effort to improve the anti-viral activity. This led to tropane derived amide analogue (**15**) which showed excellent anti-viral activity ( $IC_{90} = 0.6 \text{ nM}$ ). However, due to unfavorable pharmacokinetic properties, **15** was subjected to further structural modifications (**Figure 15**).<sup>58, 59</sup>

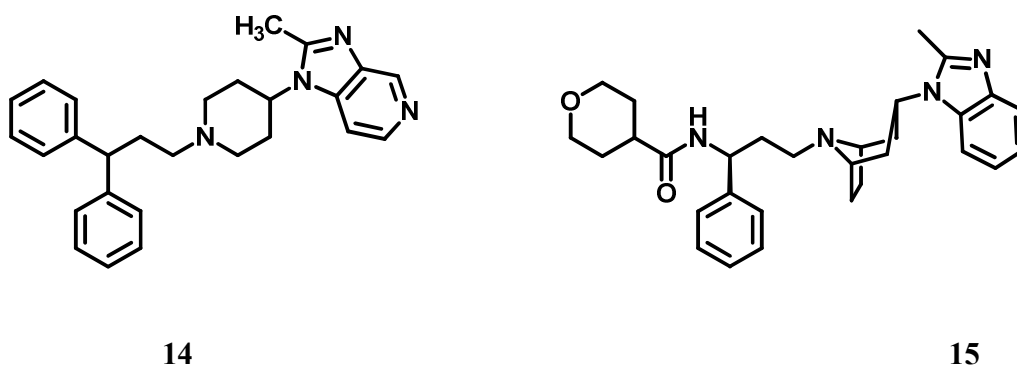


**Figure 15:** Initial leads for CCR5 antagonists developed by Pfizer.

Structural modifications of **15** were made to afford compound **16**. This compound demonstrated good anti-viral potency with an  $IC_{90}$  of 8 nM. A major drawback associated with this compound was cardiovascular side effects. It did not provide the desirable safety window and hence, could not be developed further. The cyclobutane moiety of compound **16** was replaced with a 4-substituted cyclohexane moiety. The compound **17** exhibited excellent anti-viral properties with an  $IC_{90}$  of 1 nM (**Figure 16**).<sup>57, 58</sup>

The CCR5 antagonist (**17**) known as Maraviroc or UK-427,857, was capable of producing a reduction in the viral load on administering a dose of 25 mg once a day. This CCR5 antagonist was very well tolerated. The US Food and Drug administration advisory

panel approved the new drug on 24<sup>th</sup> April, 2007. On August 6, 2007 maraviroc received full FDA approval for use in treatment experienced patients.<sup>84</sup>

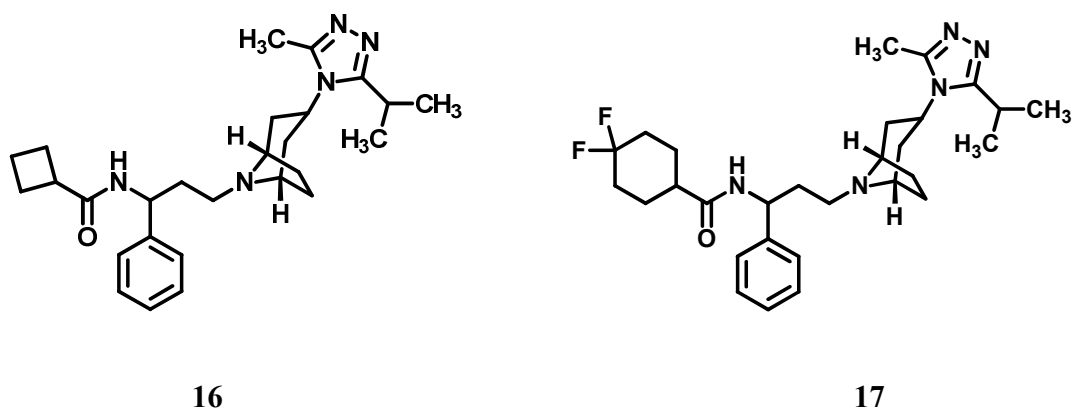


**Figure 16:** Pfizer CCR5 antagonists

#### **4. Project Objectives and Design**

The chemokine receptor CCR5 is involved in the progression and development of a number of disease states like cancer and AIDS. Thus, targeting this receptor serves as a therapeutic approach. Since both CCL5 and CCR5 are over-expressed in cancer cells and tissues specifically prostate and breast cancer, CCR5 antagonists may prevent cancer progression and metastasis. Also, due to the involvement of CCR5 as a co-receptor in the entry of HIV into the host cell, blocking this receptor with CCR5 antagonists may block the entry of the virus into host cell, thus preventing infection.

A number of pharmaceutical companies have developed CCR5 antagonists by conducting high throughput screenings. Barring Maraviroc, the remaining antagonists could not pass the clinical trial studies. Long-term toxicity and adverse events were the shortcomings of the CCR5 antagonists reported so far which necessitates the need for new drugs. Also, most of these antagonists interact with the transmembrane (TM) domains of the receptor. However, the extracellular loop 2 (EL-2) part of CCR5 interacts with gp120 for the virus to enter into the host cell.

Based on these observations, the primary objective of this project was to synthesize small molecule CCR5 antagonists with structural features to interact with EL2 of CCR5. A novel approach, molecular based drug design, was used by our lab to design and develop CCR5 antagonists. These CCR5 antagonists would serve as novel anti-cancer agents and entry inhibitors in HIV therapeutics.

The background work, including molecular modeling studies, and the project design are discussed herein.

#### 4.1 Background Work:

Like most of the GPCRs, the crystal structure of CCR5 receptor has not been resolved. Thus, a homology model of the receptor was built based on the X-ray crystal structure of bovine rhodopsin.<sup>77</sup> In order to characterize the binding site of the CCR5 antagonists, the lowest energy conformation of known CCR5 antagonists e.g. SCH-C, SCH-D, and TAK-779 (**Figure 17**) were superimposed. When this background work was done, Maraviroc, Aplaviroc, and other CCR5 antagonists had not been reported then. Therefore, they were not analyzed along with SCH-C, Vicriviroc, and TAK-779.

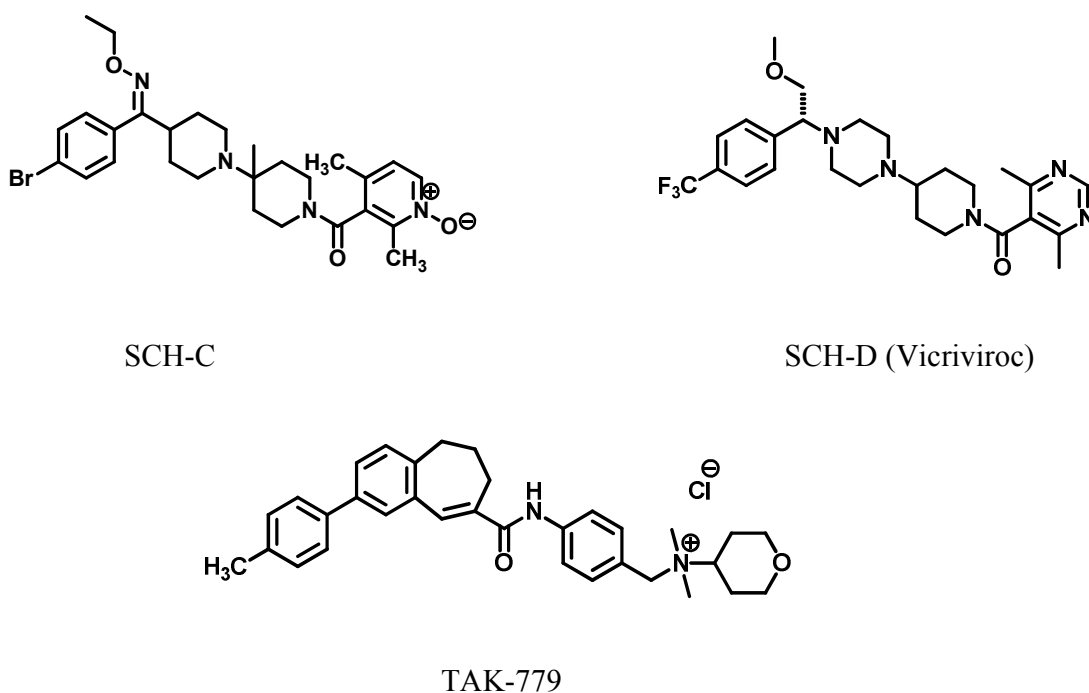


**Figure 17:** CCR5 antagonists

By superimposing their lowest energy conformations, a molecular scaffold (**Figure 18**) was built. According to the molecular scaffold that was constructed, a secondary or tertiary amine moiety was present at a distance of 5-7 Å from an amide group. The secondary or tertiary amine was linked to a hydrophobic moiety (with or without a polar group attached) at a distance of 4.5-6 Å. An aromatic moiety was attached to the amide group at a distance of 3.5-5.5 Å. This entire molecular scaffold was in a bent form.

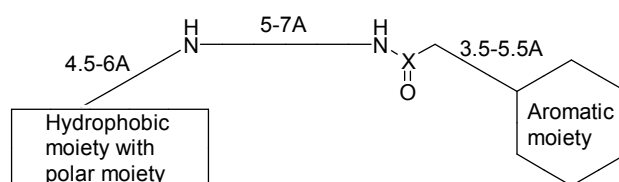


**Figure 18:** Molecular scaffold.

To determine the interactions of this scaffold with the key amino acid residues of the receptor, the CCR5 antagonist SCH-D was docked into the receptor (**Figure 19**) with emphasis on evaluating the binding pocket interactions. The central amino group of the molecule formed a putative salt bridge with Glu283 on TM7. A lipophilic pocket which was formed by Ile 110, Leu107 which were a part of TM3, Tyr251 (TM6), and His289 (TM7) served as the binding site for the hydrophobic moiety in the scaffold. The aromatic moiety in the molecular scaffold was located in an aromatic binding cavity formed by Phe112 (TM3), and Tyr244 and Trp248 which were a part of TM6.



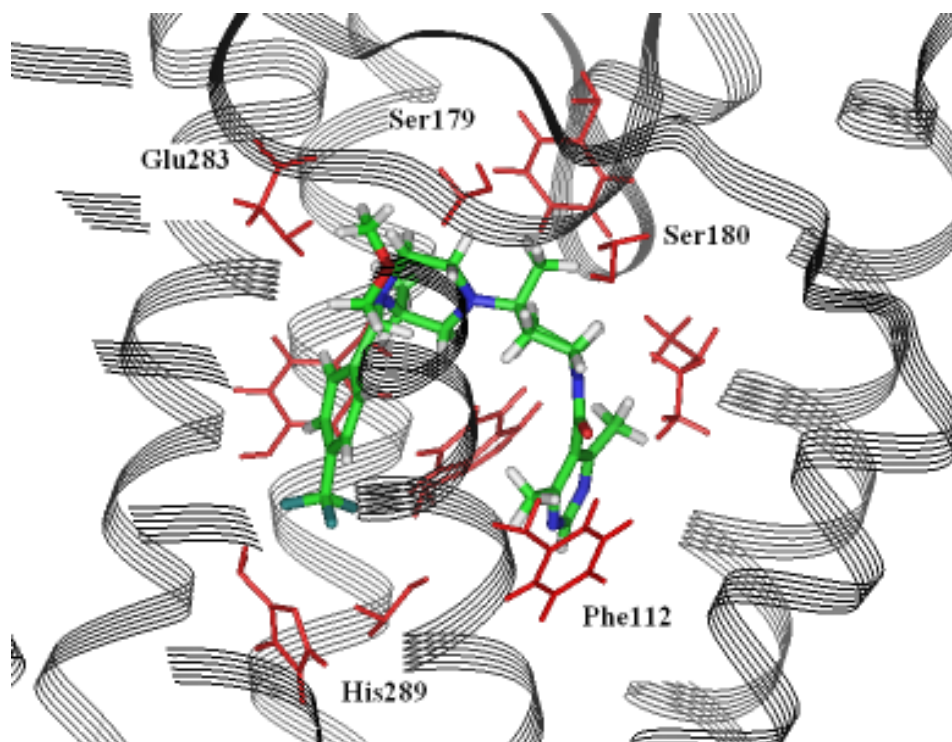


**Figure 19:** SCH-D docked into CCR5 receptor.

Through the study of the binding interface of CCR5 receptor and SCH-D, it was observed that the interface between extracellular loop 2 (EL2) and spacer of the ligand which includes the hydrophobic moiety (Phe182) and a hydrophilic area (Ser179, Ser180) was not fully satisfied by SCH-D, nor by other known CCR5 ligands reported by that point of time. Since extracellular loop 2 is very important for the binding of gp120 of HIV-1, novel ligands with a potential to interact with extracellular loop 2 were designed.

The molecular scaffold was further elaborated to afford a novel skeleton (**Figure 20**) based on the interaction of the important structural features of SCH-D with the amino acid residues in the binding pocket of the receptor. This new skeleton satisfied all the structural aspects necessary for interaction with the receptor.

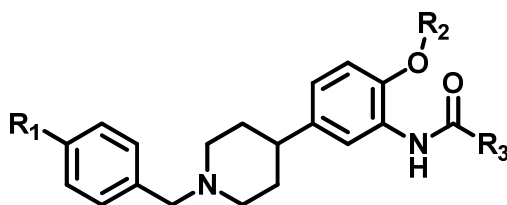


**Figure 20:** Novel skeleton

The amino and amide moieties were connected by means of a trisubstituted phenyl ring. A hydrogen bond accepting group was introduced at R<sub>2</sub> position. An aromatic moiety was introduced at R<sub>3</sub>. These structural features would satisfy the binding pocket requirements of extracellular loop 2. To verify the molecular design, a model compound (**Figure 21**) was formulated and docked into the binding cavity of the receptor (**Figure 22**).

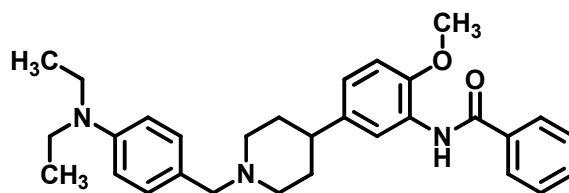


**Figure 21:** Model Compound

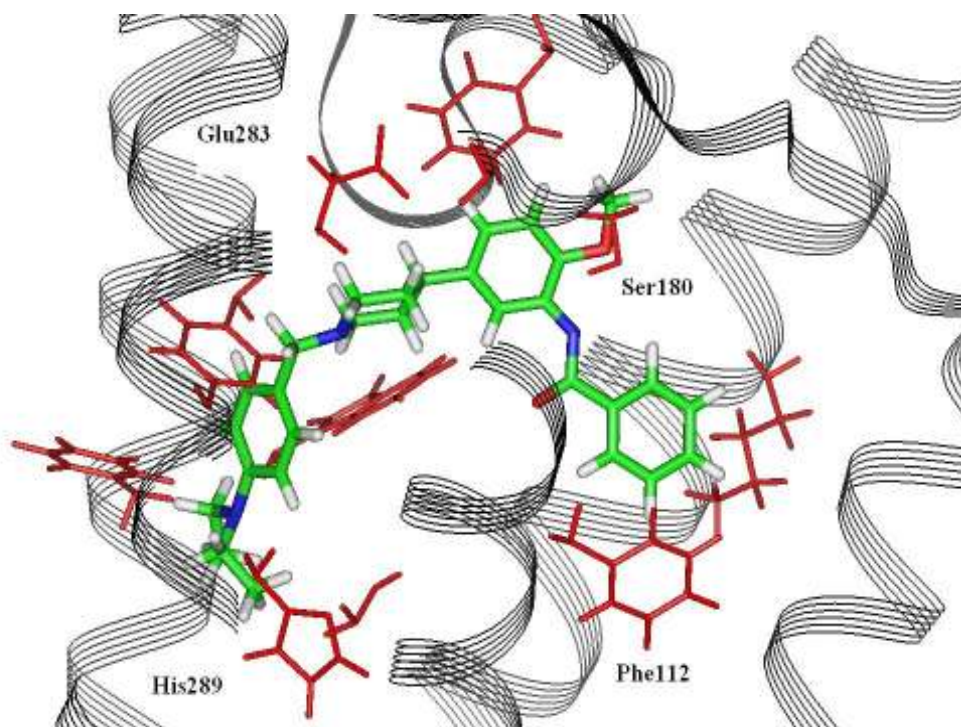



**Figure 22:** Model compound docked into binding pocket of CCR5.

As shown in the above **Figure 22**, the model compound satisfies the requirements of the binding pocket of CCR5. **Table 2** summarizes the possible substituents that could be

introduced at R<sub>1</sub>, R<sub>2</sub> and R<sub>3</sub>. The first round of chemical synthesis included the syntheses of 24 compounds.

**Table 2:** Possible substituents at R<sub>1</sub>, R<sub>2</sub>, and R<sub>3</sub>

Position	Substitution in the ligands
R <sub>1</sub>	-N(CH <sub>2</sub> CH <sub>3</sub> ) <sub>2</sub> , -NH <sub>2</sub> , -NCOCH <sub>3</sub> , -NO <sub>2</sub>
R <sub>2</sub>	-CH <sub>3</sub> , -CH <sub>2</sub> CH <sub>3</sub> , -CH(CH <sub>3</sub> ) <sub>2</sub>
R <sub>3</sub>	

These first 24 compounds were then tested for their anti-HIV activity. These compounds were tested in CEM-SS cells with laboratory derived strains (RF). In this assay, the virus, cells and drugs were incubated for six days. The cytopathic effect of HIV-1 to cells with or without the compound was measured. A lead compound was obtained (**Figure 23**) which had an EC<sub>50</sub> of 2.64 μM to inhibit HIV invasion. Based on this result, further molecular modeling studies were performed.

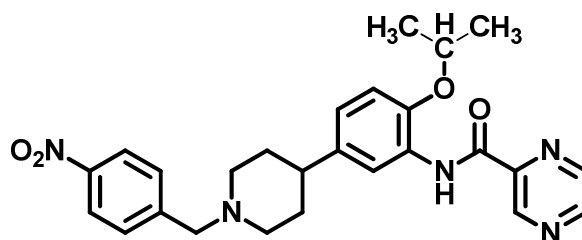
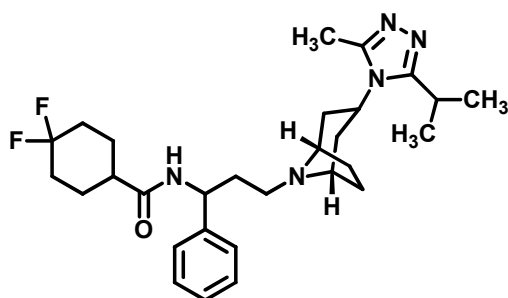


**Figure 23:** Lead compound.

#### 4.2 Molecular Modeling based drug design:

Further molecular modeling studies were done based on the results obtained from the first round of chemical synthesis. More recently reported two CCR5 antagonists, Maraviroc and Aplaviroc, were docked into the homology model of CCR5 to study their binding mode.

Maraviroc, developed by Pfizer, was docked into the homology model of CCR5 receptor to study the binding interactions of its structural features with the binding pocket of the receptor. It was observed that Glu283, Tyr108, and Ile198 were important amino acid residues in the binding pocket of Maraviroc (**Figure 24**). This was supported by site-directed mutagenesis study. Glu283 forms a putative salt bridge with the charged amino acid residue. E283A mutant showed 2000-fold loss of the binding ability of Maraviroc. Also, the binding of Maraviroc to CCR5 reduced markedly in I198A mutant. This may be due to a hydrophobic interaction between Maraviroc and Ile198. Tyr251, which is a part of the binding pocket, is believed to be flexible enough to move in and out depending on the size and electrostatic nature of the compound.<sup>77, 43</sup>



Maraviroc

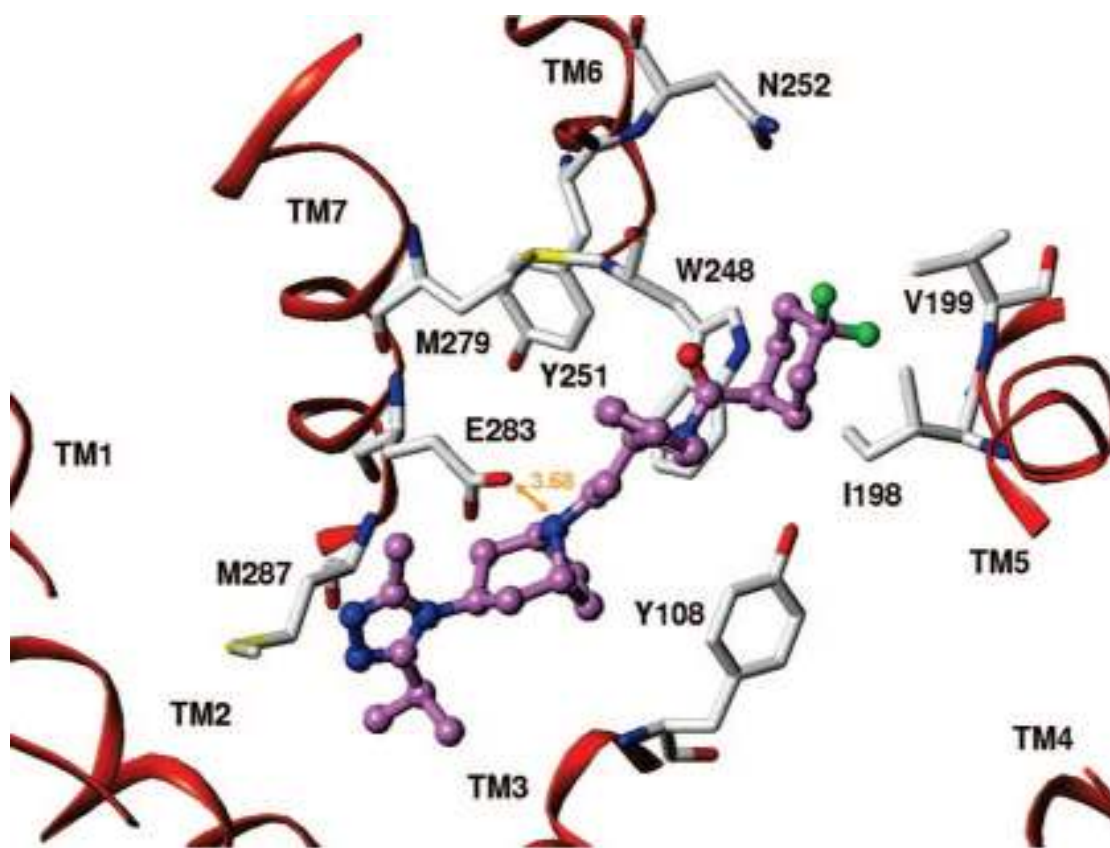
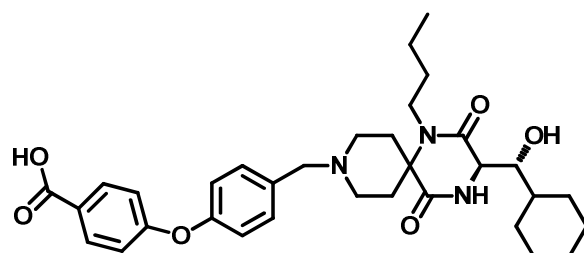


Figure 24: Binding mode of Maraviroc (purple) in the homology model of CCR5.<sup>77</sup>

Aplaviroc, developed by Ono pharmaceuticals, was also docked into the CCR5 receptor. It was observed that Aplaviroc had similar interactions with the binding pocket in the homology model of CCR5 (**Figure 25**). Ser180 may form hydrogen bond interaction with the molecule. The other key residues in the binding pocket of Aplaviroc were Tyr108, Phe112, Tyr251, and Glu283. Y108A drastically reduced the binding of Aplaviroc to the CCR5 mutant. An exclusive ionic or hydrogen bond interaction was observed between the carboxylic acid moiety and Lys197.<sup>77, 43, 78</sup>

Based on these docking studies of CCR5 antagonists into the homology model of the receptor, it was observed that there was a large hydrophobic binding pocket. This binding pocket was primarily constituted by Ile198 and Tyr 108. Mutation of these residues by alanine drastically reduced the binding affinity of Maraviroc and Aplaviroc. This hydrophobic binding pocket was able to accommodate bulky hydrophobic groups with or without polar substituents.

Further molecular modeling studies were carried wherein three CCR5 antagonists were aligned together in their lowest energy conformation. These included Maraviroc, Aplaviroc, and a compound designed and synthesized by our lab. This compound was similar to the lead compound (**Figure 23**) which only lacked the para nitro group. These three compounds are shown in **Figure 26** and their alignment is shown in **Figure 27**.



Aplaviroc

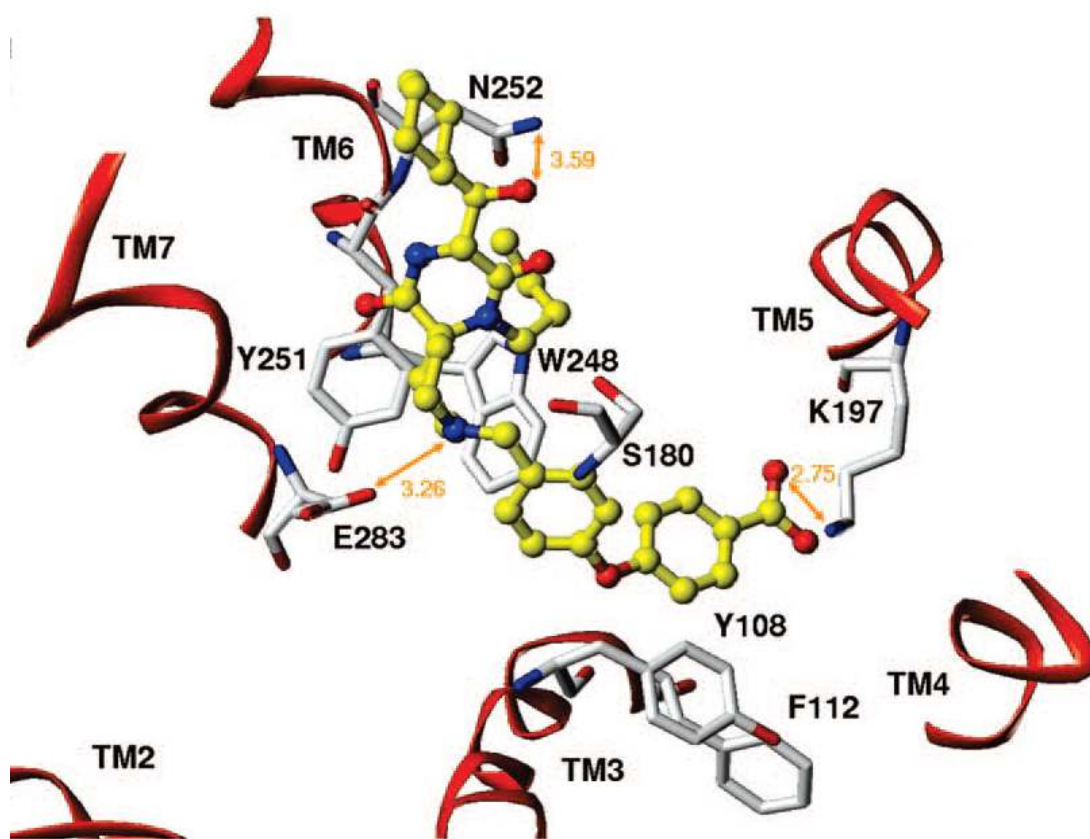
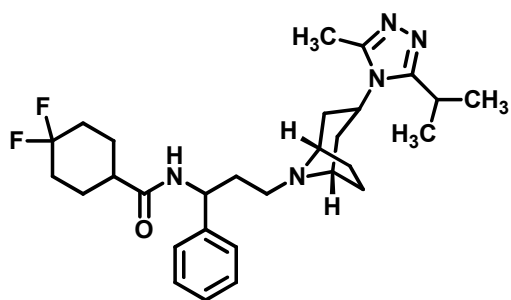
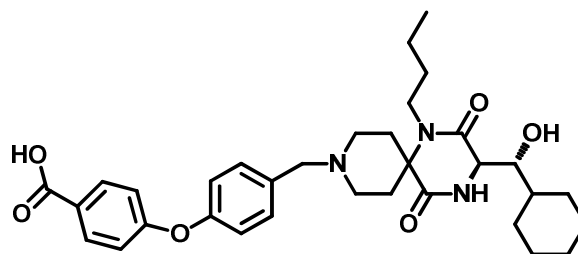


Figure 25: Binding mode of Aplaviroc (yellow) in the homology model of CCR5.<sup>77</sup>

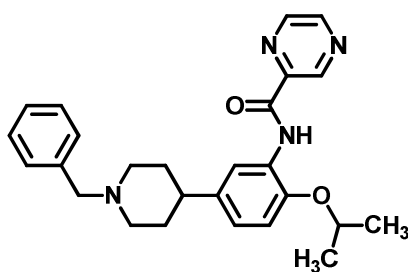




Maraviroc



Aplaviroc



Compound designed and synthesized by our lab which is similar to the lead compound (Figure 23).

**Figure 26:** The three compounds that were aligned together.

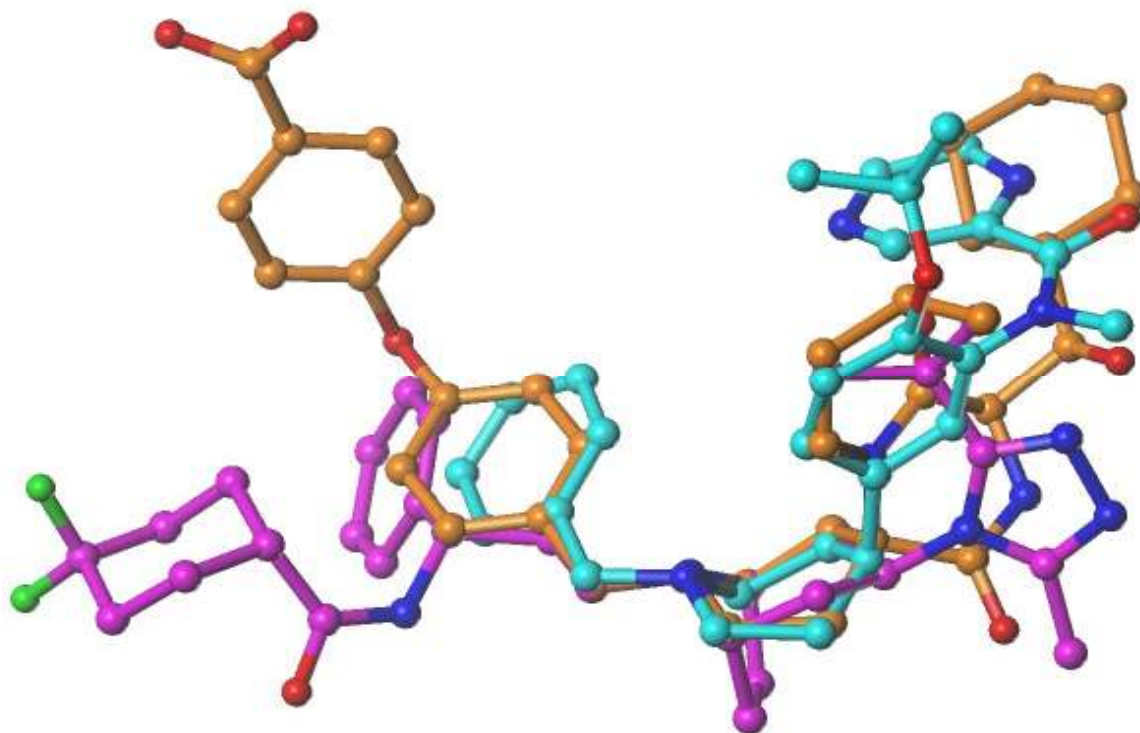
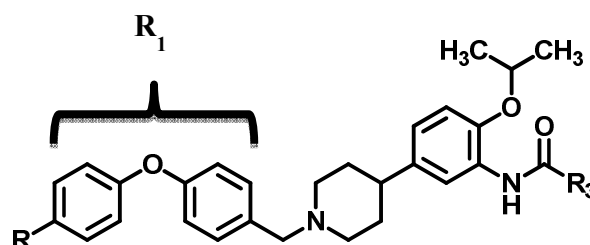


**Figure 27:** Maraviroc (purple), Aplaviroc (orange) and compound from our lab (cyan) aligned together.

On further analyzing, it was observed that the compound designed in our lab was in good alignment with the other two compounds. However; it lacked a longer arm at the end of the hydrophobic portion of the moiety. This additional hydrophobic arm probably fits into a hydrophobic binding pocket in the receptor. The need for this additional hydrophobic arm was consistent with molecular modeling and site-directed mutagenesis studies. Therefore, the molecular scaffold initially designed was further modified to accommodate additional bulky hydrophobic groups that would satisfy the hydrophobic binding pocket requirements of the receptor.

#### 4.3 Project Design:

In order to satisfy the binding pocket requirements, bulky, and hydrophobic groups were introduced as  $R_1$  (**Figure 28**).

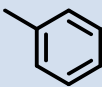
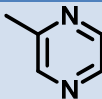


**Figure 28:** Molecular skeleton with new substituents as  $R_1$ .

To probe the electronic characteristics of the binding pocket, the molecular skeleton was modified such that various substituents could be incorporated as  $R_1$  (**Table 3**). Electron donating groups ( $-\text{CH}_3$  and  $-\text{OCH}_3$ ), electron releasing groups ( $-\text{NO}_2$ ,  $-\text{CF}_3$ ,  $-\text{Cl}$ ), and  $-\text{H}$

would be substituted at R and phenyl and pyrazinyl groups would be substituted at R<sub>3</sub>. By doing so, twelve different final compounds would be obtained.

**Table 3:** Possible substituent at R<sub>1</sub> and R<sub>3</sub>.

R	-H	-CH <sub>3</sub>	-OCH <sub>3</sub>	-NO <sub>2</sub>	-CF <sub>3</sub>	-Cl
R <sub>3</sub>						

However, due to synthetic difficulties, only the -CF<sub>3</sub> substituted compounds were synthesized. The synthesis of the remaining compounds was unsuccessful. The precursors that had to be prepared with the rest of the five different R<sub>1</sub> substituents were either unstable or difficult to prepare. This observation was consistent with the commercial sources as it was noticed that none of them were available. Thus, some other commercially available similar precursors carrying bulky hydrophobic groups were incorporated. **Figure 29** lists these commercially available precursors.

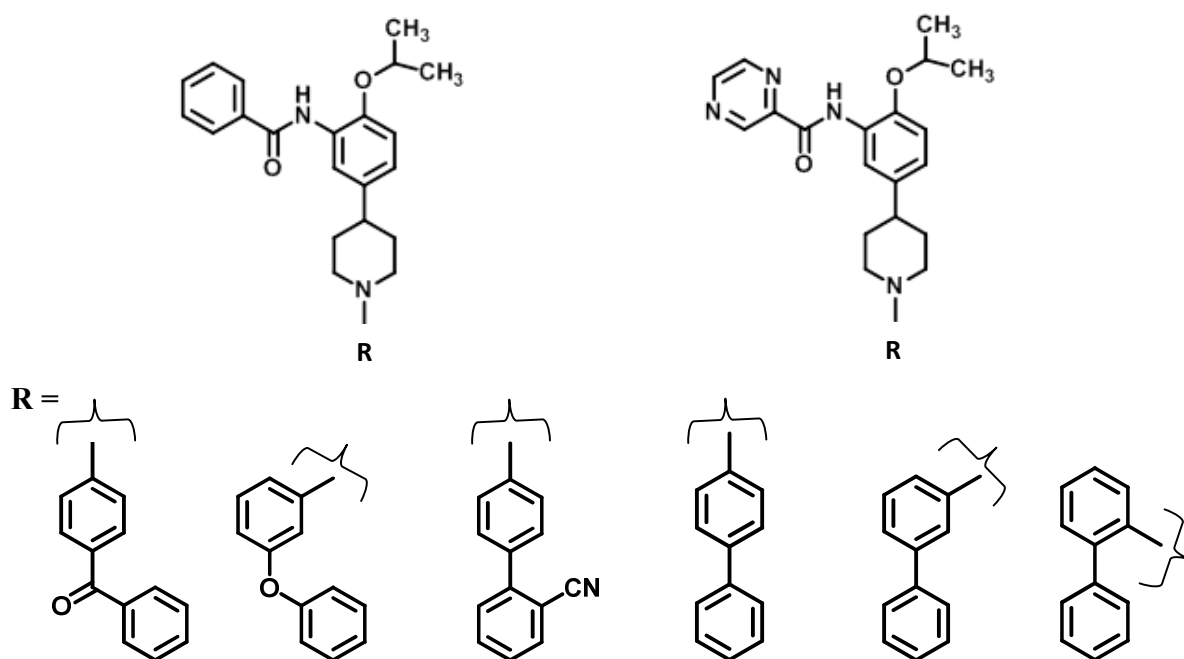


**Figure 29:** The different commercially available hydrophobic substituents.

#### 4.4 Project Objectives:

The primary objective of this project was to test our hypothesis that a bulky, hydrophobic group is necessary to satisfy the binding pocket requirements of the receptor. Fourteen CCR5 antagonists with varied substituents at  $R_1$  and  $R_3$  were synthesized to test this hypothesis. The synthetic route used for the synthesis of the previous batch of compounds was modified to introduce bulky, hydrophobic substituents at  $R_1$ . Two aromatic groups, phenyl and pyrazinyl, were tested at  $R_3$ .

These CCR5 antagonists were then evaluated for their biological activity. Two assays, the calcium mobilization assay and anti-proliferation assay, were performed. The

calcium mobilization assay is a functional assay. The ability of CCR5 antagonists in inhibiting the intracellular calcium release stimulated by endogenous ligand, RANTES was evaluated. CCR5 antagonists that have a high affinity for the receptor will be capable of inhibiting the binding of RANTES to the receptor. The second assay was the anti-proliferation assay which was tested in two different prostate cancer cell lines, PC-3, and M12. These prostate cancer cell lines express CCR5 on their cell surface. The goal of this assay was to test the anti-proliferative activity of the antagonists by binding to the CCR5 receptor. The colorimetric reagent WST-1 was used in the anti-proliferation assays.

The data obtained from these assays would help in testing our hypothesis as well as establishing a structure-activity relationship to facilitate the design of the next generation of compounds.

## 5. Results and Discussion

### 5.1 Chemical Synthesis of CCR5 Antagonists:

The synthetic route used to prepare the previous batch of compounds was adopted to prepare the new series of CCR5 antagonists. Two series of compounds were prepared which differed in the substitution at R3 position. The first series consisted of phenyl substituted compounds and the second series consisted of pyrazinyl substituted compounds. The first two reactions of the synthetic route are outlined in **Figure 30**.

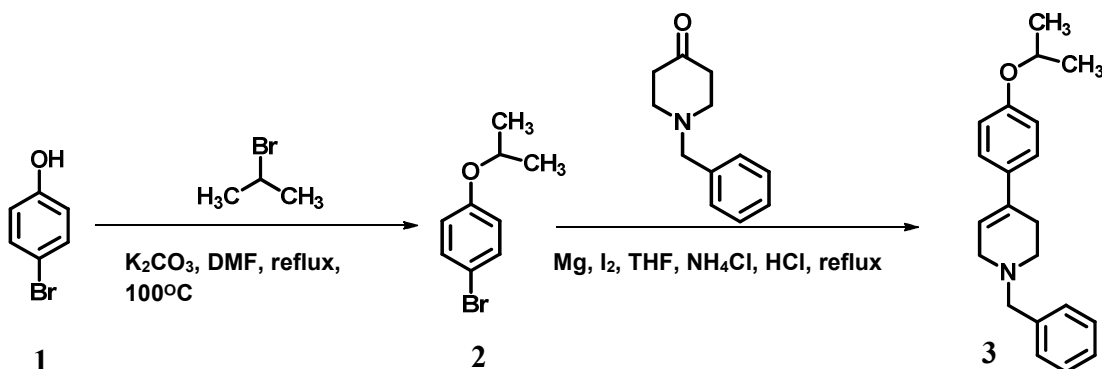


**Figure 30:** Substitution and Grignard reactions.

The first reaction in the synthetic route was a substitution reaction where the hydroxyl group of 4-bromophenol (**1**) reacted with isopropyl bromide to form an isopropoxyl moiety. This reaction was performed with dimethyl formamide (DMF) as the solvent. The reaction mixture was refluxed overnight at  $90^\circ\text{C}$ . The work up involved washing the reaction mixture with brine (50 mL) followed by washing with water (25 mL). Compound **2** was obtained in 86% yields.

The Grignard reaction was then conducted for conversion of 1-bromo-4-isopropoxybenzene (**2**) to 1-benzyl-4-(4-isopropoxyphenyl)-1,2,3,6-tetrahydropyridine (**3**). The experimental set-up of the Grignard reaction is shown in **Figure 31**. This was a challenging reaction as the reaction atmosphere had to be anhydrous and devoid of oxygen. This is because Mg, which was used in the reaction to form the Grignard reagent, decomposes in the presence of oxygen. All the glassware needed for this reaction was dried and placed in an oven overnight. Small pieces of Mg were cut just before the reaction was performed. Vacuum was introduced in the entire experimental set up to remove any trace moisture. This was followed by flushing the experimental setup with nitrogen gas.

The alkyl bromide, (**2**) prepared from the previous reaction, was added drop-wise over a period of 30 minutes to a mixture of Mg pieces and iodine in tetrahydrofuran (THF), which was the solvent of this reaction. This led to the formation of the Grignard reagent. This was followed by addition of the ketone, 1-benzyl-4-piperidone, to form the product (**3**). The resulting mixture was refluxed for about 3 hours with ammonium chloride and 6N hydrochloric acid. This was done to consume any remaining unreacted Grignard reagent. This reaction had a yield of 65%. The yield did not improve even if the reaction was allowed to run for a longer time.



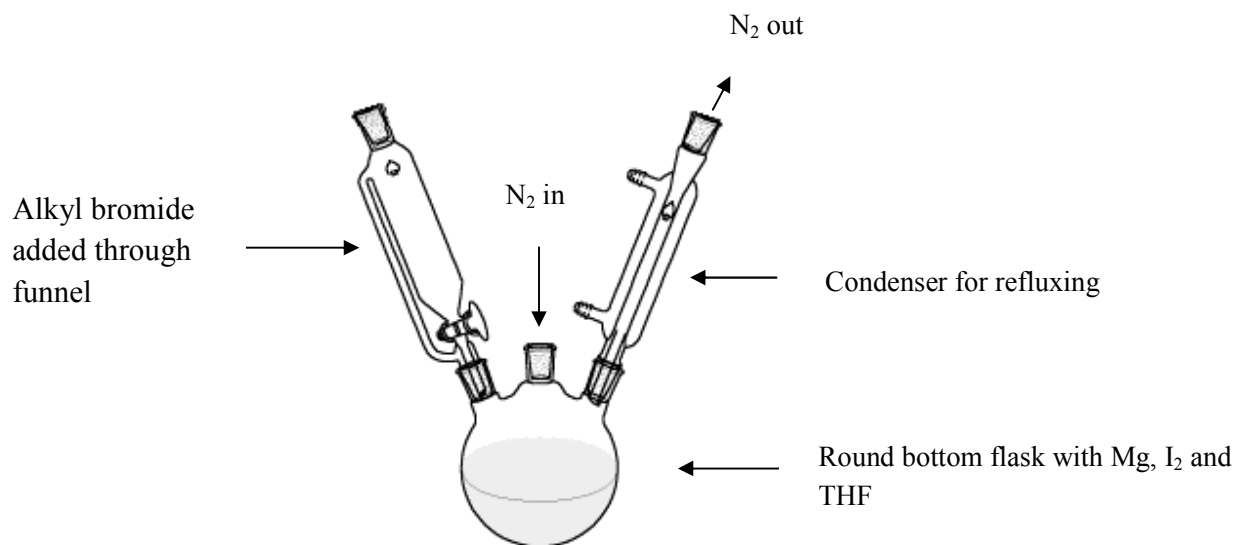


Figure 31: Experimental set-up for Grignard reaction.<sup>76</sup>

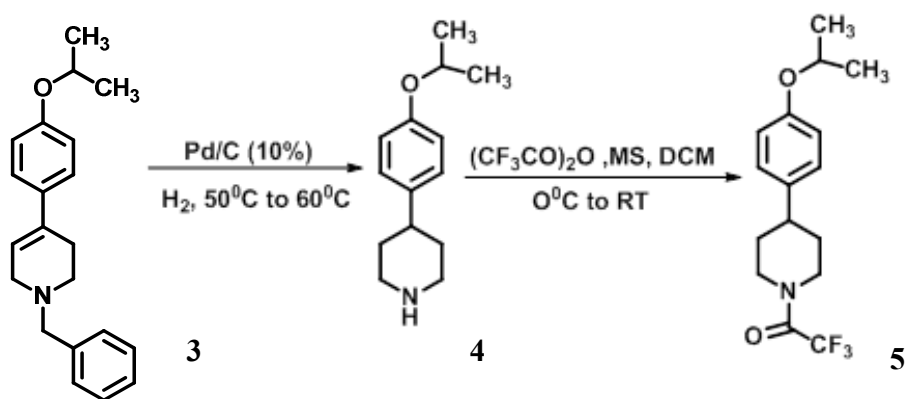


Figure 32: Hydrogenation and protection reactions.

Debenzylation and double bond reduction was the next step in the synthetic route (**Figure 32**). This reaction was carried out using a Parr-hydrogenator in an atmosphere of hydrogen. The catalyst used was Pd/C (10%). This reaction was tried out many times but the reaction did not proceed to completion. Literature reported such a reaction to be extremely slow which would take some days or weeks to go to completion. Despite running the reaction for 5-7 days, thin layer chromatography (TLC) showed that the starting material (**3**) was not consumed, thus, indicating that the reaction had not taken place.

Therefore, the starting material used in the reaction was analyzed. Earlier, the starting material had been purified by column chromatography. To further purify the starting material, it was re-crystallized from hot ethanol. Despite carrying out the reaction with the re-crystallized starting material, the reaction did not proceed to completion. The starting material (**3**), a tertiary amine, was then converted to the corresponding hydrochloride salt by adding 1.3 equivalents of 1M HCl. The resulting salt was then used in the reaction instead of the free base. The reaction was allowed to run for seven days at an elevated temperature of about 50<sup>0</sup>C by using a heating pad. 10% of the catalyst was used. At the end of seven days, TLC showed that the starting material was totally consumed. The consumption of the starting material was accompanied by the appearance of a new spot on TLC. Separation was done by column chromatography using a 20:1 dichloromethane methanol solvent system with 10% ammonium hydroxide. Characterization by NMR confirmed the new spot to be the product, compound **4**. This

reaction had a yield of 84%. Therefore, the key factors for this reaction to proceed to completion were purification of the starting material and using the tertiary amine starting material as the hydrochloride salt.

Debenzylation of the tertiary amine (**3**) leads to a secondary amine (**4**) which was not very stable. Thus, protection of the secondary amine was the next step in the overall synthetic route (**Figure 33**). Trifluoro acetic anhydride was used as the protecting agent. The reaction was carried out in an ice-water bath with dichloromethane as the solvent. Molecular sieves were added to the reaction mixture to remove any residual of water. The reaction proceeded from 0°C to room temperature. It was allowed to react for about 12 hours. The product of this reaction (**5**) was obtained in yields of 90%.

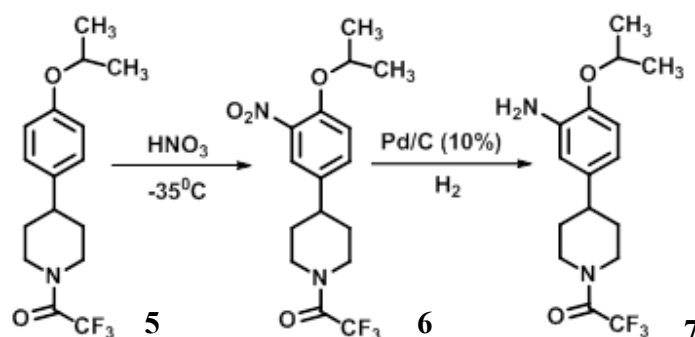


**Figure 34:** Nitration and reduction reactions

Introduction of a single nitro group on the benzene ring ortho to the isopropoxy moiety was the next reaction in the synthetic route (**Figure 34**). The reaction was carried out at a temperature of about  $-35^\circ\text{C}$  in the presence of nitric acid. This temperature was maintained in an acetone-dry ice bath. Initially the temperature was allowed to go as low

as  $-70^{\circ}\text{C}$ . At this temperature, nitric acid was added. The temperature was then raised to  $-35^{\circ}\text{C}$  by removing pieces of dry ice from the acetone-dry ice bath. The temperature was maintained constant for six hours for the reaction to proceed to completion. The reaction was quenched by pouring the contents into ice. The organic phase was extracted with dichloromethane. Product **6** was obtained in 80% yields.

The nitro group in compound **6** had to be reduced to form the corresponding primary amine in the next reaction (**Figure 34**). This was done in an atmosphere of hydrogen using the Parr hydrogenator with methanol as the solvent. Pd/C (10%) was used as the catalyst. The reaction was carried out for about 5 hours. The work up included filtering the reaction mixture through celite to afford removal of the catalyst. The product **7** was obtained in a yield of 50%.

The primary amine in **7** was then coupled with an acid to form the amide bond. The acid used was either benzoic acid or pyrazine-2-carboxylic acid (**Figure 35**). There were two factors which were important to this reaction. The first factor was absence of water and hence molecular sieves were used. The second factor was the sequence in which the reactants had to be added. The acid (either benzoic acid or pyrazine-2-carboxylic acid) was stirred with EDCI (*N*-(3-dimethylaminopropyl)-*N*'-ethylcarbodiimide hydrochloride), HOBT (1-hydroxybenzotriazole hydrate), TEA (triethylamine), DMF and molecular sieves in an ice-water bath for about 15 minutes initially. This was followed by the addition of the primary amine (**6**) to the activated carboxylic acid. The reaction was allowed to proceed to room temperature overnight. Compounds **8** or **9** were obtained when

benzoic acid or pyrazine-2-carboxylic acid was used respectively. The benzoic acid coupled product (**8**) was obtained in 87.3% yield whereas the pyrazine-2-carboxylic acid coupled product (**9**) was obtained in yields of 84.6%.

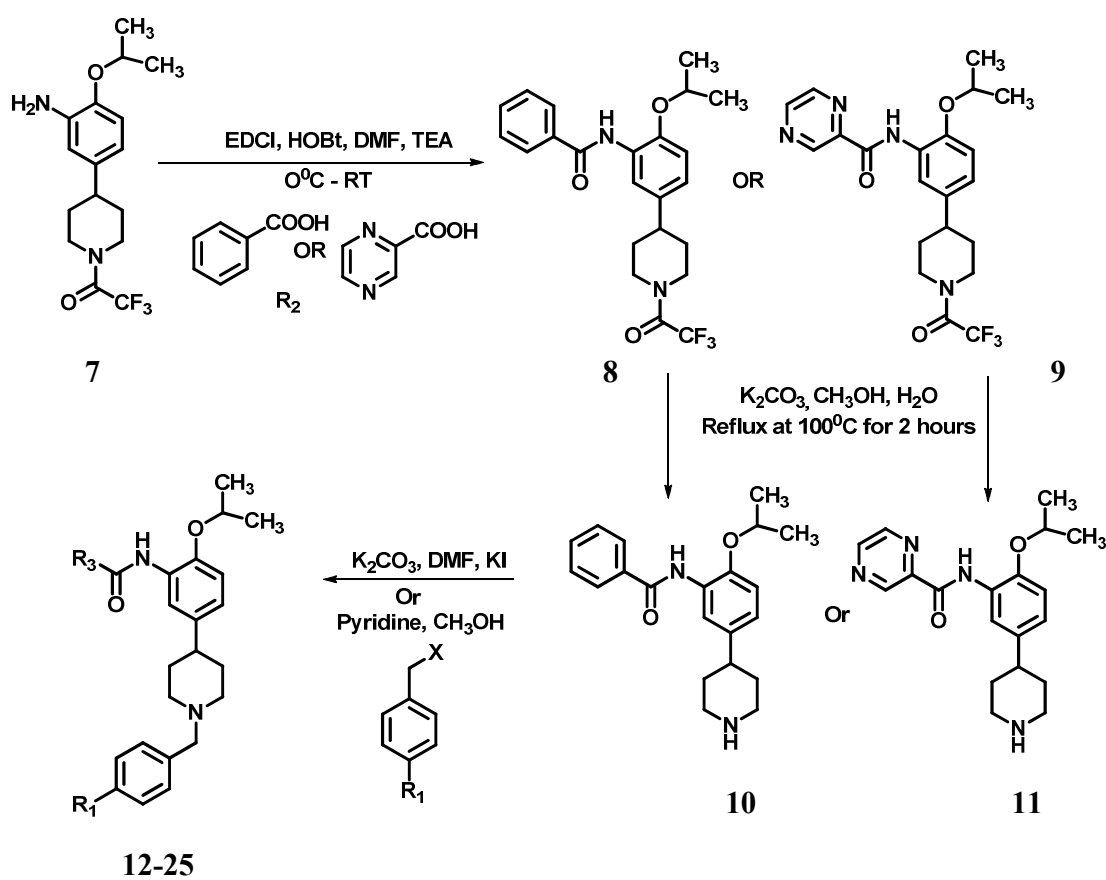


**Figure 35:** Amide formation and base catalyzed de-protection reactions.

De-protection of the piperidine amine to form a secondary amine was the next step. This was done using methanol and water mixture as the solvent system. Potassium carbonate was used as the base. The reaction mixture was refluxed at about 100<sup>0</sup>C for 3 hours. The reaction mixture was then evaporated to remove methanol and water. This was followed by dissolving the contents in dichloromethane followed by extraction with a saturated solution of sodium bicarbonate. On evaporating the organic phase, the product precipitated. The product, compounds **10** or **11**, was obtained in yield of around 98.8%.

The last step in the synthetic route was coupling of diaryl ether moieties which had different substituents at R<sub>1</sub> to the secondary amines **10** and **11** (**Figure 36**).

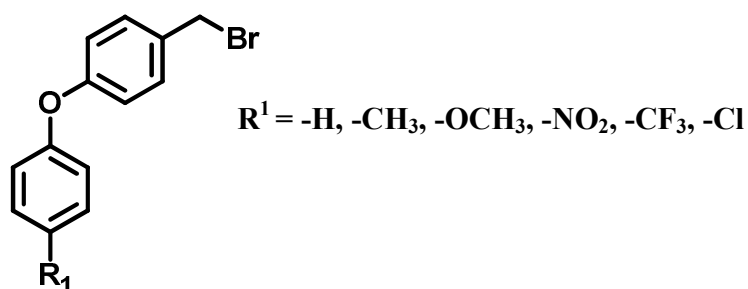


**Figure 36:** Diaryl ethers with six different substituents at R<sup>1</sup>.

These diaryl ether side chains had to be prepared in two steps. The first step was an Ullmann coupling reaction. This involved the coupling between p-cresol and bromobenzenes with different substituents at R<sub>1</sub>. **Figure 37** shows the different bromobenzenes that were to be coupled to p-cresol.

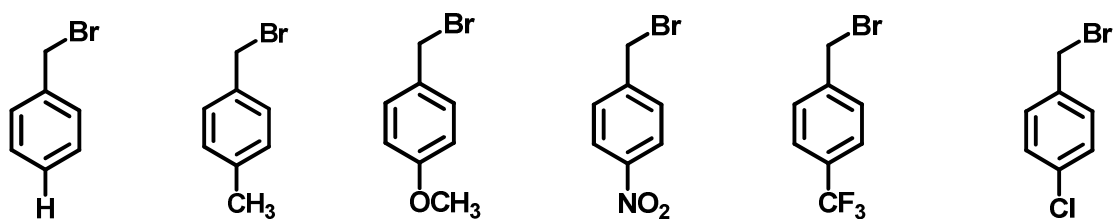


**Figure 37:** Bromobenzenes to be coupled with p-cresol.

The Ullmann coupling reaction was used to couple the bromobenzenes with an electron donating group at  $R_1$  to p-cresol. In this reaction, cesium carbonate was the base, copper bromide was used as the catalyst and N-methylpyrrolidone (NMP) was the solvent. The reaction mixture was refluxed for 16 hours at  $160^\circ\text{C}$  under nitrogen protection. The resulting diaryl ether product was purified by column chromatography. Bromobenzenes with  $-\text{H}$ ,  $-\text{OCH}_3$ , and  $-\text{CH}_3$  were coupled to p-cresol by the Ullmann coupling reaction (**Figure 38**).<sup>81</sup>

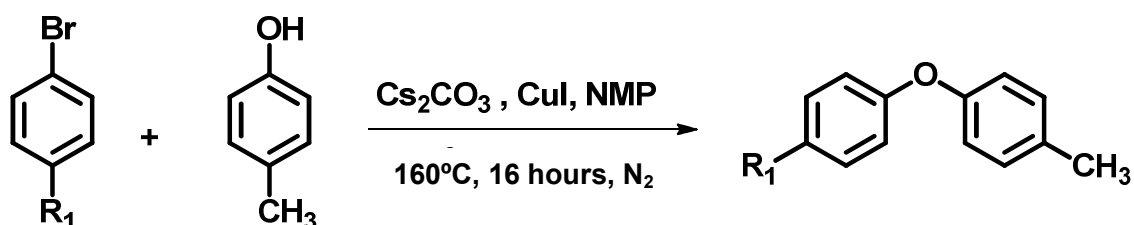


**Figure 38:** Ullman coupling reaction for electron donating groups.<sup>81</sup>

The Ullmann coupling reaction for electron withdrawing groups was done in a microwave at  $125^\circ\text{C}$  for 25 minutes (**Figure 39**). The microwave reaction was reported in literature due to the reduced reactivity of those bromobenzenes with an electron withdrawing group at  $R^1$ . The base used in the reaction was potassium tert-butoxide, the

catalyst was copper iodide and tetramethyl ethylenediamine (TMEDA) was the ligand used. However, only the  $-\text{CF}_3$  substituted bromobenzene coupled to p-cresol. The remaining substituted bromobenzenes did not react under microwave conditions successfully. Thus, refluxing the reaction mixture overnight at  $125^\circ\text{C}$  was tried. Under these conditions, the starting material was consumed and the reaction proceeded to completion.<sup>82</sup>

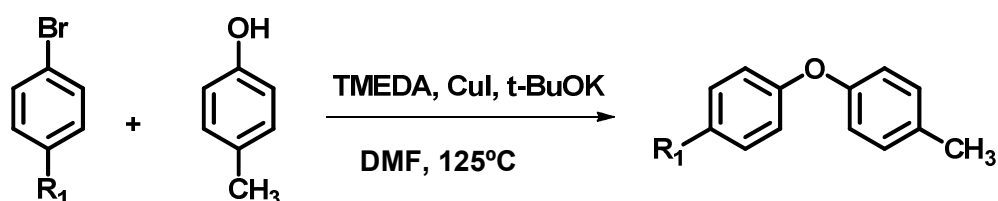
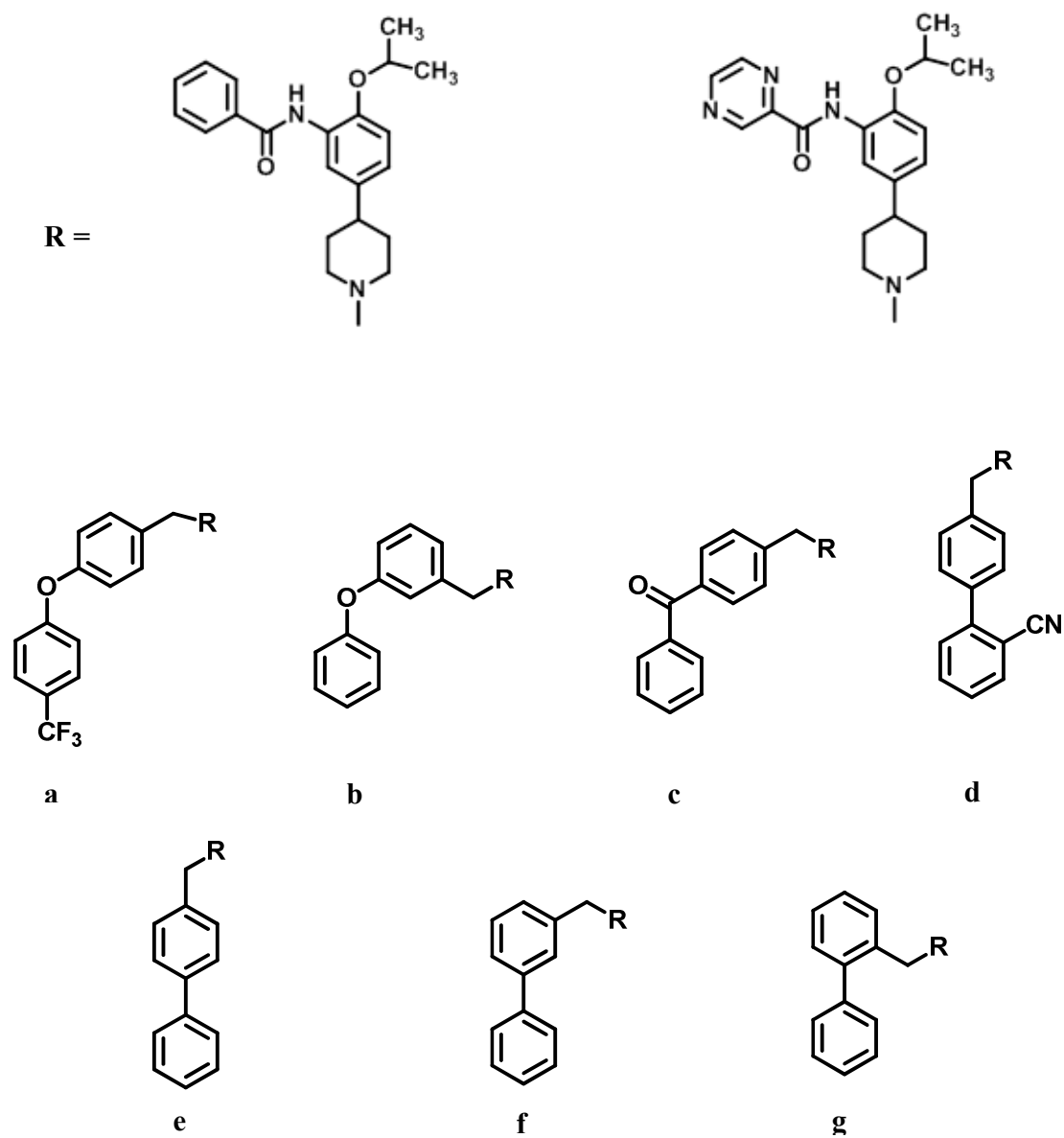


**Figure 39:** Ullmann Coupling reaction for electron withdrawing groups.<sup>82</sup>

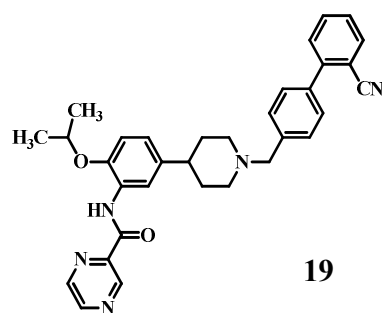
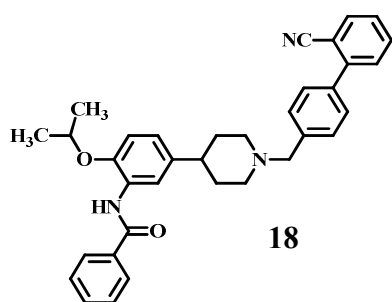
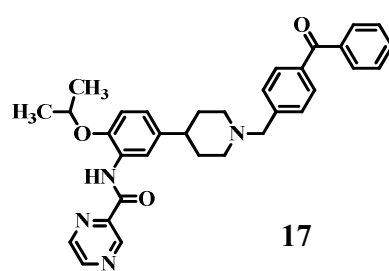
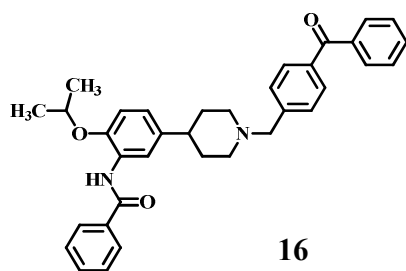
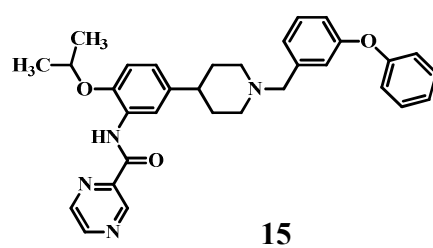
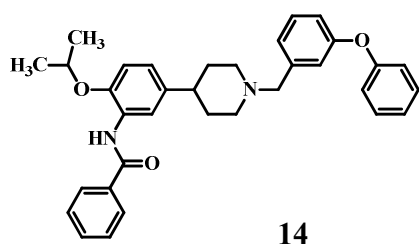
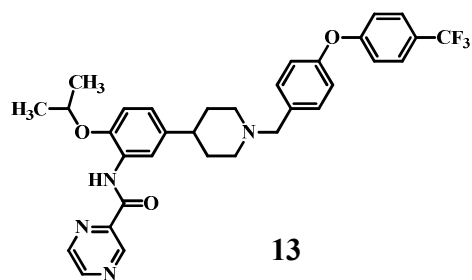
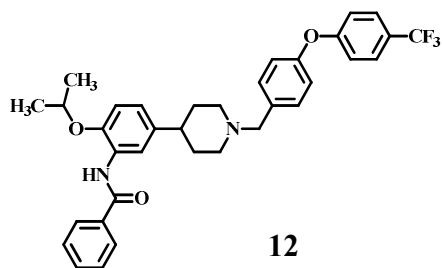
The methyl group in the diaryl ether had to be brominated to afford a benzyl bromide which could be coupled to the secondary amine. In the presence of NBS (N-bromosuccinimide) and azobisisobutyronitrile (AIBN) with  $\text{CCl}_4$  as the solvent, the methyl group would be brominated to form  $-\text{CH}_2\text{Br}$ .<sup>83</sup> However, only the reaction with the  $-\text{CF}_3$  substituted starting material proceeded to completion. The remaining diaryl ethers that were prepared either did not proceed to completion or were unstable and hence could not be purified. The reason for this may be the fact that the free radical intermediate formed in this reaction is either destabilized or consumed prior to reaction with NBS. Thus, bromination of these side chains was discontinued and other commercially available benzyl bromides or benzyl chlorides were applied to prepare the final compounds. Six



different commercially available benzyl bromides or benzyl chlorides (**b** through **g**) were coupled to compounds **10** and **11**.



**Figure 40:** Different substituents that were attached to **10** and **11**



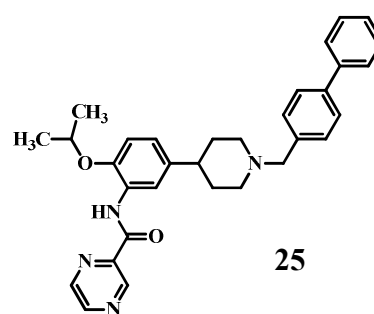
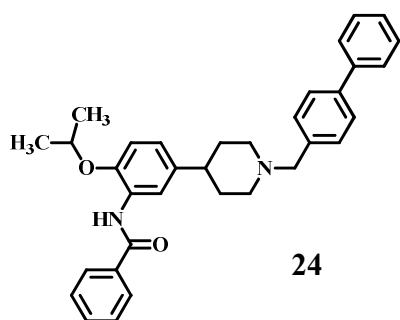
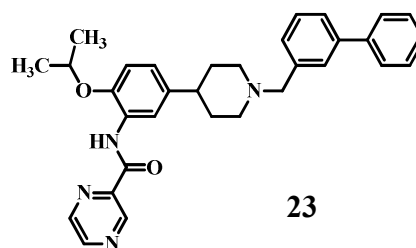
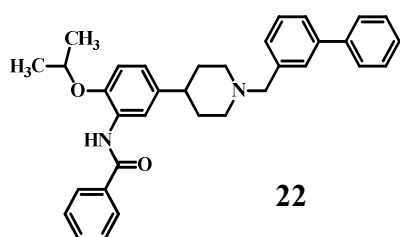
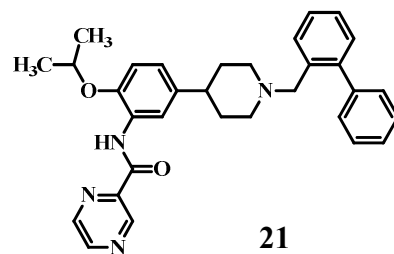
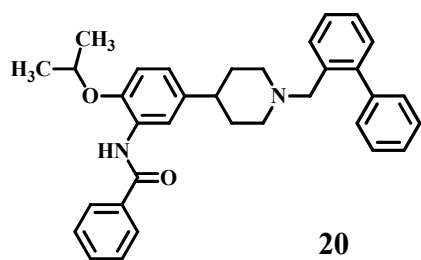
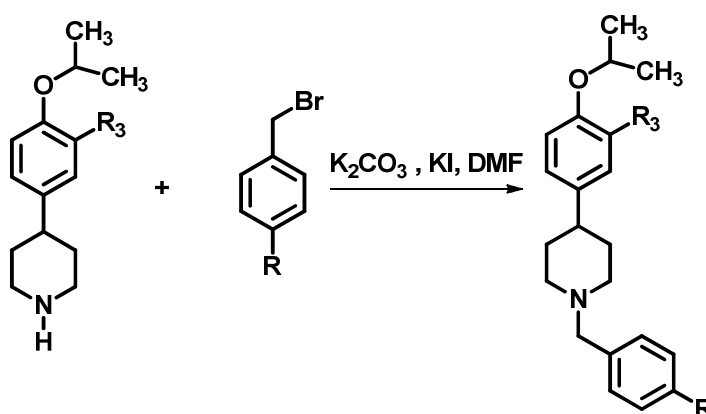


Figure 41: Final compounds.

Fourteen final compounds were prepared (**Figure 41**). Two methods were used for the preparation of the final compounds. The first method utilized potassium carbonate as the base for abstraction of the proton from the secondary amine, compounds **10** and **11** (**Figure 42**). DMF was used as the solvent. The reaction was allowed to run overnight. It proceeded from 0°C to room temperature. Those reactions which had a substituent at the para position at **R** proceeded to completion.



**Figure 42:** Reaction for para substituents at R.

However, the synthesis of compounds **14**, **15**, **20**, **21**, **22** and **23** failed when this method was used. TLC showed that the starting material had not reacted at all even after two days. Steric hindrance was thought to be the reason due to which compounds **20** and **21** could not be prepared using this method. The bulky phenyl group ortho to  $-\text{CH}_2\text{Br}$  would hinder the secondary amine (compound **10** and **11**) from reacting with it. Literature search did not provide any help as no such reaction was reported. It was postulated that refluxing the reaction mixture may overcome the steric hindrance. Methanol, with a boiling point of just 65°C as compared to DMF with a boiling point of 153°C, was chosen

as the solvent. Also, methanol is not as sticky as DMF. The latter is quite difficult to remove from the reaction mixture. Since potassium carbonate, an inorganic base, is not very soluble in methanol an organic base, such as pyridine, which is soluble in methanol, was chosen. On carrying out this reaction at a temperature of 70<sup>0</sup>C overnight resulted in completion of the reaction. The excess of pyridine left unreacted in the reaction mixture was removed by washing with 1N HCl. On purifying by column chromatography, compounds **20** and **21** were obtained (**Figure 43**).

Compounds **14**, **15** and **22**, **23** could not be prepared using the first method with potassium carbonate as the base and DMF as the solvent. Both of these compounds have an electron donating group at the meta position. This would deactivate the entire moiety and render it un-reactive towards the reaction. Once again, no such reaction was reported in literature. The method used to prepare compounds **20** and **21** was tried for the preparation of **14**, **15**, **22** and **23** as well. On refluxing over night with pyridine as the base in methanol, the compounds **14**, **15** and **22**, **23** were obtained (**Figure 43**).

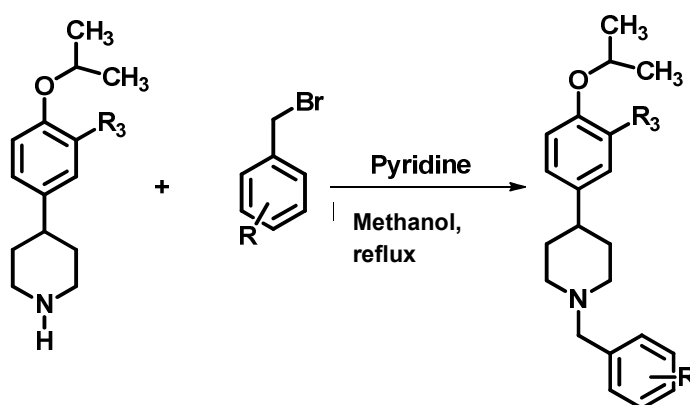


**Figure 43:** Reaction for ortho and meta substituted R.

Compounds **12** and **13** were prepared in two additional steps. The first step was an Ullmann coupling reaction (**Figure 44**). This gave compound **26**, which is diaryl ether. The methyl group of **26** had to be brominated in the next step. The resulting benzyl bromide (compound **27**) was used for coupling to the secondary amine to obtain compounds **11** and **12** (**Figure 44**).

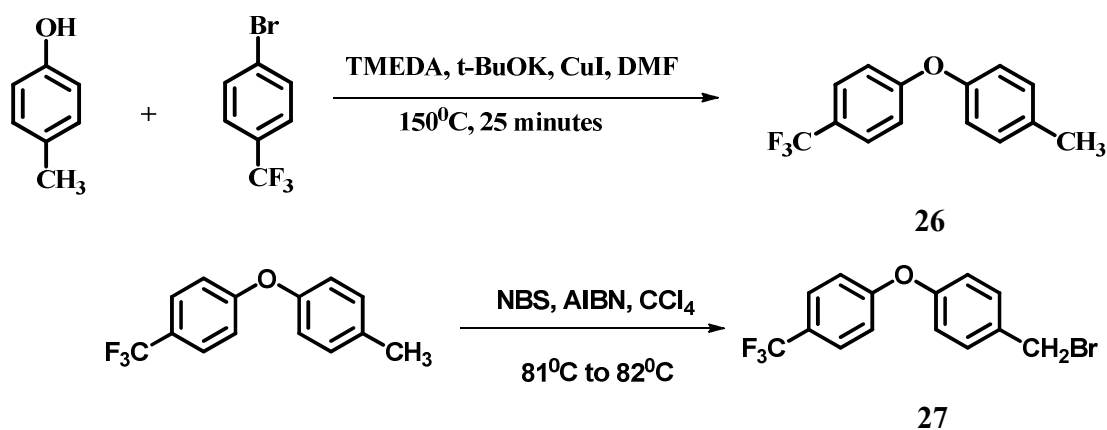


**Figure 44:** Ullmann coupling and bromination reactions.

All the final compounds (compounds **12** through **25**) were obtained in their free base form. They were then converted to the corresponding hydrochloride salts by using 1.3 equivalents of 1M HCl in ether solution. The final compounds were characterized by proton and carbon nuclear magnetic resonance spectroscopy (NMR), infrared (IR) spectroscopy, mass spectroscopy, and high performance liquid chromatography (HPLC). Also, their melting points were recorded. The hydrochloride salts of all the fourteen final compounds were used to perform biological screenings.

## 5.2 Biological Screening:

The fourteen CCR5 antagonists that were synthesized were evaluated for their biological activity. Two assays were performed: the calcium mobilization assay and the anti-proliferation assay.

### **5.2.1 Calcium Mobilization Assay:**

The calcium mobilization assay, a functional assay, was conducted to evaluate the ability of the compounds to inhibit the RANTES induced intracellular calcium release. The cell line used was MOLT-4 which expresses the chemokine receptor CCR5 on its membrane. The dye used in this assay was Fluo-4, a fluorescent dye, which has high affinity for calcium ions. This dye has a very low emission at rest; however there is a large increase in the emission intensity when it binds calcium. On stimulation of the cells with the agonist RANTES, it increases the intracellular levels of calcium. The changes in calcium concentrations can be detected by the Fluo-4 dye.<sup>81</sup> CCR5 antagonists bind to the receptor thus, preventing RANTES from interacting with the receptor. As a result, the increase in intracellular calcium levels is inhibited leading to lower emission intensity of the Fluo-4 dye. The fourteen final compounds that were tested are shown in **Figure 41**.

The IC<sub>50</sub> values obtained for the antagonists are summarized in the following **Table 4**.

**Table 4:** IC<sub>50</sub> values from the calcium mobilization assay

<b>Compound</b>	<b>IC<sub>50</sub> (μM)</b>
12	57.17± 12.81
13	189.87± 139.15
14	46.49± 28.75
15	28.60± 14.33
16	51.74± 17.04
17	54.87± 18.93
18	61.44± 53.16
19	15.41± 6.45
20	169.47± 112.15
21	36.91± 8.85
22	>200
23	190.81± 152.80



24	26.75± 12.40
25	59.00± 41.40
Maraviroc	4.13± 0.02

### Discussion:

Based on the  $IC_{50}$  values from the calcium mobilization assay, compound **19** was the most potent CCR5 antagonist in inhibiting the intracellular calcium release stimulated by RANTES with an  $IC_{50}$  of 15.41  $\mu$ M. This can be interpreted that compound **19** was able to inhibit the binding of 50% RANTES to the CCR5 receptor at a concentration of 15.41  $\mu$ M.

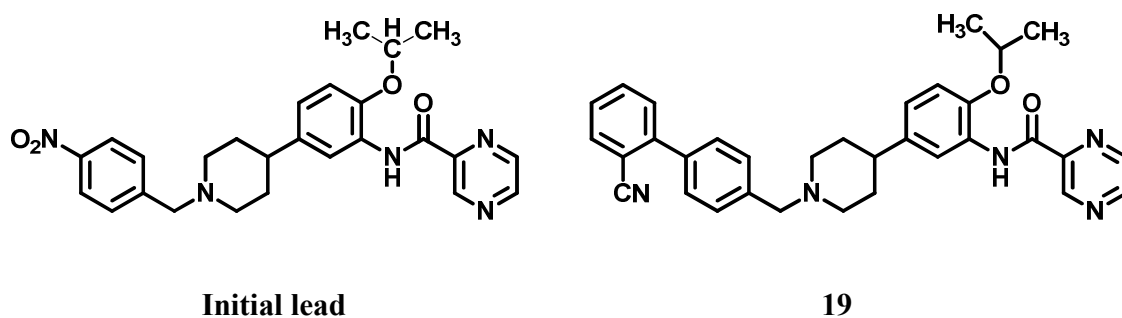


**Figure 45:** Our initial lead and compound **19**.

The  $IC_{50}$  of the initial lead in the calcium mobilization assay was 65.7  $\mu$ M. Thus, compound **19** has a greater ability to bind to CCR5 and inhibit the calcium release stimulated by RANTES. On comparing the structure of the two antagonists, we can infer

that introduction of a hydrophobic group at R<sub>1</sub> has increased the compound's affinity for the CCR5 receptor. Besides compound **19**, most of the other compounds **12**, **14**, **15**, **16**, **17**, **18**, **21**, **24** and **25** have an IC<sub>50</sub> value lower than the initial lead. This further strengthens our hypothesis that a large, hydrophobic binding pocket is present in the CCR5 receptor which is capable of accommodating bulky substituents. However, a clear structure-activity relationship can not be established. This is due to the small number of ligands (fourteen) that were synthesized and tested.

### **5.2.2 Anti-proliferation Assay:**

The anti-proliferation assay was performed to determine the anti-prostate cancer activity of the CCR5 antagonists synthesized. Two different prostate cancer cell lines which express the CCR5 receptor were used. These were PC-3 and M12. The two cell lines had a similar assay protocol that had to be followed.

WST-1 reagent has a tetrazolium salt in its structure which is cleaved by mitochondrial dehydrogenase which leads to the formation of formazan dye (**Figure 46**). The formazan dye is soluble in water and has a characteristic dark red color to it. Only those cells which are viable contain the mitochondrial dehydrogenase. Hence, only those wells with viable cells can facilitate the formation of the dark red colored formazan dye.<sup>80</sup>

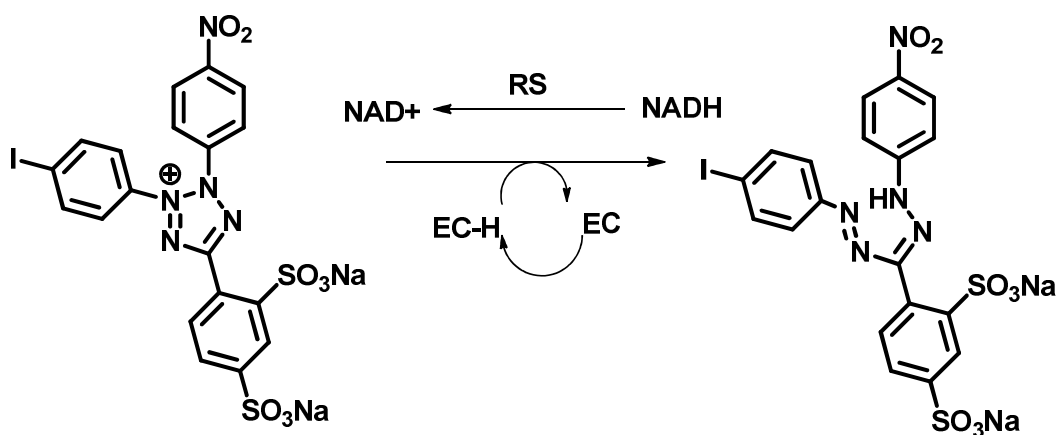


**Figure 46:** Role of WST-1 in the Anti-proliferation Assay.<sup>80</sup>

The fourteen compounds that were tested are shown in **Figure 41**, and the  $IC_{50}$  values obtained for each compound in each cell line is represented in the **Table 5**. The concentration range that was tested for both PC-3 and M12 were 3  $\mu$ M, 10  $\mu$ M, 30  $\mu$ M and 100  $\mu$ M.

**Table 5:** The IC<sub>50</sub> values for PC-3 and M12 cell lines.

<b>Compound</b>	<b>PC-3 IC<sub>50</sub> (μM)</b>	<b>M12IC<sub>50</sub> (μM)</b>
<b>12</b>	66.10 ± 9.03	37.52± 2.73
<b>13</b>	68.80 ± 7.13	62.57± 2.62
<b>14</b>	97.50 ± 1.14	20.04± 0.42
<b>15</b>	>100	49.13± 2.58
<b>16</b>	78.90 ± 25.30	>200
<b>17</b>	88.10 ± 15.90	>200
<b>18</b>	77.80 ± 18.70	>200
<b>19</b>	35.80 ± 7.14	56.33± 11.01
<b>20</b>	89.00 ± 15.0	152.97± 10.07
<b>21</b>	>100	68.63± 1.84
<b>22</b>	>100	72.86± 1.82
<b>23</b>	>100	85.12± 1.66
<b>24</b>	>100	25.58± 0.29

25	>100	>200
Anibamine	1.13± 0.01	3.26 ±0.35

### Discussion:

Based on the IC<sub>50</sub> values obtained from the calcium mobilization assay, compound **19** was the most potent CCR5 antagonist in inhibiting the intracellular calcium release stimulated by RANTES with an IC<sub>50</sub> of 15.41 μM. This was consistent with the IC<sub>50</sub> value obtained from the anti-proliferation assay in the PC-3 cell line where compound **19** showed an IC<sub>50</sub> of 35.80 μM, as the most active one among others on its anti-proliferative activity in PC-3 cell line. To be noticed, our initial lead compound had an IC<sub>50</sub> of greater than 100 μM in the anti-proliferation assay in the PC-3 cell line. Thus, our hypothesis regarding the presence of a hydrophobic binding pocket in the receptor is partially supported by the data obtained. Besides compound **19**, other ligands **12**, **13**, **14**, **16**, **17**, **18**, and **20** also showed higher anti proliferation activity than our initial lead compound in the PC-3 cell line.

In the M12 cell line, the anti-proliferative activity of compound **19** was much lower with an IC<sub>50</sub> of 56.33 μM. However, the proliferation of M12 cells were greatly inhibited by compounds **14** and **24** with IC<sub>50</sub> values of 20.04 μM and 25.58 μM respectively (**Figure 47**). Our initial lead compound had an IC<sub>50</sub> of 32.66 μM in the anti-proliferation assay in M12 cell lines. Thus, two compounds (**14**, **24**) were more potent than the lead as of prostate cancer cell proliferation agents.

A structure-activity relationship that could be established from the calcium mobilization assay as well as the anti-proliferation assay was the observation that in general pyrazinyl substituted ligands showed better activity than the phenyl substituted compounds. For example, compounds **18** and **19** (**Figure 41**) shared the same bulky hydrophobic para biphenyl moiety present in their structure. The only difference in their structures was the present of a phenyl or a pyrazinyl group at R3 position. However, compound **19** has an  $IC_{50}$  value of 15.41  $\mu$ M and compound **18** has an  $IC_{50}$  value of 61.44  $\mu$ M in the calcium mobilization assay (**Table 4**). This observation is also consistent with our initial lead compound which has a pyrazinyl group present in its structure.

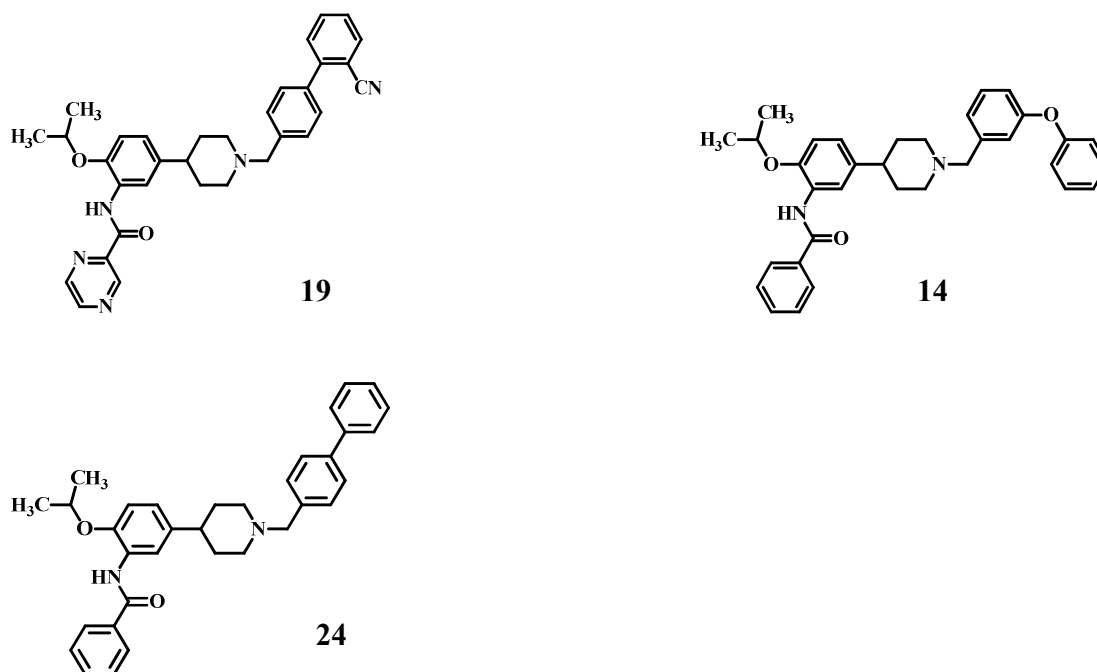


**Figure 47:** Compounds **19**, **14**, and **24**.

It can be clearly seen that the activity of the same compound showed different trend regarding different cell lines. Compound **19** was the most potent CCR5 antagonist in the calcium mobilization assay and had the best anti-proliferative activity in the PC-3 prostate cancer cell line among others. However, when tested in the M12 prostate cancer cell line, antagonist **19** showed lower anti-proliferative activity compared with other ligands. Similarly, compounds **4** and **14** were not the most potent antagonists in the calcium mobilization assay while they showed the highest anti-proliferative activity in the M12 prostate cancer cell line.

This difference in activity of the same compound in different cell lines can be affected by various factors. One reason for the difference in activity could be the varied expression of CCR5 in each cell line. This difference amongst cell lines in the expression level of CCR5 could affect the function of our compounds. For example, PC-3 cell expresses lower level of CCR5 than M12 one<sup>28</sup> while most of the compounds showed better anti-proliferative activity in M12 cells than in PC-3 cells. Also, the downstream signaling pathways may compensate differently to the antagonism of CCR5 among different cancer cell lines.

Second, CCR5 antagonism may not necessarily correlate with inhibition of proliferation of prostate cancer cell lines. Some potent CCR5 antagonists, e.g. Maraviroc, did not show significant anti-prostate cancer proliferation activity under our experimental conditions. The G-protein-coupled receptors are capable of adopting multiple active states. They can be stabilized differently by the ligands which are specific so that only a subset of

the entire signaling pathway can be selectively activated. This concept is known as “functional selectivity”.<sup>85</sup> Each individual ligand leads to differential and independent coupling of the GPCR to different intracellular effectors.<sup>86</sup> In the case of the ligands synthesized in our lab, an explanation for the differential inhibition in calcium mobilization activity and anti-proliferative activity could be functional selectivity of ligands. Despite binding to the same receptor, they cause distinct functional changes. One of the mechanisms could be atypical conformational changes induced by ligand binding.<sup>87</sup> This may result in conformational change that may differentially affect the anti-proliferation activity and calcium mobilization activity.

A comprehensive structure-activity relationship could not be established due to a limited number of ligands synthesized in this series. This limits the number of factors that can be accounted for to establish the quantitative structure activity relationship though some qualitative conclusion can be drawn. However, these studies are the beginning of a thorough analysis of the CCR5 antagonist binding pocket in the CCR5 receptor. Further examination may result in identification of a new lead compound to develop our next generation of CCR5 antagonists.



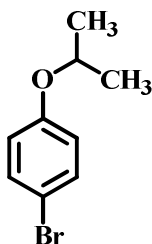
## 6. Experimental Section

### 6.1 Chemical Synthesis:

Melting points were determined on a Fisher-Scientific melting point apparatus. <sup>1</sup>H-NMR and <sup>13</sup>CNMR spectra were obtained on a Bruker 400 MHz spectrometer and tetramethylsilane was used as an internal standard. Infrared spectra were obtained on a Smart iTR diamond ATR spectrometer. Column chromatography was performed on silica gel (grade 60 mesh; Bodman Industries, Aston, PA). Routine thin-layer chromatography (TLC) was performed on silica gel GHIF plates (250 μm, 2.5 x 10 cm; Analtech Inc., Newark, DE). Preparative HPLC was performed on a Varian Microsorb 100-5 C18 column (250 x 4.6mm), using Prostar 325 UV-Vis (254 nm) as the detector.

#### 6.1.1 Synthesis of Intermediates:

##### 1-bromo-4-isopropoxybenzene (5).

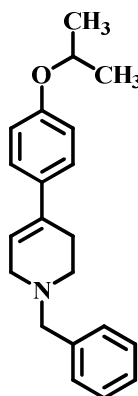


To a solution of 1 equivalent of 4-bromophenol (10.0 g, 57.803 mmol) in 15 mL dimethylformamide (DMF), 1.2 equivalents of potassium carbonate (9.58 g, 69.38 mmol) and 1.5 equivalents of 2-bromopropane (10.66 g, 8.1312 mL, d. 1.311 g/mL, 86.66 mmol) were added while stirring. The suspension was refluxed for 24 hours at 100<sup>0</sup>C on a pre-

heated mantel. The resulting suspension was filtered; the filtrate was concentrated under vacuum to remove DMF. The residue was partitioned between water (40 mL) and dichloromethane (80 mL). The organic layer was washed with brine, dried over sodium sulfate and concentrated to give 1-bromo-4-isopropoxybenzene (9.29 g, 86% yield) as colorless oil.  $^1\text{H NMR}$  (400 MHz,  $\text{CDCl}_3$ )  $\delta$  7.36 (m, 2H), 6.77 (m, 2H), 4.49 (m,  $J= 6.05$  Hz, 1H), 1.33 (d,  $J= 6.08$ , 6H).

**1-benzyl-4-(4-isopropoxyphenyl)-1,2,3,6-tetrahydropyridine (7).**

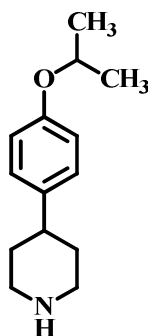
A solution of 1.1 equivalents of 1-bromo-4-isopropoxybenzene (7.5 g, 40.1 mmol) in 5 mL tetrahydrofuran (THF) was added dropwise over a period of 30 minutes to a stirred mixture



of magnesium (0.88 g, 36.4 mmol) and iodine (catalytic amount) in a 500 mL flask. The resulting suspension was refluxed at  $90^{\circ}$  C for 30 minutes on a pre-heated mantel. A solution of 0.9 equivalents of 1-benzyl-4-piperidone (6.2 g, 32.8 mmol) was then added to the suspension drop wise over a period of 30 minutes. The suspension was refluxed at  $90^{\circ}$

C for 40 minutes. After cooling down, ammonium chloride (60 mL) and water (30 mL) were added. The mixture was allowed to stand for some time followed by the addition of 60 mL of 6N HCl. This suspension was refluxed at 100<sup>0</sup> C for 3 hours. The suspension was concentrated in vacuum to remove THF. The product precipitated from the water layer. On filtration, the crude product was obtained. This was purified by column chromatography on silica gel with a hexane: ethyl acetate (20: 1) solvent system to obtain pure 1-benzyl-4-(4-isopropoxyphenyl)-1,2,3,6-tetrahydropyridine (6.6 g, 65.4% yield) as a pale yellow solid. <sup>1</sup>H NMR (400 MHz, CDCl<sub>3</sub>) δ 7.72 (m, 2H), 7.46 (m, 3H), 7.29 (m, 2H), 6.85 (m, 2H), 5.87 (s, 1H), 4.55 (m, *J*= 6.08 Hz, 1H), 4.23 (m, 2H), 3.97 (m, 1H), 3.62 (m, 1H), 3.50 (m, 1H), 3.15 (m, 2H), 2.68 (m, 1H), 1.33 (d, *J*=6.04 Hz, 6H).

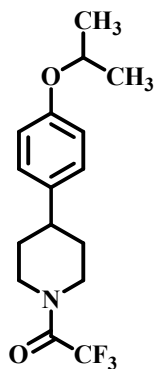
#### 4-(4-isopropoxyphenyl)piperidine (11).



A solution of 1 equivalent of 1-benzyl-4-(4-isopropoxyphenyl)-1,2,3,6-tetrahydropyridine (6 g, 19.51 mmol) in methanol was hydrogenated in a 500 mL hydrogenation flask at 50<sup>0</sup>C-60<sup>0</sup>C in the presence of 10% w/w Pd/C (10%), HCl (0.372 mmol/mL) and HBr (0.2546 mmol/mL) under hydrogen atmosphere at 57 psi for 5 days.

The resulting suspension was filtered over celite to remove catalyst. The filtrate was neutralized with sodium carbonate and concentrated to give 4-(4-isopropoxyphenyl)piperidine (4.19 g, 84% yield) as a pale yellow solid.  $^1\text{H}$  NMR (400MHz,  $\text{CDCl}_3$ ):  $\delta$  7.11 (m, 2H), 6.8 (m, 2H), 4.4 (m,  $J= 6.08$  Hz, 1H), 3.18 (m, 2H), 2.73(m, 2H), 2.55 (m, 1H), 1.82 (m, 2H), 1.61 (m, 2H), 1.31 (d,  $J= 6.04$  Hz, 6H).

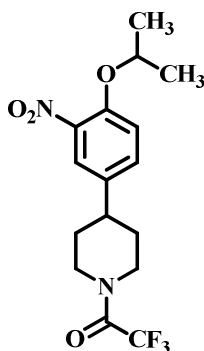
**2,2,2-trifluoro-1-(4-(4-isopropoxyphenyl)piperidine-1-yl)ethanone (14).**



A solution of 1 equivalent of 4-(4-isopropoxyphenyl)piperidine (4 g, 15.63 mmol) and 2.2 equivalents of pyridine (2.71 g, 34.399 mmol) in dichloromethane in a 200 mL flask were stirred on an ice-bath for ten minutes with molecular sieves. To this solution, 1.1 equivalents of trifluoroacetic anhydride (3.61 g, 17.19 mmol) were added dropwise over a period of ten minutes. After stirring at room temperature overnight, the solution was filtered, the filtrate was washed with 1N HCl twice, brine and dried over sodium sulfate. The resulting dichloromethane solution was concentrated to give 2,2,2-trifluoro-1-(4-(4-isopropoxyphenyl)piperidine-1-yl)ethanone (4.43 g, 90% yield) as a reddish-brown oil.  $^1\text{H}$  NMR (400MHz,  $\text{CDCl}_3$ ):  $\delta$  7.08 (m, 2H), 6.83 (m, 2H), 4.66 (m, 1H), 4.5 (m,  $J= 6.08$  Hz,

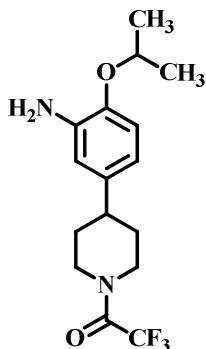
1H), 4.11 (m, 1H), 3.22 (m, 1H), 2.79 (m, 2H), 1.95 (m, 2H), 1.67 (m, 2H), 1.32 (d,  $J=6.08$  Hz, 6H).

**2,2,2-trifluoro-1-(4-(4-isopropoxy-3-nitrophenyl)piperidine-1-yl)ethanone (16).**



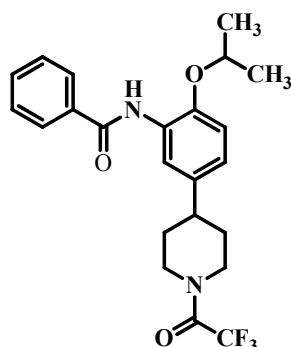
A solution of 1 equivalent of 2,2,2-trifluoro-1-(4-(4-isopropoxyphenyl)piperidine-1-yl)ethanone (4 g, 12.68 mmol) in 20 mL acetic anhydride in a 100 mL flask was stirred in a dry-ice acetone bath at  $-70^{\circ}\text{C}$  for fifteen minutes. To this solution, 10 equivalents of concentrated nitric acid (7.99 g, 5.28 mL, d. 1.512 g/mL, and 126.8 mmol) were added drop wise over a period of thirty minutes. The reaction mixture was stirred at  $-30^{\circ}\text{C}$  for 6 hours. The mixture was then poured into ice (50 mL). The water phase was extracted with 100 mL dichloromethane three times, washed with brine and dried over sodium sulfate. On concentration, 2,2,2-trifluoro-1-(4-(4-isopropoxy-3-nitrophenyl)piperidine-1-yl)ethanone (3.65 g, 80% yield) was obtained as a pale yellow oil.  $^1\text{H}$  NMR (400MHz,  $\text{CDCl}_3$ ):  $\delta$  7.60 (d,  $J=2.32$ , 1H), 7.31 (dd,  $J=2.36$ ,  $J=8.68$  Hz, 1H), 7.03 (d,  $J=8.72$  Hz, 1H), 4.70 (m, 1H), 4.64 (m,  $J=6.04$  Hz, 1H), 4.14 (m, 1H), 3.23 (m, 1H), 2.82 (m, 2H), 1.95 (m, 2H), 1.67 (m, 2H), 1.37 (d,  $J=6.04$ , 6H).

**1-(4-(3-amino-4-isopropoxyphenyl)piperidin-1-yl)-2,2,2-trifluoroethanone (33).**



A solution of 1 equivalent of 2,2,2-trifluoro-1-(4-(4-isopropoxy-3-nitrophenyl)piperidine-1-yl)-ethanone (3.5 g, 9.71 mmol) and 1.2 equivalents of HCl (0.425 g, 0.4051 mL, d. 1.049 g/mL, 11.65 mmol) in methanol was hydrogenated in a 500 mL hydrogenation flask at room temperature. The reaction was carried out in the presence of 10% Pd/C (10%) under an atmosphere of hydrogen for 10 hours. The resulting suspension was filtered over celite to remove catalyst. The filtrate was neutralized with sodium carbonate and concentrated to give 1-(4-(3-amino-4-isopropoxyphenyl)piperidin-1-yl)-2,2,2-trifluoroethanone (1.76 g, 55% yield) as a pale yellow oil.  $^1\text{H}$  NMR (400MHz,  $\text{CDCl}_3$ ):  $\delta$  7.53 (d,  $J= 1.96$  Hz, 1H), 7.12 (dd,  $J= 1.96$  Hz,  $J= 8.6$  Hz, 1H), 6.92 (d,  $J= 8.64$  Hz, 1H), 4.65 (m, 1H), 4.48 (m,  $J= 6.04$  Hz, 1H), 4.11 (m, 1H), 3.19 (m, 1H), 2.79 (m, 2H), 1.95 (m, 2H), 1.65 (m, 2H), 1.39 (d,  $J= 6.04$  Hz, 6H).

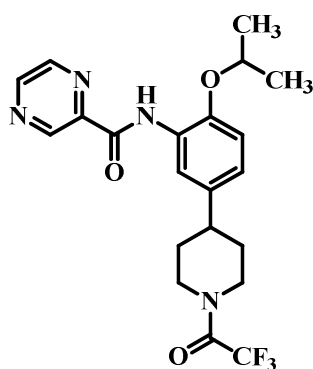
**N-(2-isopropoxy-5-(1-(2,2,2-trifluoroacetyl)piperidine-4-yl)phenyl)benzamide(34):**



On an ice-water bath, to a solution of 2 equivalents of benzoic acid (638.62 mg, 5.598 mmol) in DMF (2 mL), 1.5 equivalents of N-(3-dimethylaminopropyl)-N'-ethylcarbodiimide hydrochloride (EDCI) (804.79 mg, 4.198 mmol), 1.5 equivalents of 1-hydroxybenzotriazole hydrate (HOBT) (567.27 mg, 4.198 mmol), 3 equivalents of triethylamine (TEA) (849.69 mg, 1.16 mL, d. 0.726 g/mL, 8.397 mmol) and molecular sieves (4Å) were added. This mixture was stirred under N<sub>2</sub> protection for 15 minutes. A solution of 1 equivalent of 1-(4-(3-amino-4-isopropoxyphenyl)piperidin-1-yl)-2,2,2-trifluoroethanone (927 mg, 2.799 mmol) in DMF (2 mL) was added to the above reaction mixture. This was allowed to react overnight and proceed from 0<sup>0</sup>C to room temperature. The resulting mixture was filtered through celite and DMF was evaporated. This was dissolved in dichloromethane, washed with brine, dried over sodium sulfate and concentrated. The residue was purified by column chromatography on silica gel with a hexane: ethyl acetate (5:1) solvent system to obtain pure N-(2-isopropoxy-5-(1-(2,2,2-trifluoroacetyl)piperidine-4-yl)phenyl)benzamide (1.1 g, 87.3% yield) as a pale yellow powder. <sup>1</sup>H NMR (400MHz, CDCl<sub>3</sub>): δ 8.67 (br, 1H), 8.49 (s, 1H), 7.87 (m, 2H), 7.52 (m,

3H), 6.87 (s, 2H), 4.69 (m, 1H), 4.63 (m,  $J= 6.08$  Hz, 1H), 4.13 (m, 1H), 3.22 (m, 1H), 2.82 (m, 2H), 2.01 (m, 2H), 1.73 (m, 2H), 1.40 (d,  $J= 6.04$  Hz, 6H).

**N-(2-isopropoxy-5-(1-(2,2,2-trifluoroacetyl)piperidine-4-yl)phenyl)pyrazine-2-carboxamide (61):**

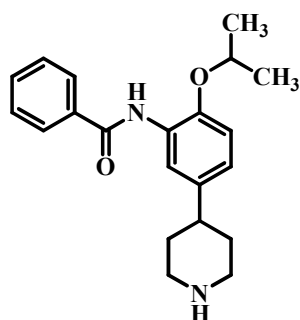


On an ice-water bath, to a solution of 2 equivalents of pyrazine-2-carboxylic acid (755.53 mg, 6.039 mmol) in DMF (2 mL), 1.5 equivalents of N-(3-dimethylaminopropyl)-N'-ethylcarbodiimide hydrochloride (EDCI) (868.06 mg, 4.528 mmol), 1.5 equivalents of 1-hydroxybenzotriazole hydrate (HOBT) (611.86 mg, 4.528 mmol), 3 equivalents of triethylamine (TEA) (916.47 mg, 1.26 mL, d. 0.726 g/mL, 9.057 mmol) and molecular sieves (4Å) were added. This mixture was stirred under N<sub>2</sub> protection for 15 minutes. A solution of 1 equivalent of 1-(4-(3-amino-4-isopropoxyphenyl)piperidin-1-yl)-2,2,2-trifluoroethanone (1 g, 3.019 mmol) in DMF (2 mL) was added to the above reaction mixture. This was allowed to react overnight and proceed from 0<sup>o</sup>C to room temperature. The resulting mixture was filtered through celite and DMF was evaporated. This was dissolved in dichloromethane, washed with brine, dried over sodium sulfate and



concentrated. The residue was purified by column chromatography on silica gel with a hexane: ethyl acetate (5:1) solvent system to obtain pure N-(2-isopropoxy-5-(1-(2,2,2,-trifluoroacetyl)piperidine-4-yl)phenyl)pyrazine-2-carboxamide (1.1 g, 84.6% yield) as a pale yellow powder.  $^1\text{H}$  NMR (400MHz,  $\text{CDCl}_3$ ):  $\delta$  10.40 (br, 1H), 9.49 (d,  $J= 1.4\text{Hz}$ , 1H), 8.79 (d,  $J= 2.4\text{ Hz}$ , 1H), 8.62 (d,d  $J=1.52\text{ Hz}$ ,  $J=2.4\text{ Hz}$ , 1H), 8.51 (s, 1H), 6.90 (s, 2H), 4.68 (m, 1H), 4.62 (m,  $J= 6.04\text{ Hz}$ , 1H), 4.13 (d, 1H), 3.24 (t, 1H), 2.85 (m, 2H), 2.01 (m, 2H), 1.73 (m, 2H), 1.42 (d,  $J= 6.08\text{ Hz}$ , 6H).

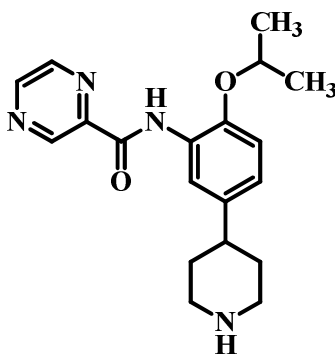
**N-(2-isopropoxy-5-(piperidinn-4-yl)phenyl)benzamide (36) :**



To a solution of 1 equivalent (200 mg, 0.5822 mmol) N-(2-isopropoxy-5-(1-(2,2,2,-trifluoroacetyl)piperidine-4-yl)phenyl)benzamide in methanol (20 mL) and water (5 mL), 5.2 equivalents of potassium carbonate (417.81 mg, 3.027 mmol) was added. The reaction mixture was refluxed at  $100^\circ\text{C}$  for 2 hours. Methanol and water were evaporated off followed by dissolving the contents in dichloromethane. This solution was then washed with saturated sodium bicarbonate solution, brine, dried over sodium sulfate and concentrated to obtain pure N-(2-isopropoxy-5-(piperidinn-4-yl)phenyl)benzamide (152

mg, 98.9% yield) as a pale yellow solid.  $^1\text{H}$  NMR (400MHz,  $\text{CDCl}_3$ ):  $\delta$  8.66 (br, 1H), 8.48 (d,  $J=1.84$  Hz, 1H), 7.88 (m, 2H), 7.51 (m, 3H), 6.91 (d,d,  $J= 1.96$  Hz,  $J= 8.4$  Hz, 1H), 8.86 (d,  $J= 8.4$  Hz, 1H), 4.61 (m,  $J= 6.08$  Hz, 1H), 3.20 (m, 2H), 2.74 (t, 2H), 6.64 (m, 1H), 1.87 (m, 2H), 1.67 (m, 2H), 1.39 (d,  $J= 6.04$  Hz, 6H).

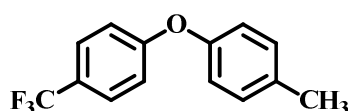
**N-(2-isopropoxy-5-(piperidinn-4-yl)phenyl)pyrazine-2-carboxamide (63) :**



To a solution of 1 equivalent (200 mg, 0.4582 mmol) N-(2-isopropoxy-5-(1-(2,2,2,-trifluoroacetyl)piperidine-4-yl)phenyl)pyrazine-2-carboxamide in methanol (20 mL) and water (5 mL), 5.2 equivalents of potassium carbonate (328 mg, 2.382 mmol) was added. The reaction mixture was refluxed at  $100^{\circ}\text{C}$  for 2 hours. Methanol and water were evaporated off followed by dissolving the contents in dichloromethane. This solution was then washed with saturated sodium bicarbonate solution, brine, dried over sodium sulfate and concentrated to obtain pure N-(2-isopropoxy-5-(piperidinn-4-yl)phenyl)pyrazine-2-carboxamide (152.5 mg, 97.75% yield) as a pale yellow solid.  $^1\text{H}$  NMR (400MHz,  $\text{CDCl}_3$ ):  $\delta$  10.37 (br, 1H), 9.49 (d,  $J= 1.44$  Hz, 1H), 8.78 (d,  $J= 2.44$  Hz, 1H), 8.61 (d,d,  $J= 1.52$  Hz,  $J= 2.44$  Hz, 1H), 8.51 (d,  $J= 2.08$  Hz, 1H), 6.94 (d,d,  $J= 2.08$  Hz,  $J= 8.44$  Hz,

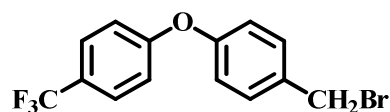
1H), 6.89 (d,  $J = 8.44$  Hz, 1H), 4.57 (m,  $J = 6.08$  Hz, 1H), 3.19 (m, 2H), 2.74 (t, 2H), 2.64 (m, 1H), 1.86 (m, 2H), 1.64 (m, 2H), 1.41 (d,  $J = 6.04$  Hz, 6H).

**1-Methyl-4-(4'-trifluoromethylphenoxy)benzene (28).**



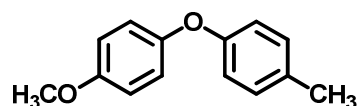
In a 10 mL glass tube, 1 equivalent of p-cresol (480.57 mg, 4.444 mmol), 0.5 equivalent of 4-trifluorobromobenzene (500 mg, 2.222 mmol), 0.1 equivalent of tetramethyl ethylene diamine (TMEDA) (51.59 mg, 0.444 mmol), 1 equivalent of potassium tert-butoxide (498.68 mg, 4.444 mmol) and 0.05 equivalent of copper iodide (70.45 mg, 0.222 mmol) were added with 1.5 mL DMF as the solvent. The glass tube was tightly closed with a cork and placed in the microwave. The temperature and time were set to 125<sup>0</sup>C and 25 minutes respectively. After 25 minutes, the contents were filtered through celite to remove the catalyst. The crude compound was purified by column chromatography on silica gel with hexane: ethyl acetate (40:1) as the solvent system. 1-Methyl-4-(4'-trifluoromethylphenoxy)benzene was obtained as white shining crystals (522 mg, 93.13% yield). <sup>1</sup>H NMR (400MHz, CDCl<sub>3</sub>):  $\delta$  7.54 (m, 2H), 7.18 (m, 2H), 7 (m, 2H), 6.94 (m, 2H), 2.35 (s, 1H).

**1-(bromomethyl)-4-(4'-(trifluoromethyl)phenoxy)benzene (40).**



In a 50 mL three-necked round bottom flask, 0.8 equivalent of 1-Methyl-4-(4'-trifluoromethylphenoxy)benzene (200 mg, 1.085 mmol) was dissolved in 4 mL carbon tetra chloride which was used as the solvent of this reaction. To this suspension, 1 equivalent of N-bromosuccinimide (NBS) (242 mg, 1.3597 mmol) and 0.02 equivalent of azobisisobutyronitrile (AIBN) (6 mg, 0.03656 mmol) were added. This reaction mixture was refluxed for 2 hours under N<sub>2</sub> protection on a pre-heated mantel at 81<sup>0</sup>C – 82<sup>0</sup>C. The solvent was evaporated and the crude compound was purified by column chromatography on silica gel using hexane: ethyl acetate (40:1) as the solvent system. 1-(bromomethyl)-4-(4'-(trifluoromethyl)phenoxy)benzene was obtained as a pale yellow oil (150 mg, 51.16% yield). <sup>1</sup>H NMR (400MHz, CDCl<sub>3</sub>): δ 7.57 (d, 2H), 7.39 (d, 2H), 7.05 (d, 2H), 6.95 (d, 2H), 4.49 (s, 1H).

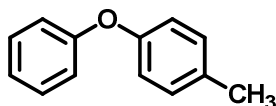
**1-methoxy-4-(p-tolyloxy)benzene (18):**



In a 50 mL three necked round bottom flask, 1 equivalent of p-cresol (1 g, 9.24 mmol), 0.769 equivalents of 4-bromoanisole (1.328 g, 7.105 mmol), 0.846 equivalents of cesium carbonate (2.5 g, 7.817 mmol), and 0.0038 equivalents of copper bromide (7.8 mg, 0.0351 mmol) were added. 1 mL of N-methylpyrrolidone (NMP) was added to the above mixture. The reaction mixture was refluxed for 16 hours on a pre-heated mantel at 160<sup>0</sup>C. The reaction was quenched with acetonitrile (5 mL). The resulting suspension was filtered

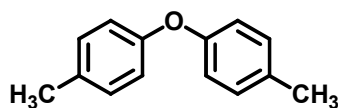
through celite to remove the catalyst. The product was purified by column chromatography on silica gel with a hexyl: ethyl acetate (40:1) solvent system. Pure 1-methoxy-4-(p-tolyloxy)benzene was obtained (1.65 g, 83.4% yield) as a pale yellow solid.  $^1\text{H}$  NMR (400MHz,  $\text{CDCl}_3$ ):  $\delta$  7.10 (m, 2H), 6.96 (m, 2H), 6.86 (m, 4H), 6.94 (m, 2H), 3.80 (s, 3H), 2.32 (s, 3H).

**1-methyl-4-phenoxybenzene (19):**



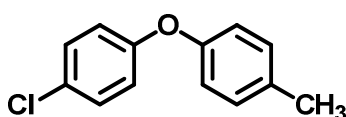
In a 50 mL three necked round bottom flask, 1 equivalent of p-cresol (1 g, 9.24 mmol), 0.769 equivalents of 4-bromobenzene (1.115 g, 7.105 mmol), 0.846 equivalents of cesium carbonate (2.5 g, 7.817 mmol), and 0.0038 equivalents of copper bromide (7.8 mg, 0.0351 mmol) were added. 1 mL of N-methylpyrrolidone (NMP) was added to the above mixture. The reaction mixture was refluxed for 16 hours on a pre-heated mantel at  $160^{\circ}\text{C}$ . The reaction was quenched with acetonitrile (5 mL). The resulting suspension was filtered through celite to remove the catalyst. The product was purified by column chromatography on silica gel with a hexyl: ethyl acetate (40:1) solvent system. Pure 1-methyl-4-phenoxybenzene was obtained (1.30 g, 76.8% yield) as a pale yellow solid.  $^1\text{H}$  NMR (400MHz,  $\text{CDCl}_3$ ):  $\delta$  7.29 (m, 2H), 7.12 (m, 2H), 7.04 (m, 1H), 6.97 (m, 2H), 6.90 (m, 2H), 2.32 (s, 3H).

**4,4'-oxybis(methylbenzene) (25):**



In a 50 mL three necked round bottom flask, 1 equivalent of p-cresol (1 g, 9.24 mmol), 0.769 equivalents of 4-bromotoluene (1.215 g, 7.105 mmol), 0.846 equivalents of cesium carbonate (2.5 g, 7.817 mmol), and 0.0038 equivalents of copper bromide (7.8 mg, 0.0351 mmol) were added. 1 mL of N-methylpyrrolidone (NMP) was added to the above mixture. The reaction mixture was refluxed for 16 hours on a pre-heated mantel at 160<sup>0</sup>C. The reaction was quenched with acetonitrile (5 mL). The resulting suspension was filtered through celite to remove the catalyst. The product was purified by column chromatography on silica gel with a hexyl: ethyl acetate (40:1) solvent system. Pure 4,4'-oxybis(methylbenzene) was obtained (1.01 g, 72% yield) as a pale yellow solid. <sup>1</sup>H NMR (400MHz, CDCl<sub>3</sub>): δ 7.12 (d, *J*= 8.16 Hz, 4H), 6.82 (d, *J*= 8.52 Hz, 4H), 2.29 (s, 6H).

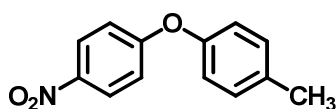
**1-chloro-4-(p-tolyloxy)benzene (24):**



In a 50 mL three necked round bottom flask, 1 equivalent of p-cresol (500 mg, 4.62 mmol), 0.769 equivalents of 4-chlorobromobenzene (777.4 mg, 3.55 mmol), 0.846 equivalents of cesium carbonate (1.2 g, 3.91 mmol), and 0.0038 equivalents of copper bromide (3.9 mg, 0.0175 mmol) were added. 1 mL of N-methylpyrrolidone (NMP) was added to the above mixture. The reaction mixture was refluxed for 16 hours on a pre-

heated mantel at 160<sup>0</sup>C. The reaction was quenched with acetonitrile (5 mL). The resulting suspension was filtered through celite to remove the catalyst. The product was purified by column chromatography on silica gel with a hexyl: ethyl acetate (40:1) solvent system. Pure 1-chloro-4-(p-tolyloxy)benzene was obtained (551 mg, 62.05% yield) as a pale yellow solid. <sup>1</sup>H NMR (400MHz, CDCl<sub>3</sub>): δ 7.29 (m, 2H), 7.17 (m, 2H), 6.89 (m, 4H), 2.31 (s, 3H).

**1-methyl-4-(4-nitrophenoxy)benzene (31):**

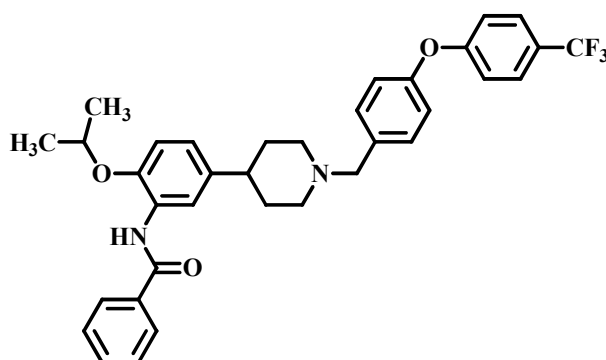


In a 50 mL three necked round bottom flask, 1 equivalent of p-cresol (535.3 mg, 4.95 mmol), 0.5 equivalents of 1-bromo-4-nitrobenzene (500 mg, 2.47 mmol), 0.1 equivalents of TMEDA (57.5 mg, 0.495 mmol), 1 equivalent of potassium tertbutoxide (555.43 mg, 4.95 mmol), and 0.05 equivalents of copper iodide (78.54 mg, 0.247 mmol) were added. 3 mL of DMF was added to the above mixture. The reaction mixture was refluxed for 16 hours on a pre-heated mantel at 125<sup>0</sup>C. The resulting suspension was filtered through celite to remove the catalyst. The product was purified by column chromatography on silica gel with a hexyl: ethyl acetate (40:1) solvent system. Pure 1-methyl-4-(4-nitrophenoxy)benzene was obtained (517 mg, 91.12% yield) as a yellow solid. <sup>1</sup>H NMR (400MHz, CDCl<sub>3</sub>): δ 8.18 (m, 2H), 7.22 (m, 2H), 6.98 (m, 4H), 2.38 (s, 3H).

## 6.1.2 Synthesis of Final Compounds:

### A. Phenyl substituted compounds:

**N-(2-Isopropoxy-5-(1-(4-(4-(trifluoromethyl)phenoxy)benzyl)piperidin-4-yl)phenyl)benzamide (41).**

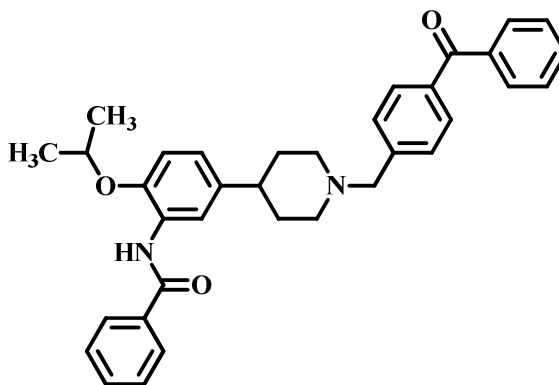


To a solution of 1 equivalent of N-(2-isopropoxy-5-(piperidin-4-yl)phenyl)benzamide (94 mg, 0.277 mmol) in 5 mL DMF, 1.5 equivalents of potassium carbonate (57.57 mg, 0.4166 mmol) and catalytic amount of potassium iodide were added. This mixture was stirred at 0°C on an ice-water bath for 15 minutes. This was followed by the addition of 1.2 equivalents of 1-(bromomethyl)-4-(4-(trifluoromethyl)phenoxy)benzene (110.33 mg, 0.3332 mmol) dropwise over a period of five minutes. This reaction mixture was allowed to run overnight from 0°C to room temperature. DMF was evaporated and the contents were dissolved in dichloromethane. The crude compound was purified by column chromatography on silica gel with dichloromethane: methanol (100:1) as the solvent system with 1% NH<sub>4</sub>OH. The pure compound was obtained as pale yellow oil (85 mg, 52% yield). <sup>1</sup>H NMR (400MHz,



CDCl<sub>3</sub>):  $\delta$  8.6 (br, 1H), 8.50 (d,  $J= 1.88$  Hz, 1H), 7.88 (m, 2H), 7.49 (m, 5H), 7.39 (m, 2H), 7.03 (m, 4H), 6.92 (d,d,  $J= 2.04$  Hz,  $J= 8.40$  Hz, 1H), 6.86 (d,  $J= 8.48$  Hz, 1H), 4.59 (m,  $J= 6.04$  Hz, 1H), 3.56 (s, 2H), 3.04 (m, 2H), 2.54 (m, 1H), 2.11 (s, 2H), 1.86 (s, 4H), 1.39 (d,  $J= 6.04$  Hz, 6H). <sup>13</sup>C NMR (400MHz, CDCl<sub>3</sub>):  $\delta$  164.93, 144.74, 135.39, 131.68, 130.94, 128.84, 128.69, 127.81, 127.15, 127.11, 127.08, 127.04, 126.91, 121.43, 119.71, 118.72, 117.79, 112.65, 71.62, 62.56, 54.23, 42.07, 33.36, 22.36. IR (Smart iTR diamond ATR, cm<sup>-1</sup>) 3421, 1672, 1325, 1246, 1105, 1064. MS m/z: 589. This compound was converted to the corresponding hydrochloride salt and a white powder was collected which had a melting point of 159<sup>0</sup>C - 160<sup>0</sup>C.

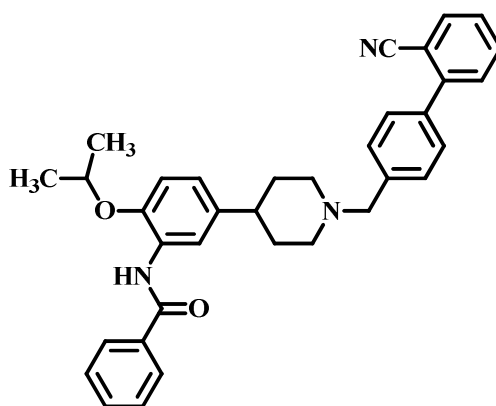
**N-(5-(1-(4-benzoylbenzyl)piperidin-4-yl)-2-isopropoxyphenyl)benzamide (67).**



To a solution of 1 equivalent of N-(2-isopropoxy-5-(piperidin-4-yl)phenyl)benzamide (70 mg, 0.2068 mmol) in 5 mL DMF, 1.5 equivalents of potassium carbonate (42.81 mg, 0.3102 mmol) and catalytic amount of potassium iodide were added. This mixture was stirred at 0<sup>0</sup>C on an ice-water bath for 15 minutes. This was followed by the addition of 1.2 equivalents of (4-(bromomethyl)phenyl)(phenyl)methanone (68.26 mg,

0.2481 mmol) drop wise over a period of five minutes. This reaction mixture was allowed to run over night from 0<sup>0</sup>C to room temperature. DMF was evaporated and the contents were dissolved in dichloromethane. The crude compound was purified by column chromatography on silica gel with dichloromethane: methanol (100:1) as the solvent system with 1% NH<sub>4</sub>OH. The pure compound was obtained as pale yellow oil (71 mg, 64.44% yield). <sup>1</sup>H NMR (400MHz, CDCl<sub>3</sub>): δ 8.6 (br, 1H), 8.51 (d, *J*= 2.0 Hz, 1H), 7.90 (m, 2H), 7.81 (m, 4H), 7.57 (m, 2H), 7.49 (m, 6H), 6.93 (d,d, *J*= 2.12 Hz, *J*= 8.40 Hz, 1H), 6.86 (d, *J*= 8.48 Hz, 1H), 4.59 (m, *J*= 6.08 Hz, 1H), 3.63 (s, 2H), 3.03 (m, 2H), 2.54 (m, 1H), 2.14 (s, 2H), 1.86 (s, 4H), 1.39 (d, *J*= 6.04 Hz, 6H). <sup>13</sup>C NMR (400MHz, CDCl<sub>3</sub>): δ 196.53, 164.91, 144.71, 137.84, 136.36, 135.40, 132.26, 131.66, 130.18, 130.03, 128.90, 128.83, 128.70, 128.24, 126.91, 121.46, 118.67, 112.62, 71.61, 63.03, 54.46, 42.12, 33.55, 22.37. IR (Smart iTR diamond ATR, cm<sup>-1</sup>) 3410, 1656, 1531, 1276. MS m/z: 533. This compound was converted to the corresponding hydrochloride salt and a white powder was collected which had a melting point of 116<sup>0</sup>C - 117<sup>0</sup>C.

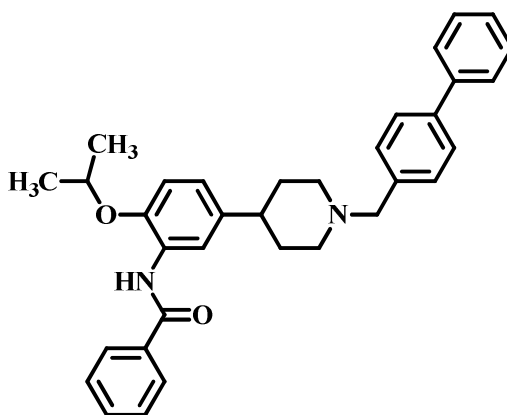
**N-(5-(1-((2'-cyano-[1,1'-biphenyl]-4-yl)methyl)piperidin-4-yl)-2-isopropoxyphenyl)benzamide (68).**



To a solution of 1 equivalent of N-(2-isopropoxy-5-(piperidin-4-yl)phenyl)benzamide (70 mg, 0.2068 mmol) in 5 mL DMF, 1.5 equivalents of potassium carbonate (42.81 mg, 0.3102 mmol) and catalytic amount of potassium iodide were added. This mixture was stirred at 0°C on an ice-water bath for 15 minutes. This was followed by the addition of 1.2 equivalents of 4'-(bromomethyl)-[1,1'-biphenyl]-2-carbonitrile (67.51 mg, 0.2481 mmol) dropwise over a period of five minutes. This reaction mixture was allowed to run over night from 0°C to room temperature. DMF was evaporated and the contents were dissolved in dichloromethane. The crude compound was purified by column chromatography on silica gel with dichloromethane: methanol (100:1) as the solvent system with 1% NH<sub>4</sub>OH. The pure compound was obtained as pale yellow oil (52 mg, 47.46% yield). <sup>1</sup>H NMR (400MHz, CDCl<sub>3</sub>): δ 8.6 (br, 1H), 8.50 (d, *J*= 1.96 Hz, 1H), 7.88 (m, 2H), 7.76 (m, 1H), 7.64 (t, *J*= 7.76 Hz, 1H), 7.52 (m, 8H), 7.42 (t, *J*= 7.64 Hz, 1H), 6.93 (d,d, *J*= 2.08 Hz, *J*= 8.40 Hz, 1H), 6.86 (d, *J*= 8.48 Hz, 1H), 4.58 (m, *J*= 6.0 Hz, 1H), 3.64 (s, 2H), 3.07 (m, 2H), 2.55 (m, 1H), 2.16 (s, 2H), 1.87 (s, 4H), 1.40 (d, *J*= 6.04 Hz, 6H). <sup>13</sup>C NMR (400MHz, CDCl<sub>3</sub>): δ 164.90, 145.38, 144.71, 135.42, 133.77, 132.78,

131.64, 130.10, 129.55, 129.43, 128.82, 128.66, 125.54, 127.40, 126.91, 121.43, 118.81, 118.76, 112.64, 111.21, 71.55, 62.94, 54.40, 42.11, 33.48, 22.37. IR (Smart iTR diamond ATR,  $\text{cm}^{-1}$ ) 3412, 2224, 1668, 1325, 1249. MS  $m/z$ : 530. This compound was converted to the corresponding hydrochloride salt and a white powder was collected which had a melting point of  $128^{\circ}\text{C}$  -  $129^{\circ}\text{C}$ .

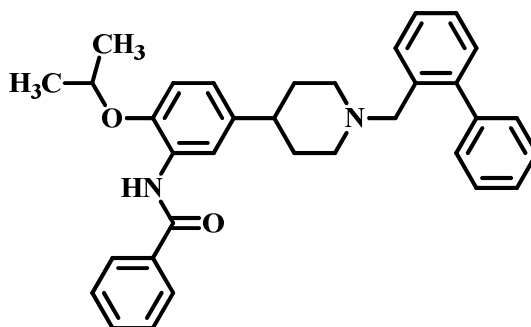
**N-(5-(1-([1,1'-biphenyl]-4-ylmethyl)piperidin-4-yl)-2-isopropoxyphenyl)benzamide (73).**



To a solution of 1 equivalent of N-(2-isopropoxy-5-(piperidin-4-yl)phenyl)benzamide (80 mg, 0.236 mmol) in 5 mL DMF, 1.5 equivalents of potassium carbonate (44.4 mg, 0.322 mmol) and catalytic amount of potassium iodide were added. This mixture was stirred at  $0^{\circ}\text{C}$  on an ice-water bath for 15 minutes. This was followed by the addition of 1.2 equivalents of 4-(chloromethyl)-1,1'-biphenyl (52.08 mg, 0.257 mmol) dropwise over a period of five minutes. This reaction mixture was allowed to run overnight from  $0^{\circ}\text{C}$  to room temperature. DMF was evaporated and the contents were

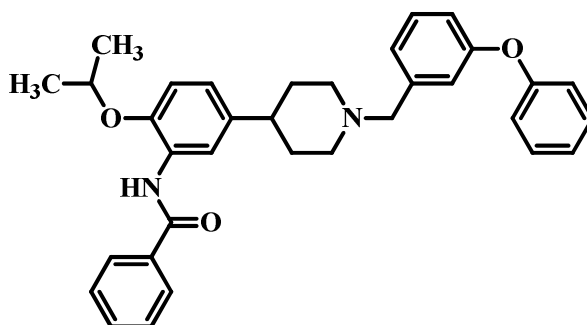
dissolved in dichloromethane. The crude compound was purified by column chromatography on silica gel with dichloromethane: methanol (100:1) as the solvent system with 1%  $\text{NH}_4\text{OH}$ . The pure compound was obtained as pale yellow oil (52 mg, 47.46% yield).  $^1\text{H}$  NMR (400MHz,  $\text{CDCl}_3$ ):  $\delta$  8.65 (br, 1H), 8.50 (d,  $J= 2.0$  Hz, 1H), 7.88 (m, 2H), 7.55 (m, 7H), 7.43 (m, 4H), 7.33 (m, 1H), 6.92 (d,d,  $J= 2.08$  Hz,  $J= 8.40$  Hz, 1H), 6.85 (d,  $J= 8.48$  Hz, 1H), 4.58 (m,  $J= 6.04$  Hz, 1H), 3.61 (s, 2H), 3.07 (m, 2H), 2.53 (m, 1H), 2.14 (s, 2H), 1.86 (s, 4H), 1.39 (d,  $J= 6.04$  Hz, 6H).  $^{13}\text{C}$  NMR (400MHz,  $\text{CDCl}_3$ ):  $\delta$  164.90, 144.71, 135.43, 129.70, 128.82, 128.72, 128.68, 127.09, 126.99, 126.92, 121.41, 118.77, 112.65, 71.61, 54.35, 42.19, 33.52, 22.37. IR (Smart iTR diamond ATR,  $\text{cm}^{-1}$ ) 3412, 1666, 1248, 1074. MS  $m/z$ : 505. This compound was converted to the corresponding hydrochloride salt and a white powder was collected which had a melting point of  $189^\circ\text{C} - 190^\circ\text{C}$ .

**N-(5-(1-([1,1'-biphenyl]-2-ylmethyl)piperidin-4-yl)-2-isopropoxyphenyl)benzamide (72).**



To a solution of 1 equivalent of N-(2-isopropoxy-5-(piperidin-4-yl)phenyl)benzamide (80 mg, 0.236 mmol) in 5 mL methanol, 1.5 equivalents of pyridine (25.44 mg, d. 0.9819 g/mL, 0.025 mL, 0.322 mmol) was added. This mixture was stirred at 60°C on a pre-heated mantel for 15 minutes. This was followed by the addition of 1.2 equivalents of 2-(bromomethyl)-1,1'-biphenyl (63.5 mg, 0.257 mmol) drop wise over a period of five minutes. The reaction mixture was refluxed overnight at 70°C. Methanol was evaporated and the contents were dissolved in dichloromethane. Pyridine was removed by washing with 20 mL 1N HCl twice followed by extraction of the organic layer with dichloromethane. The crude compound was purified by column chromatography on silica gel with dichloromethane: methanol (100:1) as the solvent system with 1% NH<sub>4</sub>OH. The pure compound was obtained as pale yellow oil (56 mg, 46.97%). <sup>1</sup>H NMR (400MHz, CDCl<sub>3</sub>): δ 8.65 (br, 1H), 8.46 (d, *J*= 1.92 Hz, 1H), 7.88 (m, 2H), 7.53 (m, 4H), 7.35 (m, 8H), 6.89 (d,d, *J*= 1.84 Hz, *J*= 8.40 Hz, 1H), 6.84 (d, *J*= 8.44 Hz, 1H), 4.57 (m, *J*= 6.04 Hz, 1H), 3.42 (s, 2H), 2.92 (m, 2H), 2.44 (m, 1H), 1.95 (m, 2H), 1.77 (s, 4H), 1.38 (d, *J*= 6.08 Hz, 6H). <sup>13</sup>C NMR (400MHz, CDCl<sub>3</sub>): δ 164.90, 144.65, 142.54, 141.62, 139.67, 136.35, 135.44, 131.63, 129.96, 129.86, 129.59, 128.82, 128.67, 127.85, 127.13, 127.09, 126.91, 126.78, 126.55, 121.48, 118.66, 114.76, 112.61, 71.62, 60.11, 54.10, 42.21, 33.73, 22.38. IR (Smart iTR diamond ATR, cm<sup>-1</sup>) 3415, 1668, 1247, 1073. MS m/z: 505. This compound was converted to the corresponding hydrochloride salt and a white powder was collected which had a melting point of 104°C - 105°C.

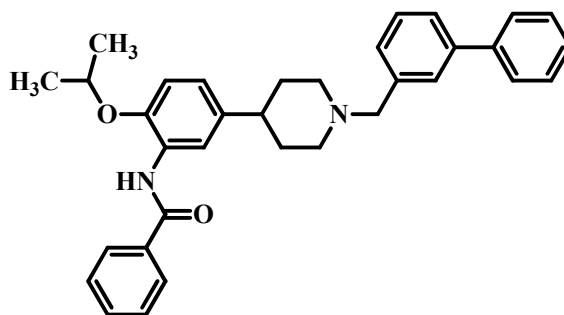
**N-(2-isopropoxy-5-(1-(3-phenoxybenzyl)piperidin-4-yl)phenyl)benzamide (74).**



To a solution of 1 equivalent of N-(2-isopropoxy-5-(piperidin-4-yl)phenyl)benzamide (80 mg, 0.236 mmol) in 5 mL methanol, 1.5 equivalents of pyridine (25.44 mg, d. 0.9819 g/mL, 0.025 mL, 0.322 mmol) was added. This mixture was stirred at 60°C on a pre-heated mantel for 15 minutes. This was followed by the addition of 1.2 equivalents of 1-(chloromethyl)-3-phenoxybenzene (56.2 mg, 0.257 mmol) drop wise over a period of five minutes. This reaction mixture was refluxed overnight at 70°C. Methanol was evaporated and the contents were dissolved in dichloromethane. Pyridine was removed by washing with 20 mL 1N HCl twice followed by extraction of the organic layer with dichloromethane. The crude compound was purified by column chromatography on silica gel with dichloromethane: methanol (100:1) as the solvent system with 1% NH<sub>4</sub>OH. The pure compound was obtained as pale yellow oil (51 mg, 42.7%). <sup>1</sup>H NMR (400MHz, CDCl<sub>3</sub>): δ 8.65 (br, 1H), 8.48 (d, *J*= 1.86 Hz, 1H), 7.86 (m, 2H), 7.55 (m, 3H), 7.31 (m, 3H), 7.03 (m, 4H), 6.90 (d,d, *J*= 2.04 Hz, *J*= 8.40 Hz, 1H), 6.85 (d, *J*= 8.44 Hz, 1H), 4.58 (m, *J*= 6.04 Hz, 1H), 3.54 (s, 2H), 3.01 (m, 2H), 2.51 (m, 1H), 2.10 (m, 2H), 1.83 (s, 4H), 1.85 (d, *J*= 6.08 Hz, 6H). <sup>13</sup>C NMR (400MHz, CDCl<sub>3</sub>): δ 164.90, 157.15, 135.43, 131.64, 129.71, 128.82, 128.13, 126.92, 123.09, 121.37, 119.74,

119.08, 118.84, 118.78, 112.65, 71.61, 63.02, 54.29, 42.12, 33.05, 22.38. IR (Smart iTR diamond ATR,  $\text{cm}^{-1}$ ) 3416, 1667, 1253, 1072. MS  $m/z$ : 521. This compound was converted to the corresponding hydrochloride salt and a white powder was collected which had a melting point of  $94^{\circ}\text{C} - 95^{\circ}\text{C}$ .

**N-(5-(1-([1,1'-biphenyl]-3-ylmethyl)piperidin-4-yl)-2-isopropoxyphenyl)benzamide (71).**



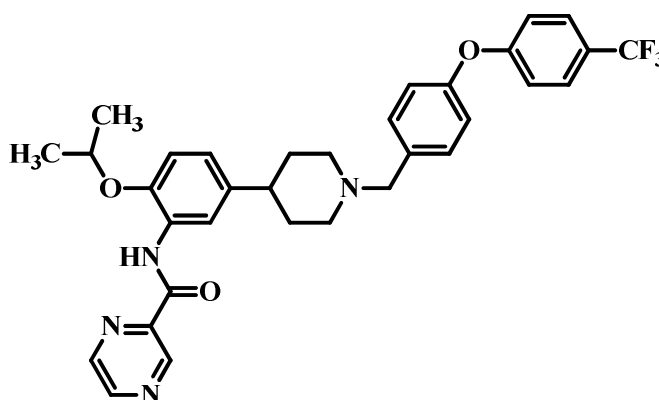
To a solution of 1 equivalent of N-(2-isopropoxy-5-(piperidin-4-yl)phenyl)benzamide (50 mg, 0.1477 mmol) in 5 mL methanol, 1.5 equivalents of pyridine (17.50 mg, d. 0.9819 g/mL, 0.017 mL, 0.2216 mmol) was added. This mixture was stirred at  $60^{\circ}\text{C}$  on a pre-heated mantel for 15 minutes. This was followed by the addition of 1.2 equivalents of 3-(bromomethyl)-1,1'-biphenyl (43.79, 0.1772 mmol) dropwise over a period of five minutes. This reaction mixture was refluxed overnight at  $70^{\circ}\text{C}$ . Methanol was evaporated and the contents were dissolved in dichloromethane. Pyridine was removed by washing with 20 mL 1N HCl twice followed by extraction of the organic layer with dichloromethane. The crude compound was purified by column chromatography on silica gel with dichloromethane: methanol (100:1) as the solvent



system with 1% NH<sub>4</sub>OH. The pure compound was obtained as pale yellow oil (37 mg, 49.63% yield). <sup>1</sup>H NMR (400MHz, CDCl<sub>3</sub>): δ 8.6 (br, 1H), 8.49 (d, *J*= 1.96 Hz, 1H), 7.87 (m, 2H), 7.61 (m, 3H), 7.53 (m, 4H), 7.42 (m, 3H), 7.34 (m, 2H), 6.92 (d,d, *J*= 2.12 Hz, *J*= 8.44 Hz, 1H), 6.85 (d, *J*= 8.44 Hz, 1H), 4.60 (m, *J*= 6.0 Hz, 1H), 3.63 (s, 2H), 3.06 (m, 2H), 2.51 (m, 1H), 2.13 (s, 2H), 1.83 (s, 4H), 1.38 (d, *J*= 6.04 Hz, 6H). ). <sup>13</sup>C NMR (400MHz, CDCl<sub>3</sub>): δ 164.87, 144.68, 141.20, 141.14, 139.41, 138.86, 135.41, 131.63, 128.81, 128.70, 128.66, 128.63, 128.22, 128.02, 127.79, 127.23, 127.18, 126.89, 125.86, 121.43, 118.74, 112.64, 71.59, 63.43, 54.35, 42.17, 33.50, 22.67. IR (Smart iTR diamond ATR, cm<sup>-1</sup>) 3416, 1667, 1249, 1074. MS *m/z*: 505. This compound was converted to the corresponding hydrochloride salt and a white powder was collected which had a melting point of 111<sup>o</sup>C - 112<sup>o</sup>C.

### B. Pyrazine substituted compounds:

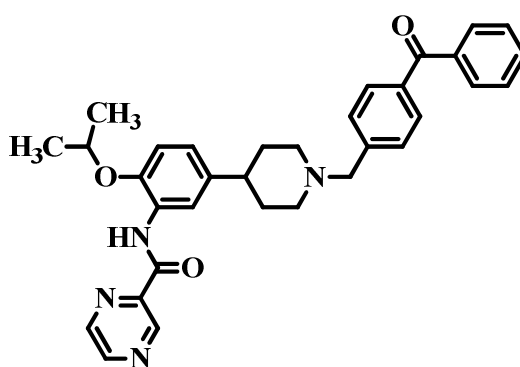
**N-(2-isopropoxy-5-(1-(4-(4-(trifluoromethyl)phenoxy)benzyl)piperidin-4-yl)phenyl)pyrazine-2-carboxamide (II-17).**



To a solution of 1 equivalent of N-(2-isopropoxy-5-(piperidin-4-yl)phenyl)pyrazine-2-carboxamide (70 mg, 0.2056 mmol) in 5 mL methanol, 1.5 equivalents of pyridine (24.37 mg, d. 0.9819 g/mL, 0.024 mL, 0.3084 mmol) was added. This mixture was stirred at 60°C on a pre-heated mantle for 15 minutes. This was followed by the addition of 1.2 equivalents of 1-(bromomethyl)-4-(4-(trifluoromethyl)phenoxy)benzene (81.68 mg, 0.2467 mmol) dropwise over a period of five minutes. This reaction mixture was refluxed overnight at 70°C. Methanol was evaporated and the contents were dissolved in dichloromethane. Pyridine was removed by washing with 20 mL 1N HCl twice followed by extraction of the organic layer with dichloromethane. The crude compound was purified by column chromatography on silica gel with dichloromethane: methanol (100:1) as the solvent system with 1% NH<sub>4</sub>OH. The pure compound was obtained as pale yellow oil (43 mg, 35.42%). <sup>1</sup>H NMR (400MHz, CDCl<sub>3</sub>): δ 10.37 (br, 1H), 9.50 (d, *J*= 1.44 Hz, 1H), 8.78 (d, *J*= 2.44 Hz, 1H), 8.60 (d,d, *J*= 1.52 Hz, *J*= 2.4 Hz, 1H), 8.53 (d, *J*= 2.04 Hz, 1H), 7.57 (d, *J*= 8.6 Hz, 2H), 7.39 (d, *J*= 8.24 Hz, 2H), 7.03 (m, 4H), 6.95 (d,d, *J*= 2.08 Hz, *J*= 8.40 Hz, 1H), 6.89 (d, *J*= 8.44 Hz, 1H), 4.56 (m, *J*= 6.04 Hz, 1H), 3.56 (s, 2H), 3.04 (m, 2H), 2.54 (m, 1H), 2.12 (s, 2H), 1.86 (s, 4H), 1.39 (d, *J*= 6.04 Hz, 6H). <sup>13</sup>C NMR (400MHz, CDCl<sub>3</sub>): δ 160.51, 147.81, 145.42, 145.18, 144.58, 142.64, 130.84, 128.29, 127.12, 127.08, 122.18, 119.71, 118.76, 117.76, 113.58, 72.14, 63.03, 54.31, 42.12, 33.55, 22.37. IR (Smart iTR diamond ATR, cm<sup>-1</sup>) 3343, 1691, 1228, 1050. MS *m/z*: 591. This compound was converted to the

corresponding hydrochloride salt and a white powder was collected which had a melting point of 210<sup>0</sup>C - 212<sup>0</sup>C

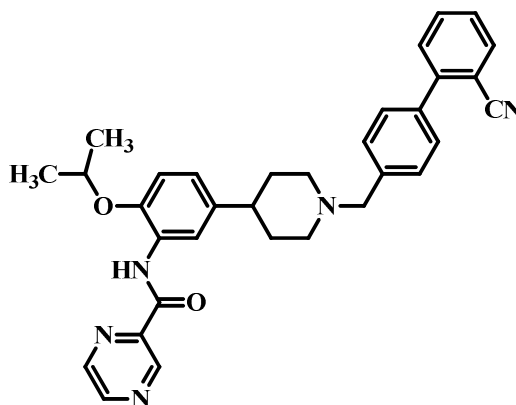
**N-(5-(1-(4-benzoylbenzyl)piperidin-4-yl)-2-isopropoxyphenyl)pyrazine-2-carboxamide (64).**



To a solution of 1 equivalent of N-(2-isopropoxy-5-(piperidin-4-yl)phenyl)pyrazine-2-carboxamide (55 mg, 0.1615 mmol) in 5 mL DMF, 1.5 equivalents of potassium carbonate (33.43mg, 0.2422 mmol) was added. This mixture was stirred at 0<sup>0</sup>C on an ice-water bath for 15 minutes. This was followed by the addition of 1.2 equivalents of (4-(bromomethyl)phenyl)(phenyl)methanone (53.32 mg, 0.1938 mmol) drop wise over a period of five minutes. This reaction mixture was allowed to run overnight from 0<sup>0</sup>C to room temperature. DMF was evaporated and the contents were dissolved in dichloromethane. The crude compound was purified by column chromatography on silica gel with dichloromethane: methanol (100:1) as the solvent system with 1% NH<sub>4</sub>OH. The pure compound was obtained as pale yellow oil (58 mg, 67.14%). <sup>1</sup>H NMR (400MHz, CDCl<sub>3</sub>): δ 10.38 (br, 1H), 9.49 (d, *J*= 1.44 Hz, 1H), 8.78 (d,

$J= 2.44$  Hz, 1H), 8.61 (d,d,  $J= 1.48$  Hz,  $J= 2.4$  Hz, 1H), 8.53 (d,  $J= 2.08$  Hz, 1H), 7.81 (m, 5H), 7.56 (m, 1H), 7.49 (m, 4H), 6.95 (d,d,  $J= 2.08$  Hz,  $J= 8.40$  Hz, 1H), 6.89 (d,  $J= 8.44$  Hz, 1H), 4.57 (m,  $J= 6.08$  Hz, 1H), 3.62 (s, 2H), 3.02 (m, 2H), 2.53 (m, 1H), 2.14 (s, 2H), 1.85 (s, 4H), 1.41 (d,  $J= 6.04$  Hz, 6H).  $^{13}\text{C}$  NMR (400MHz,  $\text{CDCl}_3$ ):  $\delta$  160.47, 144.71, 137.84, 136.36, 135.40, 132.26, 131.66, 130.18, 130.03, 128.90, 128.83, 128.70, 128.24, 126.91, 121.46, 118.67, 112.62, 71.61, 63.03, 54.46, 42.12, 33.55, 22.37. IR(Smart iTR diamond ATR,  $\text{cm}^{-1}$ ) 3368, 1681, 1635, 1223, 1051. MS  $m/z$ : 535. This compound was converted to the corresponding hydrochloride salt and a white powder was collected which had a melting point of  $130^\circ\text{C} - 131^\circ\text{C}$ .

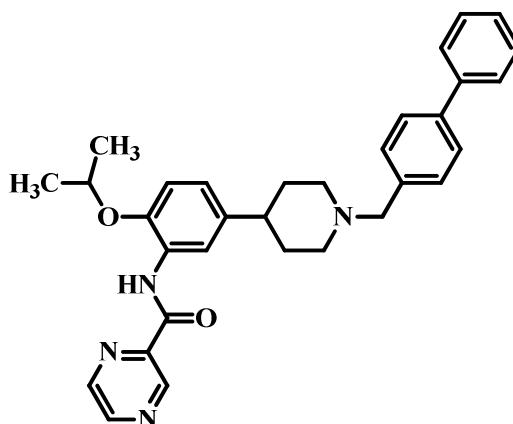
**N-(5-(1-((2'-cyano-[1,1'-biphenyl]-4-yl)methyl)piperidin-4-yl)-2-isopropoxyphenyl)pyrazine-2-carboxamide (II-3).**



To a solution of 1 equivalent of N-(2-isopropoxy-5-(piperidin-4-yl)phenyl)pyrazine-2-carboxamide (73 mg, 0.2144 mmol) in 5 mL methanol, 1.5 equivalents of pyridine (44.38 mg, d. 0.9819 g/mL, 0.044 mL, 0.3216 mmol) was added.

This mixture was stirred at 60<sup>0</sup>C on a pre-heated mantel for 15 minutes. This was followed by the addition of 1.2 equivalents of 4'-(bromomethyl)-[1,1'-biphenyl]-2-carbonitrile (70.05 mg, 0.2573 mmol) dropwise over a period of five minutes. This reaction mixture was refluxed overnight at 70<sup>0</sup>C. Methanol was evaporated and the contents were dissolved in dichloromethane. Pyridine was removed by washing with 20 mL 1N HCl twice followed by extraction of the organic layer with dichloromethane. The crude compound was purified by column chromatography on silica gel with dichloromethane: methanol (100:1) as the solvent system with 1% NH<sub>4</sub>OH. The pure compound was obtained as a pale yellow oil (40 mg, 35.08%). <sup>1</sup>H NMR (400MHz, CDCl<sub>3</sub>): δ 10.37 (br, 1H), 9.50 (d, *J*= 1.44 Hz, 1H), 8.77 (d, *J*= 2.40 Hz, 1H), 8.61 (d,d, *J*= 1.56 Hz, *J*= 2.36 Hz, 1H), 8.53 (d, *J*= 2.04 Hz, 1H), 7.76 (m, 1H), 7.64 (t, *J*= 7.68 Hz, 1H), 7.50 (m, 5H), 7.42 (t, *J*= 7.64 Hz, 1H), 6.96 (d,d, *J*= 2.04 Hz, *J*= 8.40 Hz, 1H), 6.89 (d, *J*= 8.44 Hz, 1H), 4.56 (m, *J*= 6.08 Hz, 1H), 3.61 (s, 2H), 3.06 (m, 2H), 2.55 (m, 1H), 2.13 (s, 2H), 1.86 (s, 4H), 1.42 (d, *J*= 6.04 Hz, 6H). <sup>13</sup>C NMR (400MHz, CDCl<sub>3</sub>): δ 160.47, 147.16, 145.39, 145.20, 144.59, 142.63, 133.78, 132.77, 130.11, 129.46, 128.63, 128.26, 127.38, 122.19, 118.79, 113.58, 111.25, 72.12, 54.46, 33.61, 22.31. IR(Smart iTR diamond ATR, cm<sup>-1</sup>) 3350, 1681, 1250, 1047. MS m/z: 532. This compound was converted to the corresponding hydrochloride salt and a white powder was collected which had a melting point of 152<sup>0</sup>C - 153<sup>0</sup>C.

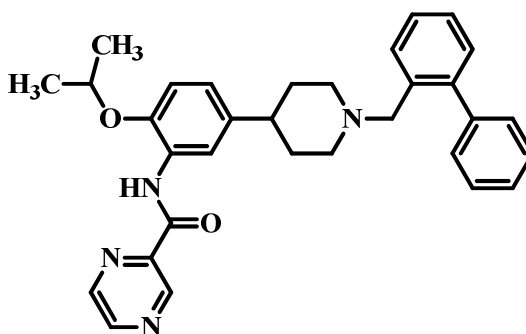
**N-(5-(1-([1,1'-biphenyl]-4-ylmethyl)piperidin-4-yl)-2-isopropoxyphenyl)pyrazine-2-carboxamide (II-14).**



To a solution of 1 equivalent of N-(2-isopropoxy-5-(piperidin-4-yl)phenyl)pyrazine-2-carboxamide (70 mg, 0.2056 mmol) in 5 mL methanol, 1.5 equivalents of pyridine (24.36 mg, d. 0.9819 g/mL, 0.024 mL, 0.3084 mmol) was added. This mixture was stirred at 60°C on a pre-heated mantel for 15 minutes. This was followed by the addition of 1.2 equivalents of 4-(chloromethyl)-1,1'-biphenyl (50 mg, 0.2467 mmol) dropwise over a period of five minutes. This reaction mixture was refluxed overnight at 70°C. Methanol was evaporated and the contents were dissolved in dichloromethane. Pyridine was removed by washing with 20 mL 1N HCl twice followed by extraction of the organic layer with dichloromethane. The crude compound was purified by column chromatography on silica gel with dichloromethane: methanol (100:1) as the solvent system with 1% NH<sub>4</sub>OH. The pure compound was obtained as a pale yellow oil (49 mg, 47.11%). <sup>1</sup>H NMR (400MHz, CDCl<sub>3</sub>): δ 10.37 (br, 1H), 9.50 (d, *J*= 1.44 Hz, 1H), 8.77 (d, *J*= 2.44 Hz, 1H), 8.60 (d,d, *J*= 1.52 Hz, *J*= 2.36 Hz, 1H), 8.52 (d, *J*= 2.08 Hz, 1H), 7.59 (m, 4H), 7.44 (m, 4H), 7.32 (m, 1H), 6.96 (d,d, *J*= 2.08 Hz, *J*= 8.40 Hz, 1H), 6.88 (d, *J*= 8.44 Hz, 1H), 4.55 (m, *J*= 6.0 Hz, 1H), 3.61 (s, 2H), 3.05 (m, 2H), 2.54 (m,

1H), 2.13 (s, 2H), 1.86 (s, 4H), 1.41 (d,  $J= 6.04$  Hz, 6H).  $^{13}\text{C}$  NMR (400MHz,  $\text{CDCl}_3$ ):  $\delta$  160.47, 147.15, 145.38, 145.18, 144.58, 142.62, 141.06, 139.94, 129.65, 128.71, 128.25, 127.11, 127.08, 126.96, 122.15, 118.79, 113.57, 72.11, 63.07, 54.36, 42.20, 33.55, 22.30. IR(Smart iTR diamond ATR,  $\text{cm}^{-1}$ ) 3357, 1683, 1255, 1047. MS  $m/z$ : 507. This compound was converted to the corresponding hydrochloride salt and a white powder was collected which had a melting point of  $209^\circ\text{C} - 210^\circ\text{C}$ .

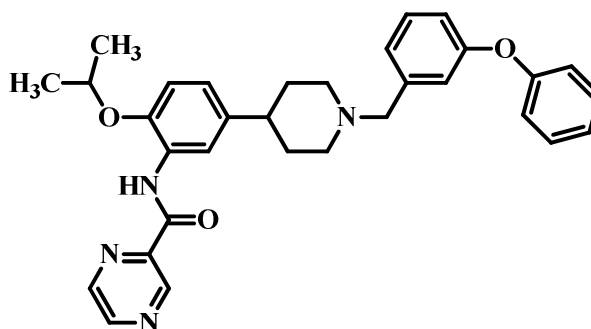
**N-(5-(1-([1,1'-biphenyl]-2-ylmethyl)piperidin-4-yl)-2-isopropoxyphenyl)pyrazine-2-carboxamide (II-10).**



To a solution of 1 equivalent of N-(2-isopropoxy-5-(piperidin-4-yl)phenyl)pyrazine-2-carboxamide (70 mg, 0.2056 mmol) in 5 mL methanol, 1.5 equivalents of pyridine (24.36 mg, d. 0.9819 g/mL, 0.024 mL, 0.3084 mmol) was added. This mixture was stirred at  $60^\circ\text{C}$  on a pre-heated mantle for 15 minutes. This was followed by the addition of 1.2 equivalents of 2-(bromomethyl)-1,1'-biphenyl (60.96 mg, 0.2467 mmol) dropwise over a period of five minutes. This reaction mixture was refluxed overnight at  $70^\circ\text{C}$ . Methanol was evaporated and the contents were dissolved in

dichloromethane. Pyridine was removed by washing with 20 mL 1N HCl twice followed by extraction of the organic layer with dichloromethane. The crude compound was purified by column chromatography on silica gel with dichloromethane: methanol (100:1) as the solvent system with 1% NH<sub>4</sub>OH. The pure compound was obtained as a pale yellow oil (65 mg, 62.39%). <sup>1</sup>H NMR (400MHz, CDCl<sub>3</sub>): δ 10.37 (br, 1H), 9.50 (d, *J*= 1.44 Hz, 1H), 8.78 (d, *J*= 2.44 Hz, 1H), 8.60 (d,d, *J*= 1.52 Hz, *J*= 2.44 Hz, 1H), 8.50 (d, *J*= 1.96 Hz, 1H), 7.63 (m, 1H), 7.36 (m, 8H), 6.93 (d,d, *J*= 2.0 Hz, *J*= 8.40 Hz, 1H), 6.88 (d, *J*= 8.48 Hz, 1H), 4.57 (m, *J*= 6.04 Hz, 1H), 3.47 (s, 2H), 2.94 (m, 2H), 2.54 (m, 1H), 1.98 (m, 2H), 1.78 (s, 4H), 1.41 (d, *J*= 6.04 Hz, 6H). <sup>13</sup>C NMR (400MHz, CDCl<sub>3</sub>): δ 160.47, 147.15, 145.34, 145.17, 144.56, 142.63, 142.56, 141.57, 139.72, 129.99, 129.90, 129.58, 128.22, 127.88, 127.18, 126.82, 126.65, 122.18, 118.69, 113.54, 72.10, 60.03, 54.06, 42.12, 33.63, 22.30. IR(Smart iTR diamond ATR, cm<sup>-1</sup>) 3350, 1683, 1256, 1074. MS m/z: 507. This compound was converted to the corresponding hydrochloride salt and a white powder was collected which had a melting point of 171<sup>0</sup>C - 172<sup>0</sup>C.

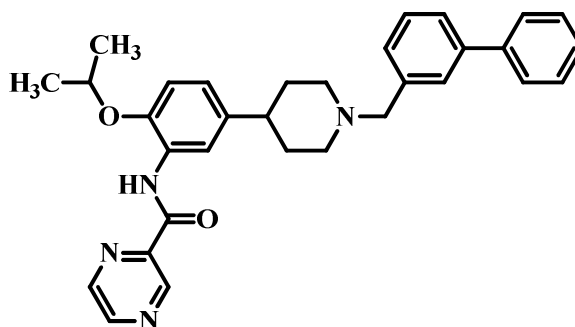
**N-(2-isopropoxy-5-(1-(3-phenoxybenzyl)piperidin-4-yl)phenyl)pyrazine-2-carboxamide (II-11).**





To a solution of 1 equivalent of N-(2-isopropoxy-5-(piperidin-4-yl)phenyl)pyrazine-2-carboxamide (70 mg, 0.2056 mmol) in 5 mL methanol, 1.5 equivalents of pyridine (24.36 mg, d. 0.9819 g/mL, 0.024 mL, 0.3084 mmol) was added. This mixture was stirred at 60°C on a pre-heated mantle for 15 minutes. This was followed by the addition of 1.2 equivalents of 1-(chloromethyl)-3-phenoxybenzene (53.95 mg, 0.2467 mmol) dropwise over a period of five minutes. This reaction mixture was refluxed overnight at 70°C. Methanol was evaporated and the contents were dissolved in dichloromethane. Pyridine was removed by washing with 20 mL 1N HCl twice followed by extraction of the organic layer with dichloromethane. The crude compound was purified by column chromatography on silica gel with dichloromethane: methanol (100:1) as the solvent system with 1% NH<sub>4</sub>OH. The pure compound was obtained as a pale yellow oil (74 mg, 68.86%). <sup>1</sup>H NMR (400MHz, CDCl<sub>3</sub>): δ 10.37 (br, 1H), 9.49 (d, *J*= 1.24 Hz, 1H), 8.77 (d, *J*= 2.40 Hz, 1H), 8.60 (d,d, *J*= 1.52 Hz, *J*= 2.32 Hz, 1H), 8.50 (d, *J*= 2.04 Hz, 1H), 7.31 (m, 3H), 7.09 (m, 5H), 7.00 (d,d, *J*= 2.00 Hz, *J*= 8.36 Hz, 1H), 6.94 (d, *J*= 8.44 Hz, 1H), 4.58 (m, *J*= 6.04 Hz, 1H), 3.57 (s, 2H), 3.04 (m, 2H), 2.53 (m, 1H), 2.13 (s, 2H), 1.85 (s, 4H), 1.41 (d, *J*= 6.08 Hz, 6H). <sup>13</sup>C NMR (400MHz, CDCl<sub>3</sub>): δ 160.47, 147.15, 145.41, 145.18, 144.57, 142.63, 141.15, 129.71, 129.53, 128.23, 128.14, 126.82, 123.13, 122.08, 119.80, 118.84, 118.80, 113.59, 72.11, 63.44, 54.19, 42.20, 33.51, 22.29. IR(Smart iTR diamond ATR, cm<sup>-1</sup>) 3357, 1683, 1255, 1047. MS m/z: 523. This compound was converted to the corresponding hydrochloride salt and a white powder was collected which had a melting point of 124°C - 125°C.

**N-(5-(1-([1,1'-biphenyl]-3-ylmethyl)piperidin-4-yl)-2-isopropoxyphenyl)pyrazine-2-carboxamide (II-15).**



To a solution of 1 equivalent of N-(2-isopropoxy-5-(piperidin-4-yl)phenyl)pyrazine-2-carboxamide (70 mg, 0.2056 mmol) in 5 mL methanol, 1.5 equivalents of pyridine (24.36 mg, d. 0.9819 g/mL, 0.024 mL, 0.3084 mmol) was added. This mixture was stirred at 60°C on a pre-heated mantel for 15 minutes. This was followed by the addition of 1.2 equivalents of 3-(bromomethyl)-1,1'-biphenyl (60.98 mg, 0.2467 mmol) dropwise over a period of five minutes. This reaction mixture was refluxed overnight at 70°C. Methanol was evaporated and the contents were dissolved in dichloromethane. Pyridine was removed by washing with 20 mL 1N HCl twice followed by extraction of the organic layer with dichloromethane. The crude compound was purified by column chromatography on silica gel with dichloromethane: methanol (100:1) as the solvent system with 1% NH<sub>4</sub>OH. The pure compound was obtained as a pale yellow oil (45 mg, 44% yield). <sup>1</sup>H NMR (400MHz, CDCl<sub>3</sub>): δ 10.36 (br, 1H), 9.49 (d, *J*= 1.44 Hz, 1H), 8.77 (d, *J*= 2.44 Hz, 1H), 8.60 (d,d, *J*= 1.52 Hz, *J*= 2.36 Hz, 1H), 8.51 (d, *J*= 2.08 Hz, 1H), 7.62 (m, 3H), 7.35 (m, 6H), 6.96 (d,d, *J*= 2.12 Hz, *J*= 8.44 Hz, 1H), 6.88 (d, *J*=

8.48 Hz, 1H), 4.54 (m,  $J= 6.04$  Hz, 1H), 3.63 (s, 2H), 3.07 (m, 2H), 2.54 (m, 1H), 2.13 (s, 2H), 1.85 (s, 4H), 1.41 (d,  $J= 6.08$  Hz, 6H).  $^{13}\text{C}$  NMR (400MHz,  $\text{CDCl}_3$ ):  $\delta$  160.47, 147.15, 145.38, 145.18, 144.57, 142.63, 141.23, 141.17, 139.59, 128.71, 128.65, 128.24, 128.04, 127.25, 127.21, 122.16, 118.80, 113.57, 72.11, 63.46, 54.35, 42.19, 33.53, 22.30. IR (Smart iTR diamond ATR,  $\text{cm}^{-1}$ ) 3350, 1680, 1250, 1047. MS  $m/z$ : 507. This compound was converted to hydrochloride salt and a white powder was collected which had a melting point of  $122^\circ\text{C}$  to  $123^\circ\text{C}$ .

## 6.2 Biological Screening:

### 6.2.1 Calcium Mobilization Assay:

The cell line used for this assay was MOLT-4. The drug solutions were prepared in varying concentrations. The assay buffer which comprised of 25 mL HBBS and 0.5 mL HEPES was used to prepare the drug dilutions. 50  $\mu\text{L}$  of drug solutions was added to each well. This was followed by the addition of MOLT-4 cells which were plated in a concentration of 80  $\mu\text{L}$  per well. The cells along with the drug were incubated for 60 minutes at  $37^\circ\text{C}$ . The reaction buffer which comprised of 5 mL of assay buffer, 100  $\mu\text{L}$  probenecid, and 40  $\mu\text{L}$  Fluo-4 dye was prepared. 50  $\mu\text{L}$  of the reaction buffer was added to the wells followed by incubation for 60 minutes at  $37^\circ\text{C}$ .

The stock solution of the agonist RANTES was prepared by adding 25  $\mu\text{L}$  of the RANTES stock solution and 2.475 mL assay buffer. The RANTES solution was added to all wells except the blank cells, to which only assay buffer was added. The Flex station

was used to add RANTES and assay buffer to the wells. The fluorescence emission signal was recorded by the Flex station. The software Prism was used to obtain the IC<sub>50</sub> values of the antagonists.

### **6.2.2 Anti-proliferation Assay:**

#### **A. Preparation of cells:**

The CCR5 antagonists were tested on two cell lines. These were PC-3 and M12 cell lines which are prostate cancer cell lines. The cells were incubated at 37<sup>0</sup>C and 5% CO<sub>2</sub>. The media which was used to grow the cells contained RPMI1640 (500 mL), 1% L-glutamine, 0.1% ITS (5 µg/mL insulin, 5 µg/mL transferin, 5 µg/mL selenium), 0.1% gentamycin and 10% fetal bovine serum (FBS). The media used for M12 cell lines contained only 5% FBS and not 10% FBS. After 24 hours of incubation of the M12 cells, the media was replaced with serum free media containing 0.1% epidermal growth factor (EGF).

#### **B. Anti-Proliferation Assay protocol:**

On day 1, both cell lines were plated in 96 well plates. The cells were plated such that 1000 cells would be present in each well. For each cell line, their respective media was used to plate them in concentrations of 100 µL per well. This was followed by incubation of the cells along with their media for 24 hours. On day 2, after 24 hours, the drug solutions were added to each well. The drug solutions were prepared in phosphate buffer solution (PBS). The negative/solvent control included cells with only PBS and

DMSO. The percentage of DMSO used was the amount that was present in the highest concentration of drug tested. 50  $\mu$ L of drug solution was added to each well. The cells were incubated with the drug solution for 72 hours. On day 5, the media, PBS and drug solutions were removed from the plate. This was followed by the addition of 100  $\mu$ L of serum free media with 10% of anti-proliferative reagent WST-1. This was incubated for 3 hours. The absorbance was then measured at 450 nM on Flex station 3. The software Prism was used to obtain the IC<sub>50</sub> values of the drugs.

## **7. Conclusion:**

The constant increase in the number of prostate cancer cases in men as well as rise in mortality due to prostate cancer metastasis necessitates the development of new approaches in the treatment of prostate cancer. Inflammation has been closely associated in the etiology of prostate cancer. Analysis of the inflammatory network in prostate cancer emphasized the role of chemokines and chemokine receptors in the progression of cancer. The chemokine receptor CCR5 and its endogenous ligand CCL5 (RANTES) was found to be overexpressed in prostate cancer cells. This was followed by the discovery that CCR5 antagonists were capable of inhibiting proliferation of prostate cancer cell lines.<sup>28</sup>

The chemokine receptor CCR5 was subsequently identified to play a critical role in the entry process of HIV in to the host cell. CCR5 served as a co-receptor along with the cell surface CD4 receptor for the entry of HIV. It was observed that the gp120 of the viral envelope interacted with the extracellular loop 2 of the CCR5 receptor. With the constantly increasing number of cases of AIDS worldwide, there is a need for novel therapeutic approaches. This led to the discovery of CCR5 antagonists that were capable of blocking the receptor and preventing the interaction between the virus and CCR5.

Due to the implication of CCR5 in various diseases, it served as a novel therapeutic target. Fourteen novel CCR5 antagonists were synthesized and their anti-proliferative activity was explored against prostate cancer cell lines PC-3 and M12. Another assay that was performed to evaluate the CCR5 antagonists was the calcium mobilization assay. The synthesis of the CCR5 antagonists followed the synthetic route

used to synthesize the previous batch of compounds by our lab. Fourteen such compounds were synthesized and their biological screening was carried out.

The anti-proliferative data for PC-3 and M12 showed different results. Compound **19** showed the greatest anti-proliferative activity in the PC-3 cell line. However, it showed only moderate activity in the M12 cell line. Compounds **14** and **24** could strongly inhibit the proliferation of M12 cells. Majority of the compounds had a strong anti-proliferative activity in the M12 cell line, thus making it hard to distinguish a clear structure-activity relationship. There are several possible reasons for compounds showing different activity in different cell lines. Difference in the level of expression of CCR5 by each cell line could be an important factor. Also, different downstream signaling pathways could affect the activity of the antagonist. Compound **19** showed the best activity in the calcium mobilization assay. From the data, it could be inferred that this compound had the greatest ability in inhibiting the RANTES stimulated increase in intracellular calcium.

In summary, a clear structure-activity relationship could not be established due to the limited number of compounds synthesized in this series. However, these studies are a beginning of a thorough analysis of the CCR5 antagonist binding pocket in the CCR5 receptor. Further optimization of the structure could lead to development of the next generation of CCR5 antagonists.

## References:

1. Balkwil, F.; Mantovani, A.; Inflammation and cancer: back to Virchow? *Lancet*, **2001**, *357*, 539-545.
2. Kempen, L.; Visser, K.; Coussens, L.; Inflammation, proteases and cancer. *European Journal of Cancer*. **2006**, *42*, 728-734.
3. Paget. S.; The distribution of secondary growths in cancer of the breast. 1889. *Cancer Metastasis Rev.* **1989**, *8*, 98-101.
4. Giles, R.; Robert, L. ; Can we Target the Chemokine Network for Cancer Therapeutics? *Current Cancer Drug Targets*, **2006**, *6*, 659-670.
5. Jin. T.; Xu, X.; Hereld, D.; Chemotaxis, chemokine receptors and human disease. *Cytokine*, **2008**, *44*, 1-8.
6. Matsushima, K.; Inflammation and Regeneration. **2011**, *31*, 11-22.
7. Fernandez, E.; Lolis, E. ; Structure, Function, and Inhibition of Chemokines. *Annu. Rev. Pharmacol. Toxicol.* **2002**, *42*, 469-499.
8. Palapattu, G.; Sutcliffe, S.; Bastian, P.; Platz, E.; De Marzo, A.; Isaacs, W.; Nelson, W.; Prostate carcinogenesis and inflammation: emerging insights. *Carcinogenesis*, **2004**, *26*(7), 1170-1181.
9. Allavena, A.; Sica, A.; Vecchi, A.; Locati, M.; Sozzani, S.; Mantovani, A.; The chemokine receptor switch paradigm and dendritic cell migration: its significance in tumor tissues. *Immunol. Rev.* **2000**, *177*, 141-149.
10. Ali. S.; Lazenec, G.; Chemokines: novel targets for breast cancer metastasis. *Cancer Metastasis Rev.* **2007**, *26*, 401-420.



11. Singh. R.; Sudhakar, A.; Lokeshwar, B.; Role of Chemokines and Chemokine Receptors in Prostate Cancer Development and Progression. *Journal of Cancer Science and Therapy*, **2010**, 2(4), 89-94.
12. Wu. X.; Lee, V.; Chevalier, E.; Hwang, S.; Chemokine Receptors as Targets for Cancer Therapy. *Current Pharmaceutical Design*, **2009**, 15, 742-757.
13. Balkwil. F.; Cancer and the chemokine network. *Nature*, **2004**, 4, 540-550.
14. Rodrigues-Frade. J.; Munoz, L.; Holgado, B.; Mellado, M.; Chemokine Receptor Dimerization and Chemotaxis. *Chemotaxis, Methods in Molecular Biology*, **2009**, 571, 179-199.
15. Ruddon, R. *Cancer Biology*, 4<sup>th</sup> ed.; Oxford University Press: New York, 2007.
16. O'Hayre, M.; Salanga, C.; Handel, T.; Allen, S.; Chemokines and cancer: migration, intracellular signaling and intercellular communication in the microenvironment. *Biochem. J.* **2008**, 409, 635-649.
17. Bohm. S.; Grady, E.; Bunnett, N.; Regulatory mechanisms that modulate signaling by G-protein-coupled receptors. *Biochem. J.* **1997**, 322, 1-18.
18. Neptune, E.; Receptors induce chemotaxis by releasing the  $\beta\gamma$  subunit of  $G\alpha_i$ , not by activating  $G_q$  or  $G_s$ . *Cell Biology*, **1997**, 94, 14489-14494.
19. Samson. M.; The Role of Human Leukocyte Antigen E and G in HIV Infection: Nef-Mediated Downregulation of Major Histocompatibility Complex Class I, *Biochemistry*, **1996**, 271, 3362-3367.

20. Combadiere. C.; Ahuja, S. ; Tiffany, H. ; Murphy, P. ; Cloning and functional expression of CC-CKR5. *Leukoc. Biol.* **1996**, *60*(1), 147-152.
21. Raport. C.; Gosling, J.; Schweickart, V.; Gray, P.; Charo, I.; Molecular cloning and functional characterization of a novel human CC chemokine receptor (CCR5) for RANTES, MIP-1beta, and MIP-1alpha. *J. Biol. Chem.* **1996**, *271*, 17161-17166.
22. Liu. R.; Paxton, W. ; Choe, S. ; Ceradini, D. ; Martin, S. ; Horuk, R. ; MacDonald, M. ; Stuhlmann, H. ; Koup, R. ; Landau, N. ; Homozygous defect in HIV-1 coreceptor accounts for resistance of some multiply-exposed individuals to HIV-1 infection. *Cell*, **1996**, *86*, 367-377.
23. Samson. M.; LaRosa, G.; Libert, F.; Paindavoine, P.; Detheux, M.; Vassart, G.; Parmentier, M.; The second extracellular loop of CCR5 is the major determinant of ligand specificity. *J. Biol. Chem.* **1997**, *272*, 24934-24941.
24. Samson. M.; Labbe, O.; Mollereau, C.; Vassart, G.; Parmentier, M.; Molecular cloning and functional expression of a new human CC-chemokine receptor gene. *Biochemistry*, **1996**, *35*, 3362-3367.
25. Blanpain. C.; Miquette, I.; Lee, B.; Vakili, J.; Doranz, B.; Govaerts, C.; Vassart, G.; Doms, R.; Parmentier, M.; CCR5 binds multiple CC-chemokines: MCP-3 acts as a natural antagonist. *Blood*, **1999**, *94*, 1899-1905.

26. Leach. K.; Charlton, S.; Strange, P.; Analysis of second messenger pathways stimulated by different chemokines acting at the chemokine receptor CCR5. *Biochemical Pharmacology*, **2007**, *74*, 881-890.
27. Oppermann. M. Chemokine receptor CCR5: insights into structure, function, and regulation. *Cellular Signaling*, **2004**, *16*, 1201-1210.
28. Vaday. G.; Peehl, D.; Kadam, P.; Lawrence, D.; Expression of CCL5 (RANTES) and CCR5 in Prostate Cancer. *The Prostate*, **2006**, *66*, 124-134.
29. Dhimi. H.; Fritz, C.; Gankin, B.; Pak, S.; Yi, W.; Seya, M.; Raffa, R.; Nagar, S.; The chemokine system and CCR5 antagonists: potential in HIV treatment and other novel therapies. *Journal of Clinical Pharmacy and Therapeutics*, **2009**, *34*, 147-160.
30. Deng. H.; Liu, R.; Ellemier, W.; Choe, S.; Unutmaz, D.; Burkhardt, M.; DiMarzio, P.; Marmon, S.; Sutton, R.; Hill, C.; Davis, C.; Peiper, S.; Schall, T.; Littman, D.; Landau, N.; Identification of Major Coreceptor for primary isolates of HIV-1. *Nature*. **1996**, *381*, 661-666.
31. Agarwal. L.; Jin, Q.; Altenburgg, J.; Meyer, L.; Tubiana, R.; Theodorou, I.; Alkhatib, G.; CCR5 $\Delta$ 32 Protein Expression and Stability Are Critical For Resistance to Human Immunodeficiency Virus Type 1 In Vivo. *Journal of Virology*, **2007**, *81*(5), 8041-8049.
32. Wang. T.; Duan, Y.; HIV Co-Receptor CCR5: Structure and Interactions with Inhibitors. *Infectious Disorders-Drug Targets*, **2009**, *9*, 279-288.

33. Shahenn. F.; Collman, R.; Co-receptor antagonists and HIV-1 entry inhibitors. *Current Opinion in Infectious Disease*, **2004**, *17*, 7-16.
34. Jones. K.; Maquire, E.; Davenport, A.; Chemokine receptor CCR5: from AIDS to atherosclerosis. *British Journal of Pharmacology*, **2011**, *162*, 1453-1469.
35. Johrer. K.; Pleyer, L.; Olivier, A.; Maizner, E.; Zelle-Reiser, C.; Greil, R.; Tumor-immune cell interactions modulated by chemokines. *Expert Opin. Biol. Ther.* **2008**, *8*, 269-290.
36. Ballistreri. C.; Carruba, G.; Calabro, M.; Campisi, I.; Di Carlo, D.; Lio, D.; Colonna-Romano, G.; Candore, G.; Caruso, C.; CCR5 Proinflammatory Allele in Prostate Cancer Risk. *Steroid Enzymes and Cancer*, **2009**, 289-292.
37. Robinson. S.; Scott, K.; Wilson, J.; Thompson, J.; Proudfoot, A.; Balkwill, F.; A chemokines receptor antagonist inhibits experimental breast tumor growth. *Cancer Res.* **2003**, *63*, 8360-8365.
38. Palapattu. G.; Sutcliffe, S.; Bastian, P.; Platz, E.; De Marzo, A.; Isaacs, W.; Nelson, W.; Prostate carcinogenesis and inflammation: emerging insights. *Carcinogenesis*. **2004**, *26*(7), 1170-1181.
39. Singh, R.; Sudhakar, A.; Lokeshwar, B.; Role of Chemokines and Chemokine Receptors in Prostate Cancer Development and Progression. *Journal of Cancer Science and Therapy*, **2010**, *2*(4), 89-94.
40. Agarwal, L.; Lu, X.; Jin, Q.; Alkhatib, G.; Anti-HIV therapy: Current and Future Directions. *Current Pharmaceutical Design*, **2006**, *12*, 2031-2055.

41. Barbaro, G.; Scozzafava, A.; Mastrolorenzo, A.; Supuran, C.; Highly active antiretroviral therapy: current state of the art, new agents and their pharmacological interactions useful for improving therapeutic outcome. *Current Pharmaceutical Design*, **2005**, *11*, 1805-1843.
42. Gilliam, B.; Clinical use of CCR5 inhibitors in HIV and beyond. *Journal of Translational Medicine*, **2010**, *9*, 1-14.
43. Kondru, R.; Zhang, J.; Ji, C.; Mirzadegan, T.; Rotstein, D.; Sankuratri, S.; Dioszegi, M.; Molecular Interactions of CCR5 with Major Classes of Small-Molecule Anti-HIV CCR5 Antagonists. *Molecular Pharmacology*. **2008**, *73* (3), 789-800.
44. Miller, B.; Ries, L.; Hankey, B.; Seer Cancer Statistics Review. *United States Department of Health and Human Services National Cancer Institute*, **1993**, *NIH Publ. No. 93-2789*, 1973-1990.
45. Luboshits, G.; Shina, S.; Kaplan, O.; Engelberg, S.; Nass, D.; Lifshitz-Mercer, B.; Chaitchik, S.; Keydar, I.; Ben-Baruch, A.; Elevated Expression of the CC chemokines Regulated on Activation, Normal T Cell Expressed and Secreted (RANTES) in Advanced Breast Carcinoma. *Cancer Research*, **1999**, *59*, 4681-4687.
46. Robinson, S.; Scott, K.; Wilson, J.; Thompson, R.; Proudfoot, A.; Balkwil, F.; A Chemokine Receptor Antagonist Inhibits Experimental Breast Tumor Growth. *Cancer Research*, **2003**, *63*, 8360-8365.

47. Proudfoot, A.; Power, C.; Hoogewerf, A.; Montjovent, M.; Borlat, F.; Offords, R.; Wells, T.; Extension of Recombinant Human RANTES by the Retention of the Initiating Methionine Produces a Potent Antagonist. *The Journal of Biological Chemistry*, **1996**, *271*(5), 2599-2603.
48. Youngs, S.; Ali, S.; Taub, D.; Rees, R.; Chemokines Induce Migrational Responses in Human Breast Carcinoma Cell Lines. *Int. J. Cancer*. **1997**, *71*, 257-266.
49. Baba, M.; Nishimura, O.; Kanzaki, N.; Okamoto, M.; Sawada, H.; Iizawa, Y.; Shiraishi, M.; Aramaki, Y.; Okonogi, K.; Ogawa, Y.; Meguro, K.; Funjino, M.; A small-molecule, nonpeptide CCR5 antagonist with highly potent and selective anti-HIV activity. *Proc. Natl. Acad.* **1999**, *96*, 5698-5703.
50. Baba, M.; Takashima, K.; Miyake, H.; Kanzaki, N.; Teshima, K.; Wang, X.; Shiraishi, M.; Iizawa, Y.; TAK-652 inhibits CCR5 Mediated Human Immunodeficiency Virus Type 1 Infection In Vitro and Has Favorable Pharmacokinetics in Humans. *Antimicrobial Agents and Chemotherapy*, **2005**, *49*(11), 4584-4591.
51. Palani, A.; Tagat, J.; Discovery and Development of Small-Molecule Chemokine Coreceptor CCR5 Antagonists. *J. Med Chem.* **2006**, *49* (10), 2851- 2855.
52. Shiraishi, M.; Aramaki, Y.; Seto, M.; Imoto, H.; Nishikawa, Y.; Kanzaki, Y.; Okamoto, M.; Sawada, H.; Nishimura, O.; Baba, M.; Fujino, M.; Discovery of Novel, Potent and Selective Small Molecule CCR5 Antagonists as Anti-HIV

- agents: Synthesis and Biological Evaluation of Anilide Derivatives with a Quaternary Ammonium Moiety. *J. Med. Chem.* **2000**, *43*, 2049-2063.
53. Kazmierski, W.; Bifulco, N.; Yang, H.; Boone, L.; DeAnda, F.; Watson, C.; Kenakin, T.; Recent Progress in Discovery of Small-Molecule CCR5 Chemokine Receptor Ligands as HIV-1 Inhibitors. *Bioorganic & Medicinal Chemistry*, **2003**, *11*, 2663-2676.
54. Palani, A.; Shapiro, S.; Clader, J.; Greenlee, W.; Blythin, D.; Cox, K.; Wagner, N.; Strizki, J.; Baroudy, B.; Dan, N.; Biological Evaluation and Interconversion Studies of Rotamers of SCH 351125, an Orally Bioavailable CCR5 Antagonist. *Bioorganic & Medicinal Chemistry Letters*, **2003**, *13*, 705-708.
55. Strizki, J.; Xu, S.; Wagner, N.; Wojick, L.; Liu, J.; Hou, Y.; Endres, M.; Palani, A.; Shapiro, S.; Clader, J.; Greenlee, W.; Tagat, J.; McCombie, S.; Cox, K.; Fawzi, A.; Chou, C.; Sivo, C.; Davies, L.; Moreno, M.; Ho, D.; Trkola, A.; Stoddart, C.; Moore, J.; Reyes, G.; Baroudy, B.; SCH-C (SCH 351125), an orally bioavailable, small molecule antagonist of the chemokines receptor CCR5, is a potent inhibitor of HIV-1 infection *in vitro* and *in vivo*. *Pnas.* **2001**, *98* (22), 12718-12723.
56. Singhal, M.; Kansara, S.; Paul, A.; CCR5 Antagonist: A New Era for Treatment of AIDS. *Pharmacologyonline*, **2010**, *3*, 484-496.
57. Norton, B.; Hicks, C.; Maraviroc: the first chemokine coreceptor 5 inhibitor. *Future Virol.* **2011**, *6*(3), 283-294.

58. Hunt, J.; Romanelli, F.; Maraviroc, a CCR5 Coreceptor Antagonist That Blocks Entry of Human Immunodeficiency Virus Type 1. *Pharmacotherapy*, **2009**, 29(3), 295-304.
59. Peek, R.; Mohla, S.; DuBois, R.; Inflammation in the Genesis and Perpetuation of Cancer: Summary and Recommendations from a National Cancer Institute-Sponsored Meeting. *Cancer Res.* **2005**, 65 (19), 8583-8586.
60. Porta, C.; Riboldi, E.; Sica, A.; Mechanisms linking pathogens-associated inflammation and cancer. *Cancer Letters*, **2011**, 305, 250-262.
61. Baniyash, M.; Chronic inflammation, immunosuppression and cancer: New insights and outlook. *Seminars in Cancer Biology*, **2006**, 16, 80-88.
62. Cancer.org.  
<http://www.cancer.org/acs/groups/content/@epidemiologysurveillance/document/document/acspc-029771.pdf> (accessed June 23rd, 2011).
63. Nelson, W.; De Marzo, A.; DeWeese, T.; Isaacs, W.; The Role of Inflammation in the pathogenesis of prostate cancer. *The Journal of Urology*, **2004**, 172, S6-S12.
64. Wolk, A.; Diet, Lifestyle and risk of prostate cancer. *Acta Oncologica*. **2005**, 44, 277-281.
65. Sutcliffe, S.; Platz, E.; Inflammation in the etiology of prostate cancer: An epidemiologic perspective. *Urologic Oncology*, **2007**, 25, 242-249.



66. Klein, E.; Silverman, R.; Inflammation, infection, and prostate cancer. *Current Opinion in Urology*, **2008**, *18*, 315-319.
67. Rajasekaran, A.; Anilkumar, G.; Christiansen J.; Is prostate specific membrane antigen a multifunctional protein? *Am J Physiol Cell Physiol*. **2005**, *288*, 975-981.
68. Colombatti, M.; Grasso, S.; Porzia, A.; Fracasso, G.; Scupoli, M.; Cingarlini, S.; Poffe, O.; Naim, H.; Heine, M.; Tridente, G.; Mainiero, F.; Ramarli, D.; The Prostate Specific Membrane Antigen Regulates the Expression of IL-6 and CCL5 in Prostate Tumor Cells by Activating the MAPK Pathways. *PLoS ONE*. **2009**, *4* (2), 1-11.
69. Jayasurya, H.; Herath, K.; Ondeyka, J.; Polishook, J.; Bills, G.; Dombrowski, A.; Springer, M.; Siciliano, S; Malkowitz, L.; Sanchez, M.; Tiwari, G.; Stevenson, D.; Borris, R.; Singh, S.; *J. Nat. Prod.* **2004**, *67*, 1036-.
70. Prabhu, V.; Farnham, P.; Hutchinson, A.; Soorapanth, S.; Heffelfinger, J.; Golden, M.; Brooks, J.; Rimland, D.; Sansom, S.; Cost-Effectiveness of HIV Screening in STD Clinics, Emergency Departments, and Inpatient Units: A Model- Based Analysis. *PLoS ONE*. **2011**, *6* (5), 1-11
71. Garzino-Demo, A.; Devico, A.; Gallo, R.; Chemokine Receptors and Chemokines in HIV Infection. *Journal of Clinical Immunology*. **1998**, *18* (4), 243-255.
72. Coussens, L.; Werb, Z.; Inflammation and cancer. *Nature*, **2002**, *420*, 860-.

73. Soria, G.; Ben-Baruch, A.; The inflammatory chemokines CCL2 and CCL5 in breast cancer. *Cancer Letters*, **2008**, *267*, 271-285.
74. Li, G.; Watson, K.; Buckheit, R.; Zhang, Y.; Total Synthesis of Anibamine, a Novel Natural Product as a Chemokine Receptor CCR5 Antagonist. *Organic Letters*, **2007**, *9* (10), 2043-2046.
75. Zhang, X.; Haney, K.; Richardson, A.; Wilson, E.; Gewirtz, D.; Ware, J.; Zehner, Z.; Zhang, Y.; Anibamine, a natural product CCR5 antagonist, as a novel lead for the development of anti-prostate cancer agents. *Bioorganic & Medicinal Chemistry Letters*, **2010**, *20*, 4627-4630.
76. Homepage.smc.edu.  
[http://homepage.smc.edu/kline\\_peggy/organic/Lab\\_Reports\\_Ch\\_24/Chem\\_24\\_Lab\\_Notes.html](http://homepage.smc.edu/kline_peggy/organic/Lab_Reports_Ch_24/Chem_24_Lab_Notes.html) (accessed May 15<sup>th</sup>, 2011)
77. Li, Guo.; Haney, K.; Kellogg, G.; Zhang, Y.; Comparative Docking Study of Anibamine as the First Natural Product CCR5 Antagonist in CCR5 Homology Models. *J. Chem. Inf. Model.* **2009**, *49*, 120-132.
78. Maeda, K.; Das, D.; Ogata-Aoki, H.; Nakata, H.; Miyakawa, T.; Tojo, Y.; Norman, R.; Takaoka, Y.; Ding, J.; Arnold, G. F.; Arnold, E.; Mitsuya, H. Structural and molecular interactions of CCR5 inhibitors with CCR5. *J. Biol. Chem.* **2006**, *281*, 12688-98.
79. Cell proliferation reagent WST-1. [www.roche-applied-science.com](http://www.roche-applied-science.com) (accessed May 31<sup>st</sup>, 2011)

80. Fluo-4-dye. <http://www.invitrogen.com/site/us/en/home/support/Newsletters-and-Journals/BioProbes-Journal-of-Cell-Biology-Applications/BioProbes-Issues-2010/BioProbes-63/Reagents-for-Changes-in-Calcium-Concentrations.html> (accessed July 5<sup>th</sup>, 2011).
81. Sperotto, E.; Vries, J.; Klink, G.; Koten, G.; Ligand-free copper (I) catalyzed N- and O- arylation of aryl halides. *Tetrahedron Letters*, **2007**, *48*, 7366-7370.
82. Xin-Hai, Z.; Gong, C.; Yan, M, Hua-Can, S.; Zun-Le, X.; Yi-Qian, W.; A General, Highly Efficient Ullmann C-O Coupling Reaction under Microwave Irradiation and the Effects of Water. *Chinese Journal of Chemistry*. **2007**, *25*, 546-552.
83. Li, C.; Han-Hong, X.; Biao-Lin, Y.; Chun, X.; Tai-Shaan, H.; Yu-Lin, W.; Synthesis and Biological Activity of Tonghaosu Analogs Containing Phenoxy-phenyl Moiety. *Chinese Journal of Chemistry*, **2004**, *22*, 984-989.
84. Westby, M.; Van der Ryst, E.; CCR5 antagonists: host-targetted antiviral agents for the treatment of HIV infection, 4 years on. *Antiviral Chemistry & Chemotherapy*. **2010**, *20*, 179-192.
85. Stewart, G.; Valant, C.; Dowell, S.; Mijaljica, D.; Devenish, R.; Scammells, P.; Sexton, P.; Christopoulos, A.; Determination of Adenosine A<sub>1</sub> Receptor Agonist and Antagonist Pharmacology using *Saccharomyces Cerevisiae*: Implications for Ligand Screening and Functional Selectivity. *J. Pharmacol. Exp. Ther.* **2009**, *331*, 277-286.

86. Leduc, M.; Breton, B.; Gales, C.; Gouill, C.; Bouvier, M.; Chemtob, S.; Heveker, N.;  
Functional Selectivity of Natural and Synthetic Prostaglandin EP<sub>4</sub> Receptor Ligands. *J. Pharmacol. Exp. Ther.* **2009**, *331*, 297-307.
87. Mailman, R. GPCR functional selectivity has therapeutic impact. *Trends. Pharmacol. Sci.* **2007**, *28*, 390-396.